NAVAL POSTGRADUATE SCHOOL
MONTEREY, CALIFORNIA

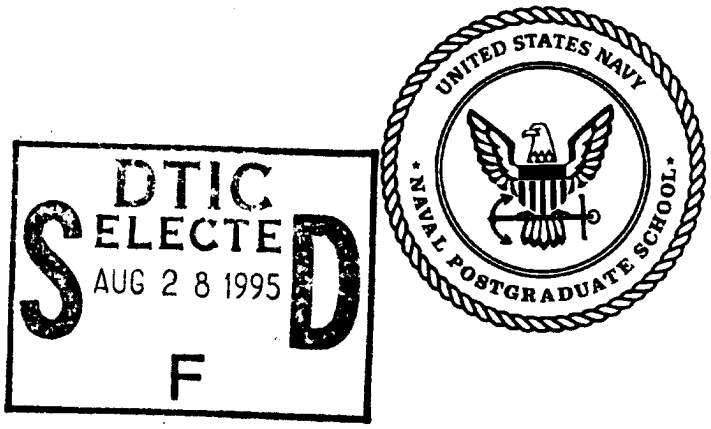

THESIS

SIMULINK SIMULATION OF PROPORTIONAL NAVIGATION AND COMMAND TO LINE OF SIGHT MISSILE GUIDANCE

by

Patrick Costello

March, 1995

Thesis Advisor: **Harold A. Titus**

Approved for public release; distribution is unlimited.

REPORT DOCUMENTATION PAGE

Form Approved OMB No. 0704-0188

1. AGENCY USE ONLY *(Leave blank)*	2. REPORT DATE	3. REPORT TYPE AND DATES COVERED
	March 1995	Master's Thesis

4. TITLE AND SUBTITLE SIMULINK SIMULATION OF PROPORTIONAL NAVIGATION AND COMMAND TO LINE OF SIGHT MISSILE GUIDANCE	5. FUNDING NUMBERS
6. AUTHOR(S) Patrick Costello	
7. PERFORMING ORGANIZATION NAME(S) AND ADDRESS(ES) Naval Postgraduate School Monterey CA 93943-5000	8. PERFORMING ORGANIZATION REPORT NUMBER
9. SPONSORING/MONITORING AGENCY NAME(S) AND ADDRESS(ES)	10. SPONSORING/MONITORING AGENCY REPORT NUMBER

11. SUPPLEMENTARY NOTES The views expressed in this thesis are those of the author and do not reflect the official policy or position of the Department of Defense or the U.S. Government.

12a. DISTRIBUTION/AVAILABILITY STATEMENT	12b. DISTRIBUTION CODE
Approved for public release; distribution is unlimited.	

13. ABSTRACT *(maximum 200 words)*

* Proportional Navigation and Command To Line Of Sight missile guidance are explored. A system flow graph is developed for each guidance technique. The block transfer functions are developed and a state space representation of the system is defined. The missile systems are then tested using one two-dimensional engagement and two three-dimensional engagement scenarios. The final three-dimensional scenario introduces measurement noise in order to evaluate the effect of noise on the guidance algorithms. The engagement results are then compared to analyze the miss distance of each type of missile guidance.

14. SUBJECT TERMS Proportional Navigation Missile, Command to Line of Sight Missile, Missile Control.	15. NUMBER OF PAGES *88
	16. PRICE CODE

17. SECURITY CLASSIFICATION OF REPORT	18. SECURITY CLASSIFICATION OF THIS PAGE	19. SECURITY CLASSIFICATION OF ABSTRACT	20. LIMITATION OF ABSTRACT
Unclassified	Unclassified	Unclassified	UL

NSN 7540-01-280-5500

Standard Form 298 (Rev. 2-89)
Prescribed by ANSI Std. 239-18 298-102

Approved for public release; distribution is unlimited.

SIMULINK SIMULATION OF PROPORTIONAL NAVIGATION AND COMMAND TO LINE OF SIGHT MISSILE GUIDANCE

by

Patrick Costello
Lieutenant, United States Navy
B.S.E.E, Marquette University, 1987

Submitted in partial fulfillment
of the requirements for the degree of

MASTER OF SCIENCE ELECTRICAL ENGINEERING

from the

NAVAL POSTGRADUATE SCHOOL
March 1995

Author: _____
Patrick Costello

Approved by: _____
Harold A. Titus, Thesis Advisor

_____
R.G. Hutchins, Second Reader

_____
for Michael A. Morgan, Chairman
Department of Electrical and Computer Engineering

ABSTRACT

Proportional Navigation and Command To Line Of Sight missile guidance are explored. A system flow graph is developed for each guidance technique. The block transfer functions are developed and a state space representation of the systems is defined. The missile systems are then tested using one two-dimensional engagement and two three-dimensional engagement scenarios. The final three-dimensional scenario introduces measurement noise in order to evaluate the effect of noise on the guidance algorithms. The engagement results are then compared to analyze the miss distance of each type of missile guidance.

TABLE OF CONTENTS

I. INTRODUCTION

A guided missile can be controlled using two different methods. The first is when the missile contains its own guidance system. This type of missile is beneficial in that once fired it will track its target. The second type of guidance has a ground fire control system to command the missile. This type of missile, called command guided, does not contain a target seeker. Two radars, or one radar capable of tracking two targets, are required at the fire control station; one will track the missile and the other the target. The fire control system will calculate the required missile acceleration commands and relay them to the missile by either a radio link or fiber optic cable.

The type of guidance system implemented is largely dependent on the missile's mission. A long range missile will need a self contained guidance system. A point defense missile will use a self contained seeker or command guidance.

The guidance system supplies the input to the missile control system. We will use a roll stabilized "skid-to-turn" missile. The roll stabilization will permit a simpler analysis because there is no coupling between pitch and yaw. Figure 1 shows a block diagram for a missile control system.

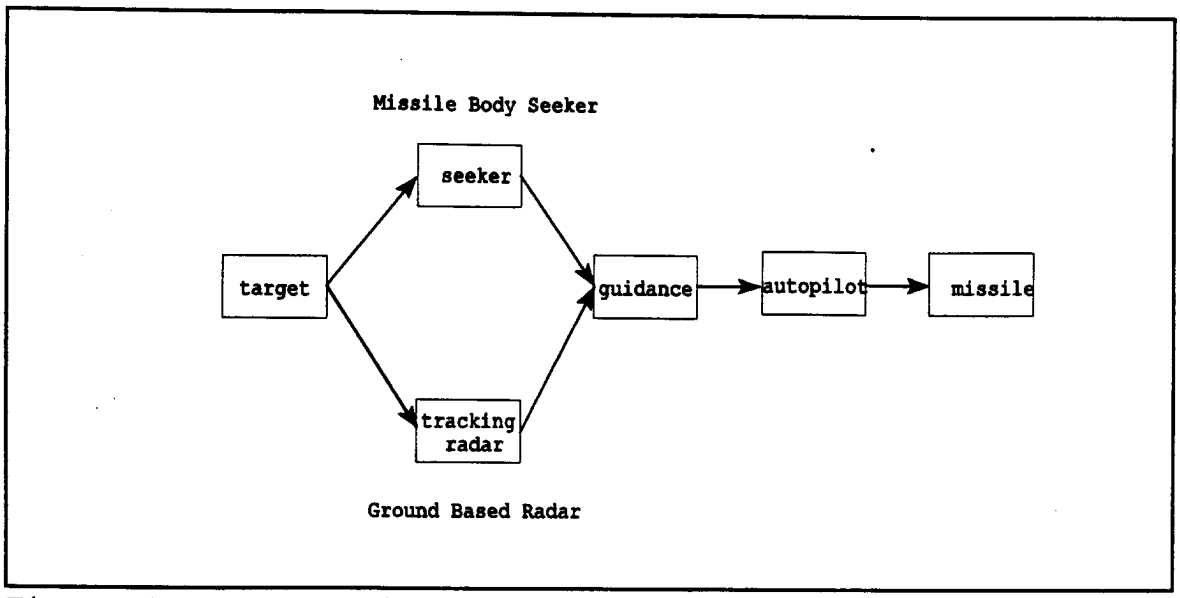

Figure 1. General Missile Guidance System

Missile interception simulations using command to line of sight and proportional navigation guidance systems are developed. Chapter II explains the guidance laws. Chapter III develops the simulation algorithms. Chapter IV tests the algorithms with known two-dimensional results and a three-dimensional problem with and without measurement noise. Chapter V discusses the simulation, conclusions, and recommendations.

II. MISSILE GUIDANCE LAWS

A. GENERAL

The missile guidance system provides the autopilot with the necessary information to produce the required acceleration commands. The missile/target intercept geometry has several important parameters. Figure 2 depicts a typical missile/target intercept scenario.

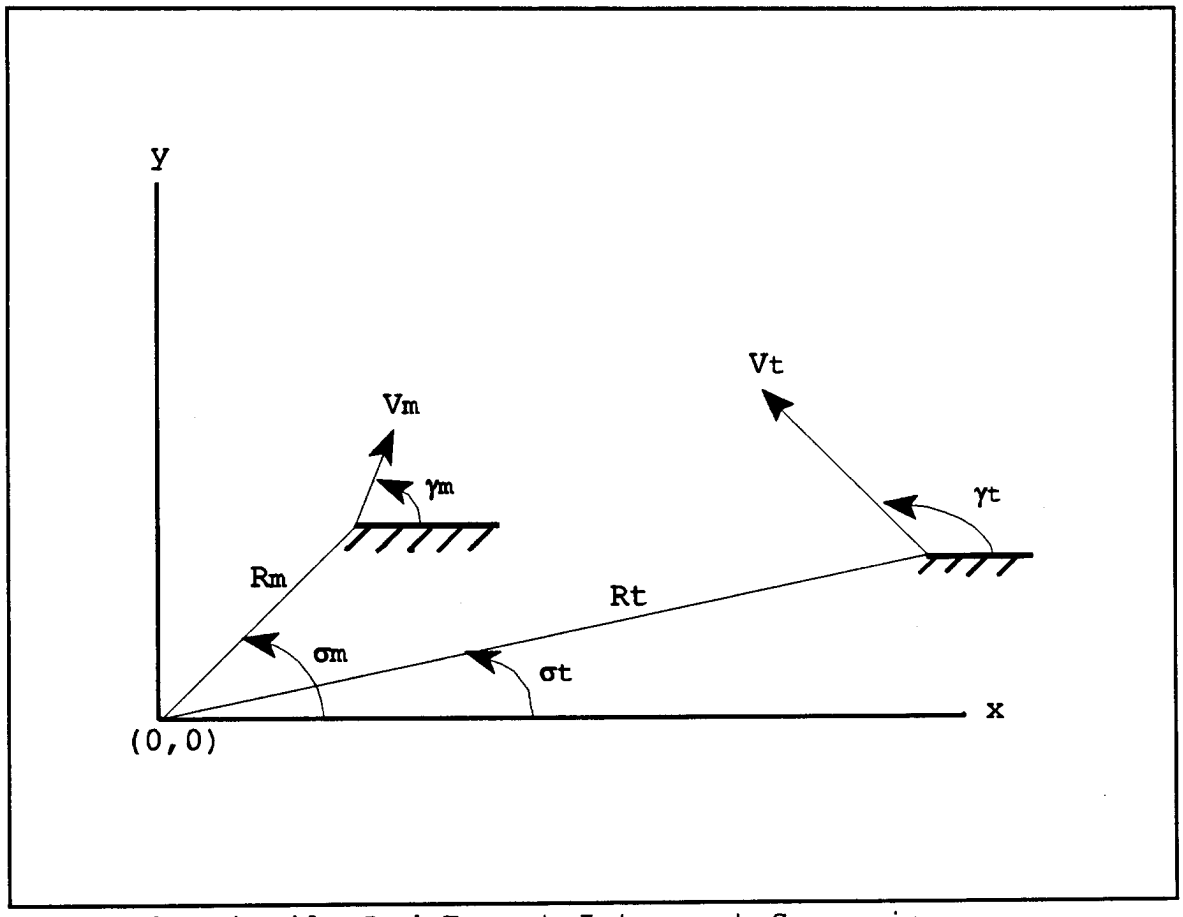

Figure 2. Missile And Target Intercept Scenario

Several important parameters can be developed by analyzing Figure 2.

R_m : Tracker to missile range

R_t : Tracker to target range

σ_m : Tracker to missile line-of-sight angle

σ_t : Tracker to target line-of-sight angle

γ_m : Missile velocity vector angle

γ_t : Target velocity vector angle

The two guidance techniques to be discussed are proportional navigation and command-to-line-of-sight.

B. PROPORTIONAL NAVIGATION

Proportional navigation missiles are guided by either reflected or emmitted energy from the target. A passive missile will be guided from the IR, EO, or RF emmitted by the target. An active missile will send an RF signal out to track the target. In each case the energy is received by a seeker which tracks the target.

Proportional navigation is based on the rate of change of the missile to target line-of-sight (LOS). The missile commanded acceleration is proportional to the rate of change of the LOS. The ratio of the missile turning rate to the LOS rate of change is called the proportional navigation constant (N).

$$N' = \frac{\dot{\gamma}_m}{\dot{\sigma}}$$
$$N = \frac{V_c}{V_m} N' \qquad (2.1)$$

The proportional navigation constant must be greater than 2 to ensure system stability. A proper value of N will ensure that the missile to target angle σ_{mt} will remain constant thus

ensuring missile intercept. Figure 3 illustates this point.

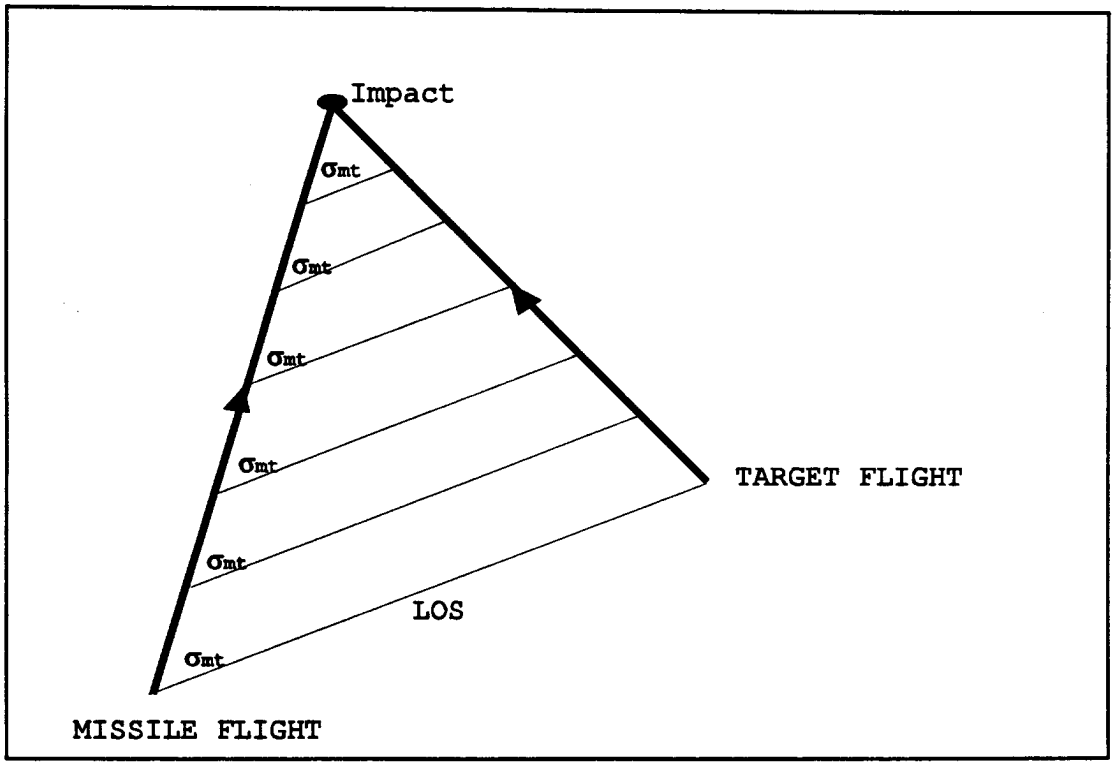

Figure 3. Missile Collision Course Theory

Assuming an acceleration is applied at right angles to the velocity vector of the missile for a period of time dt, the missile's velocity will then be $V_m(t+dt)$. The velocity vector will have changed direction by $d\gamma_m$.
Assuming a small angle approximation yields

$$a_m dt = V_m d\gamma_m$$
$$a_m = V_m \dot{\gamma}_m \qquad (2.2)$$

Combining (2.1) and (2.2) leads to

$$a_m = V_m N \dot{\sigma} \qquad (2.3)$$

This result is the proportional navigation law that will be

implemented in this simulation.

C. COMMAND GUIDANCE

The Command To Line Of Sight (CLOS) missile is given guidance commands that keep the missile in the LOS between the launch point and the target. The distance between the missile and the LOS is defined as the cross range error (CRE). The fire control system will supply the proper commanded acceleration to drive the CRE to zero.

Since two separate radars are required for this type of guidance the problem geometry is slightly different than previously described. Figure 4 shows the CLOS system geometry.

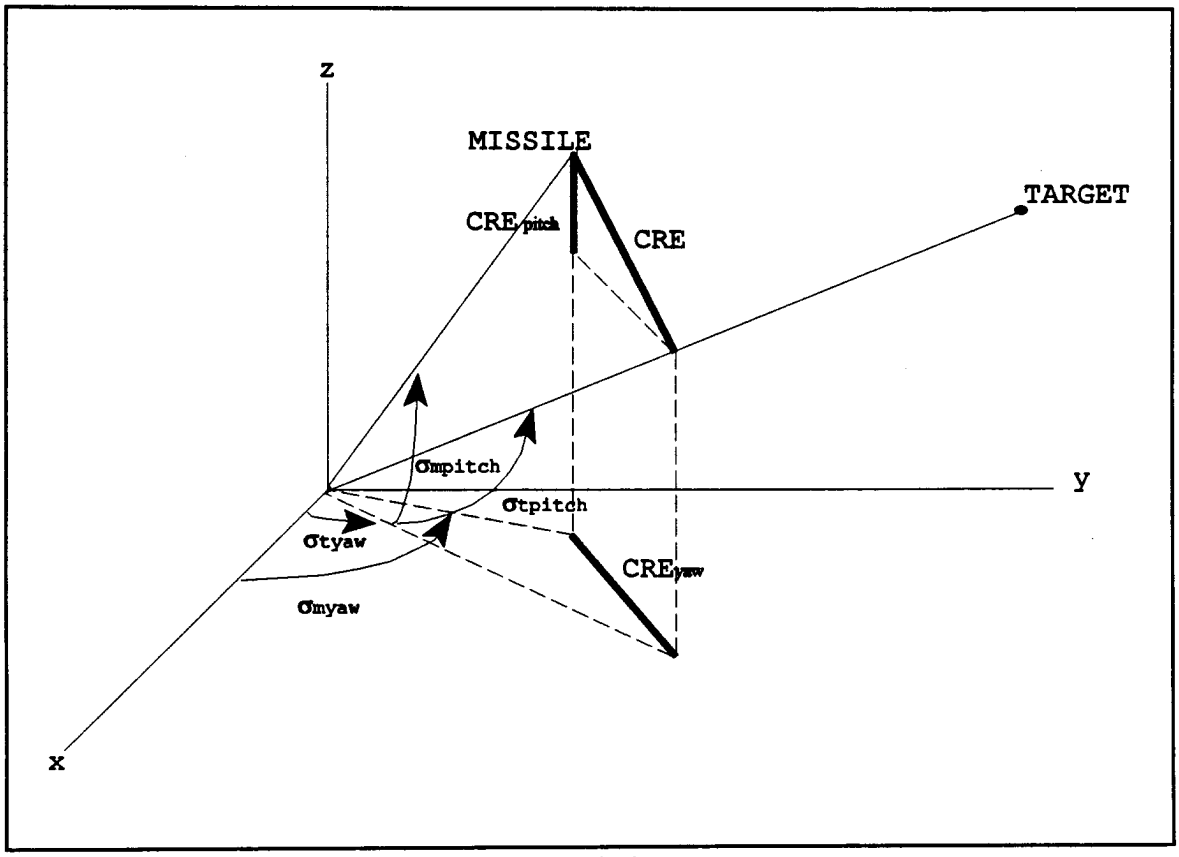

Figure 4. Command To Line Of Sight Geometry

III. SYSTEM DEVELOPMENT

A. OVERVIEW

The system block diagram is shown in Figure 1. The block transfer functions, system dynamics, and simulation equations will be developed for the simulation.

B. RADAR DEVELOPMENT

Target flight is tracked using angles in the pitch and yaw planes. The pitch plane is defined as the vertical plane that contains the target and the radar. The yaw plane is defined as the xy plane.

1. Proportional Navigation

Proportional navigation system geometry is shown in Figure 5.

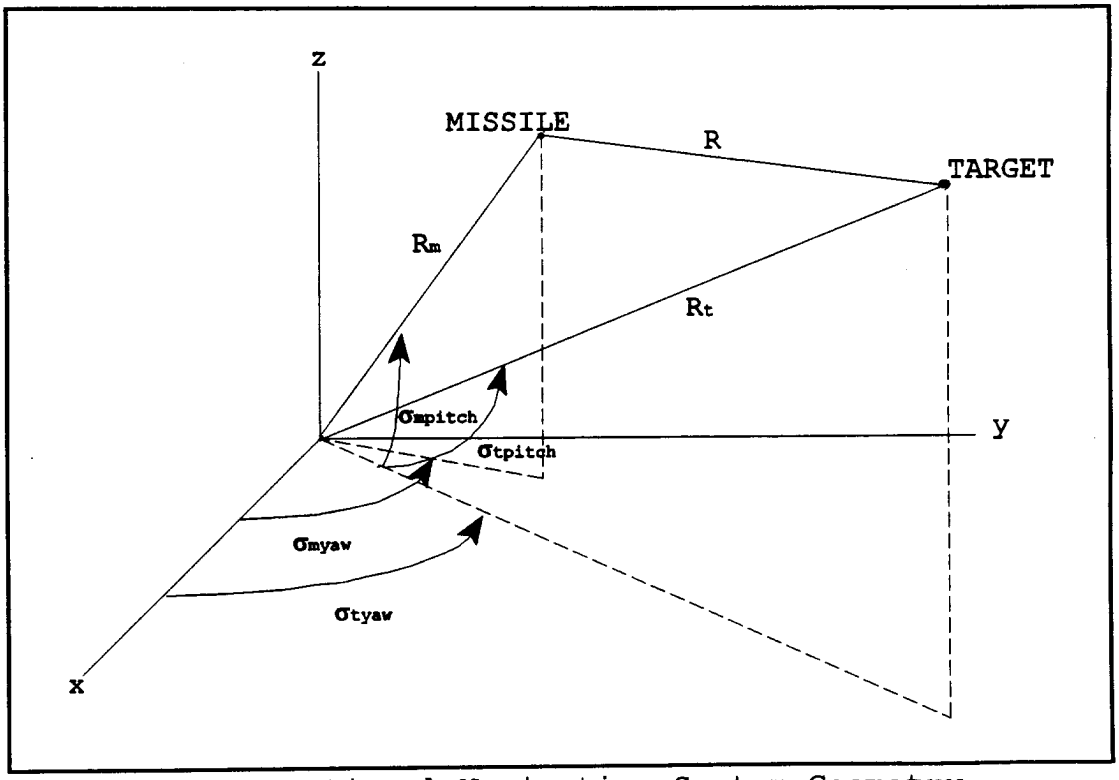

Figure 5. Proportional Navigation System Geometry

From Figure 5 the following angles can be defined:

σ_{myaw} : Missile yaw angle

σ_{mpitch} : Missile pitch angle

σ_{tyaw} : Target yaw angle

σ_{tpitch} : Target pitch angle

The system requires that the following ranges be defined:

R_m : Radar to missile range

R_t : Radar to target range

R : Missile to target range

By applying elementary trigonometry to the cartesian system geometry defined in Figure 5, the following equations can be derived

$$\sigma_{m_{yaw}} = \arctan\left(\frac{y_m}{x_m}\right)$$

$$\sigma_{m_{pitch}} = \arctan\left(\frac{z_m}{\sqrt{x^2{}_m + y^2{}_m}}\right)$$

$$\sigma_{t_{yaw}} = \arctan\left(\frac{y_t}{x_t}\right) \qquad (3.1)$$

$$\sigma_{t_{pitch}} = \arctan\left(\frac{z_t}{\sqrt{x^2{}_t + y^2{}_t}}\right)$$

$$R_m = \sqrt{x_m^2 + y_m^2 + z_m^2}$$

$$R_t = \sqrt{x_t^2 + y_t^2 + z_t^2}$$

$$R = \sqrt{(x_t - x_m)^2 + (y_t - y_m)^2 + (z_t - z_m)^2}$$

The radar system will produce the following angles

σ_{yaw} : Missile to target yaw plane angle

σ_{pitch} : Missile to target pitch plane angle

The angles are given by the equations

$$\sigma_{yaw} = \arctan\left(\frac{(y_t-y_m)}{(x_t-x_m)}\right)$$

$$\sigma_{pitch} = \arctan\left(\frac{(z_t-z_m)}{\sqrt{(x_t-x_m)^2+(y_t-y_m)^2}}\right) \qquad (3.2)$$

The radar will send these angles to the respective yaw and pitch seeker elements.

2. Command Guidance

The CLOS radar will produce a cross range error signal and relay this signal to the missile autopilot. The cross range error is the distance between the missile and the radar to target LOS. Figure 4 shows the CLOS geometry.

From Figure 4 and vector calculus the cross range error of the missile can be defined as follows

$$|\vec{CRE}| = \frac{|\vec{R}_m \times \vec{R}_t|}{|\vec{R}_t|} \qquad (3.3)$$

This calculation yields the following equation

$$|\vec{CRE}| = \frac{1}{|\vec{R}_t|}\sqrt{(y_m z_t - y_t z_m)^2+(x_t z_m - x_m z_t)^2+(x_m y_t - x_t y_m)^2} \qquad (3.4)$$

The missile autopilot requires that the cross range error be broken into the yaw and pitch components. Analyzing Figure 4 yields the following equations

$$CRE_{yaw} = \sqrt{x_m^2 + y_m^2}\,\sin(\sigma_{t_{yaw}} - \sigma_{m_{yaw}})$$
$$CRE_{pitch} = \sqrt{CRE^2 - CRE_{yaw}^2}\;sign(\sigma_{t_{pitch}} - \sigma_{m_{pitch}}) \qquad (3.5)$$

The sign function ensures that the pitch plane cross range error can be positive or negative. A positive cross range error indicates that the missile is leading the LOS. A negative cross range error indicates the missile is trailing the LOS.

C. SEEKER DEVELOPMENT

1. Proportional Navigation

The seeker for proportional navigation measures the rate of change of the missile to target LOS angle. A simple gimballed seeker will use the angular rate of change of the seeker head as an estimate of the rate of change of the LOS angle. Figure 6 shows the seeker.

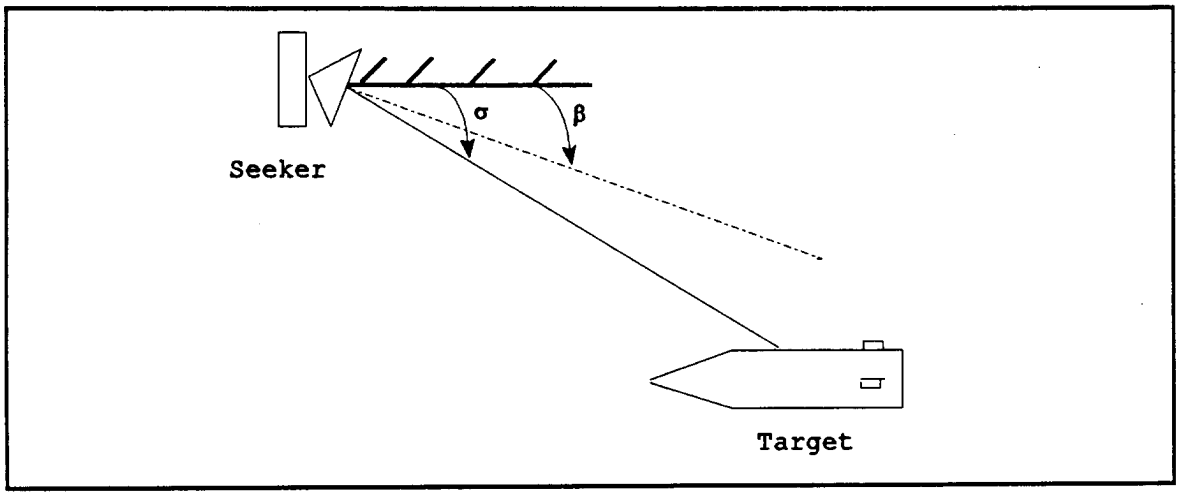

Figure 6. Seeker Head Model

The equation of motion of the seeker head will yield the estimate of the angular rate of change of the LOS. The seeker head equations for the pitch and yaw planes will be identical. We will develop the equations for only the yaw plane. The equation of motion for the seeker head is given by

$$T = I_{seeker}\,\ddot{\beta} \tag{3.6}$$

where

T = Torque applied to the seeker head

I = Moment of inertia of the seeker head

β = Seeker bore sight angle

Solving (3.6) yields

$$\ddot{\beta} = \frac{T}{I} = -k_1(\beta-\sigma) - k_2\dot{\beta} = -k_2\dot{\beta}-k_1\beta+k_1\sigma \tag{3.7}$$

Taking the Laplace transform of (3.7) gives

$$s^2\beta(s) = -k_2 s\beta(s)-k_1\beta(s)+k_1\sigma(s) \tag{3.8}$$

Then we solve for the seeker transfer function

$$\frac{\beta(s)}{\sigma(s)} = \frac{k_1}{s^2+k_2 s+k_1} = \frac{k_1}{\left(s+\frac{1}{\tau_{SH}}\right)^2} \tag{3.9}$$

where τ_{SH} is the seeker head time constant.

A typical seeker head time constant is τ_{SH}= 1/8, using this value produces the following constants

$$k_1 = \left(\frac{1}{\tau_{SH}}\right)^2 = \left(\frac{1}{.125}\right)^2 = 64$$
$$k_2 = 2\left(\frac{1}{\tau_{SH}}\right) = \frac{2}{.125} = 16 \qquad (3.10)$$

The signal flow graph, using these constants, can be seen in Figure 7.

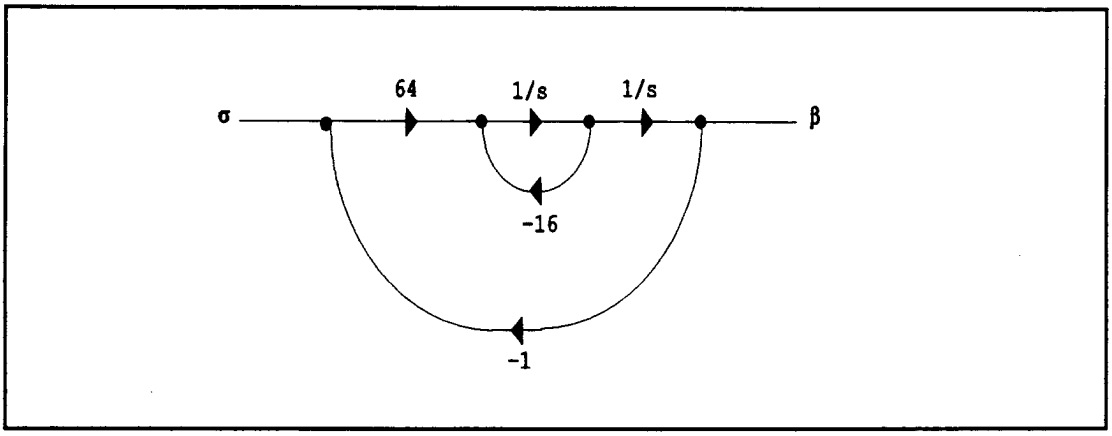

Figure 7. Proportional Navigation Seeker SFG

The following state space representation can then be implemented

$$\dot{x}_{SH} = \begin{bmatrix} 0 & 1 \\ -64 & -16 \end{bmatrix} x_{SH} + \begin{bmatrix} 0 \\ 64 \end{bmatrix} u_{SH}$$
$$x_{SH} = \begin{bmatrix} x_1 \\ x_2 \end{bmatrix} = \begin{bmatrix} \beta \\ \dot{\beta} \end{bmatrix} \qquad (3.11)$$
$$u_{SH} = \sigma$$

2. Command Guidance

The CLOS missile control system does not contain a seeker head. All missile control functions are processed and developed by the fire control system located at the radar site.

D. GUIDANCE DEVELOPMENT

1. Proportional Navigation

The missile guidance system implements the proportional navigation law explained in Chapter II. The major difference is that an estimate of the angular LOS rate is used vice a measurement of the actual LOS rate. Therefore, the rate of change of the missile's velocity vector is given by

$$\dot{\gamma}_m = N \hat{\beta} \tag{3.12}$$

This leads to the following state variable representation

$$\begin{bmatrix} \dot{\gamma}_{m\,pitch} \\ \dot{\gamma}_{m\,yaw} \end{bmatrix} = \begin{bmatrix} N & 0 \\ 0 & N \end{bmatrix} \begin{bmatrix} \hat{\beta}_{pitch} \\ \hat{\beta}_{yaw} \end{bmatrix} \tag{3.13}$$

2. Command Guidance

The guidance for a CLOS missile is developed from the rate of change of the missile's cross range error. The missile acceleration is equal to the rate of change of the cross range error. This rate of change is then used as a commanded acceleration in the autopilot.

The commanded acceleration is developed to provide good missile response. To ensure good response the missile acceleration must be of the form

$$s^2 + (\alpha + \beta)s + \alpha\beta \tag{3.14}$$

This will provide the damping necessary for the missile to perform correctly.

Using equation (3.14) the following commanded acceleration is developed

$$a_{cmd} \doteq \ddot{CRE} + \alpha \dot{CRE} + \rho CRE \qquad (3.15)$$

Taking the Laplace transform of (3.15) yields

$$\frac{a_{cmd}(s)}{CRE(s)} = s^2 + \alpha s + \rho \qquad (3.16)$$

α = 40 and ρ = 196 produces two real roots at s=-5.7171 and s=-34.2829.

The signal flow graph for the guidance system is shown in Figure 8.

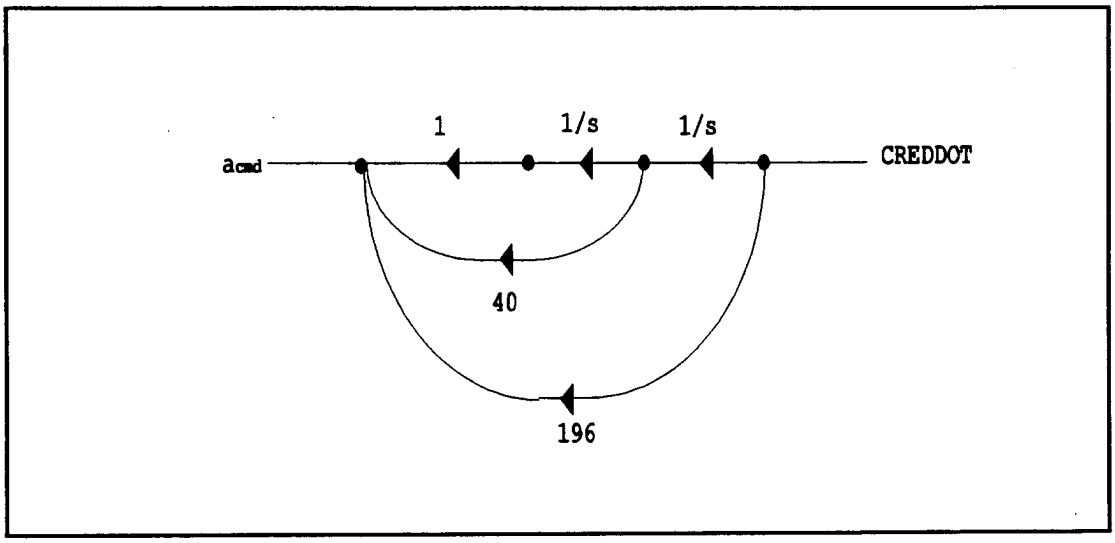

Figure 8. Command To Line Of Sight Guidance SFG

A state space representation of the guidance system is

$$\begin{bmatrix} a_{cmd_{pitch}} \\ a_{cmd_{yaw}} \end{bmatrix} = \begin{bmatrix} 196 & 40 & 0 & 0 \\ 0 & 0 & 196 & 40 \end{bmatrix} \begin{bmatrix} CRE_{pitch} \\ \dot{CRE}_{pitch} \\ CRE_{yaw} \\ \dot{CRE}_{yaw} \end{bmatrix} \tag{3.17}$$

E. AUTOPILOT DEVELOPMENT

1. Proportional Navigation

A simple autopilot can be developed by applying a torque about the center of gravity of the missile. Analyzing the equation of motion

$$T = I_{CG}\ddot{\gamma}_m \tag{3.18}$$

and noting that this must also satisfy equation (3.14) to achieve stable performance, yields the following relationship

$$\ddot{\gamma}_m = \frac{T}{I_{CG}} = -K\dot{\gamma}_m + KN\dot{\beta} \tag{3.19}$$

Taking the Laplace transform of (3.19) yields

$$\frac{\dot{\gamma}_m(s)}{\dot{\beta}(s)} = \frac{KN}{s + K} \tag{3.20}$$

and defining τ_{AP} as the autopilot time constant produces

$$K = \frac{1}{\tau_{AP}} \tag{3.21}$$

The signal flow graph for the autopilot, with k=1, is shown in Figure 9.

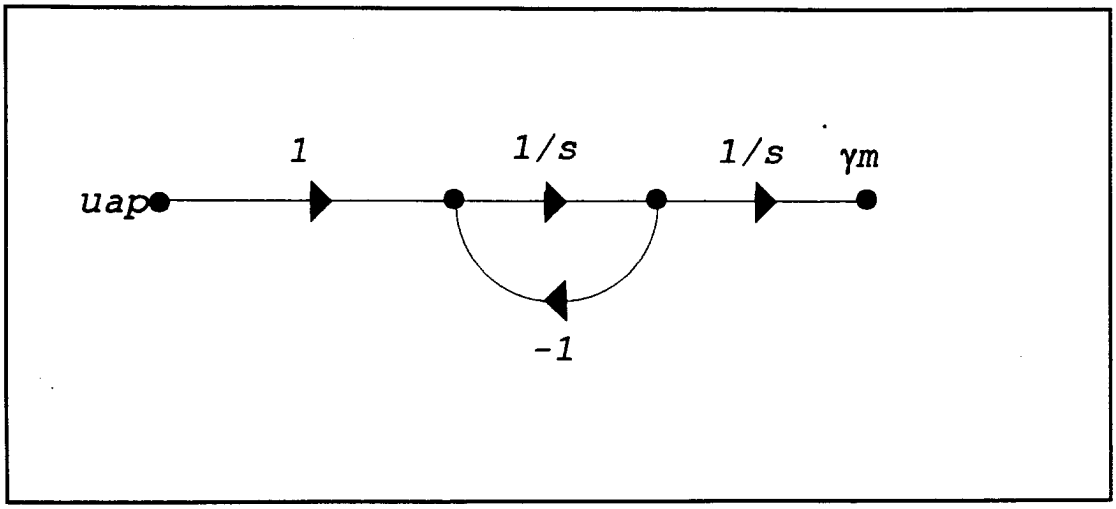

Figure 9. Proportional Navigation Autopilot SFG

The state space representation can be written as follows

$$\begin{bmatrix} \ddot{Y}_{m_{pitch}} \\ \ddot{Y}_{m_{yaw}} \end{bmatrix} = \begin{bmatrix} -1 & 0 \\ 0 & -1 \end{bmatrix} \begin{bmatrix} \dot{Y}_{m_{pitch}} \\ \dot{Y}_{m_{yaw}} \end{bmatrix} + \begin{bmatrix} 1 & 0 \\ 0 & 1 \end{bmatrix} u_{AP}$$

$$u_{AP} = \begin{bmatrix} N & 0 \\ 0 & N \end{bmatrix} \begin{bmatrix} \dot{\beta}_{m_{pitch}} \\ \dot{\beta}_{m_{yaw}} \end{bmatrix} \qquad (3.22)$$

The missile acceleration commands can be derived by looking at the missile's velocity vectors. Figure 10 shows the two-dimensional missile acceleration geometry.

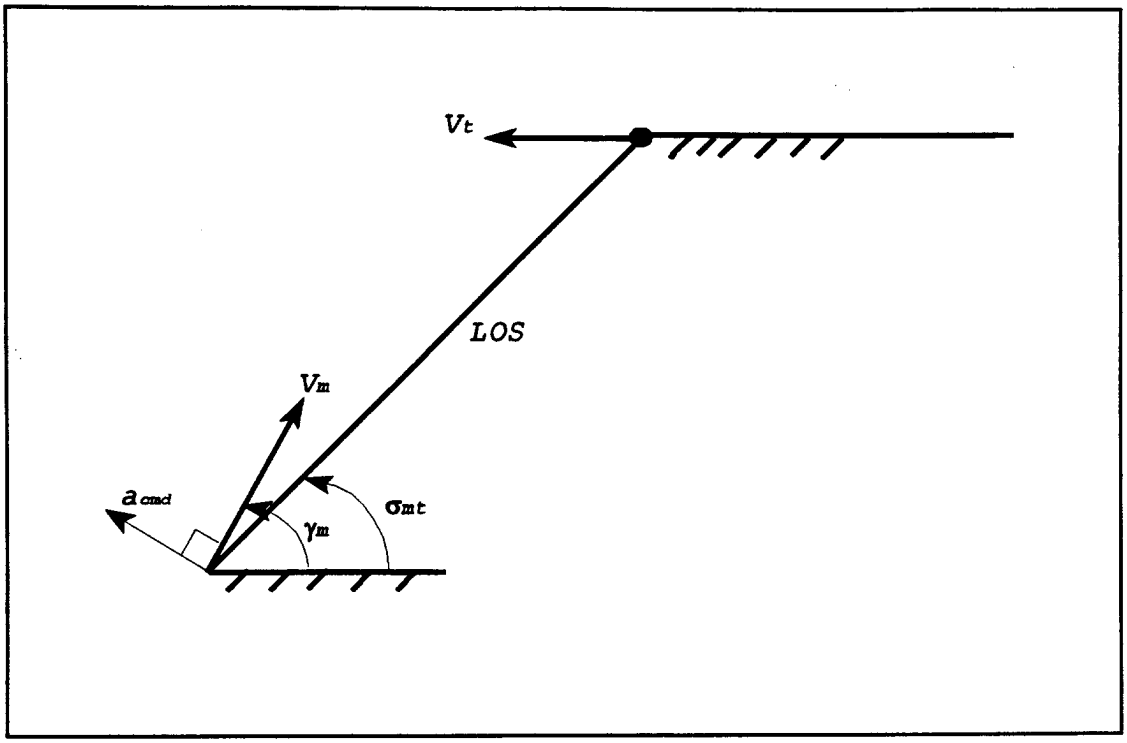

Figure 10. Missile Acceleration Geometry

It can be shown that the velocity in the pitch and yaw planes is given by

$$V_{m_{yaw}} = V_m \cos(\gamma_{m_{yaw}} - \sigma_{m_{yaw}})$$
$$V_{m_{pitch}} = V_m \cos(\gamma_{m_{pitch}}) \qquad (3.23)$$

The acceleration components are then a function of the angular rate of change of the velocity vector

$$a_{m_{pitch}} = V_{m_{pitch}} \dot{\gamma}_{m_{pitch}}$$
$$a_{m_{yaw}} = V_{m_{yaw}} \dot{\gamma}_{m_{yaw}} \qquad (3.24)$$

The angular acceleration commands are then distributed to the missile's cartesian coordinate accelerations using the following geometric relationships

$$\ddot{x}_{m_{pitch}} = -a_{m_{pitch}} \sin(\sigma_{pitch}) \cos(\sigma_{yaw})$$

$$\ddot{y}_{m_{pitch}} = -a_{m_{pitch}} \sin(\sigma_{pitch}) \sin(\sigma_{yaw})$$

$$\ddot{z}_{m_{pitch}} = a_{m_{pitch}} \cos(\sigma_{pitch}) \qquad (3.25)$$

$$\ddot{x}_{m_{yaw}} = -a_{m_{yaw}} \sin(\sigma_{yaw})$$

$$\ddot{y}_{m_{yaw}} = a_{m_{yaw}} \cos(\sigma_{yaw})$$

The missile acceleration in each plane is then

$$\ddot{x}_m = \ddot{x}_{m_{pitch}} + \ddot{x}_{m_{yaw}}$$

$$\ddot{y}_m = \ddot{y}_{m_{pitch}} + \ddot{y}_{m_{yaw}} \qquad (3.26)$$

$$\ddot{z}_m = \ddot{z}_{m_{pitch}}$$

and the total missile acceleration is

$$a_m = \sqrt{\ddot{x}_m^2 + \ddot{y}_m^2 + \ddot{z}_m^2} \qquad (3.27)$$

2. Command Guidance

The CLOS autopilot also takes the guidance commands and translates them into missile accelerations. Similar to the proportional navigation autopilot, this autopilot translates the angular accelerations into cartesian coordinate accelerations.

The commanded angular accelerations of equation (3.15) are translated to cartesian accelerations using the following relationships

$$
\begin{aligned}
\ddot{x}_{m_{pitch}} &= -a_{cmd_{pitch}} \sin(\sigma_{pitch}) \cos(\sigma_{yaw}) \\
\ddot{y}_{m_{pitch}} &= -a_{cmd_{pitch}} \sin(\sigma_{pitch}) \sin(\sigma_{yaw}) \\
\ddot{z}_{m_{pitch}} &= a_{cmd_{pitch}} \cos(\sigma_{pitch}) \\
\ddot{x}_{m_{yaw}} &= -a_{cmd_{yaw}} \sin(\sigma_{yaw}) \\
\ddot{y}_{m_{yaw}} &= a_{cmd_{yaw}} \cos(\sigma_{yaw})
\end{aligned}
\tag{3.28}
$$

The overall missile accelerations are also given by equations (3.26) and (3.27).

F. MISSILE AND TARGET KINEMATICS

The missile and target kinematics can be developed using the state space representation

$$
\begin{aligned}
x_m &= \left[x_m \;\; \dot{x}_m \;\; y_m \;\; \dot{y}_m \;\; z_m \;\; \dot{z}_m\right]^T \\
x_t &= \left[x_t \;\; \dot{x}_t \;\; y_t \;\; \dot{y}_t \;\; z_t \;\; \dot{z}_t\right]^T
\end{aligned}
\tag{3.29}
$$

The system is then represented by

$$
\begin{aligned}
\dot{x}_m &= A_m x_m + B_m u_m \\
\dot{x}_t &= A_t x_t + B_t u_t
\end{aligned}
\tag{3.30}
$$

where

$$A_m = A_t = \begin{bmatrix} 0 & 1 & 0 & 0 & 0 & 0 \\ 0 & 0 & 0 & 0 & 0 & 0 \\ 0 & 0 & 0 & 1 & 0 & 0 \\ 0 & 0 & 0 & 0 & 0 & 0 \\ 0 & 0 & 0 & 0 & 0 & 1 \\ 0 & 0 & 0 & 0 & 0 & 0 \end{bmatrix} \tag{3.31}$$

$$u_m = \begin{bmatrix} \ddot{x}_m & \ddot{y}_m & \ddot{z}_m \end{bmatrix}^T$$

$$u_t = \begin{bmatrix} \ddot{x}_t & \ddot{y}_t & \ddot{z}_t \end{bmatrix}^T$$

A signal flow graph for the missile and target kinematics can be seen in Figure 11.

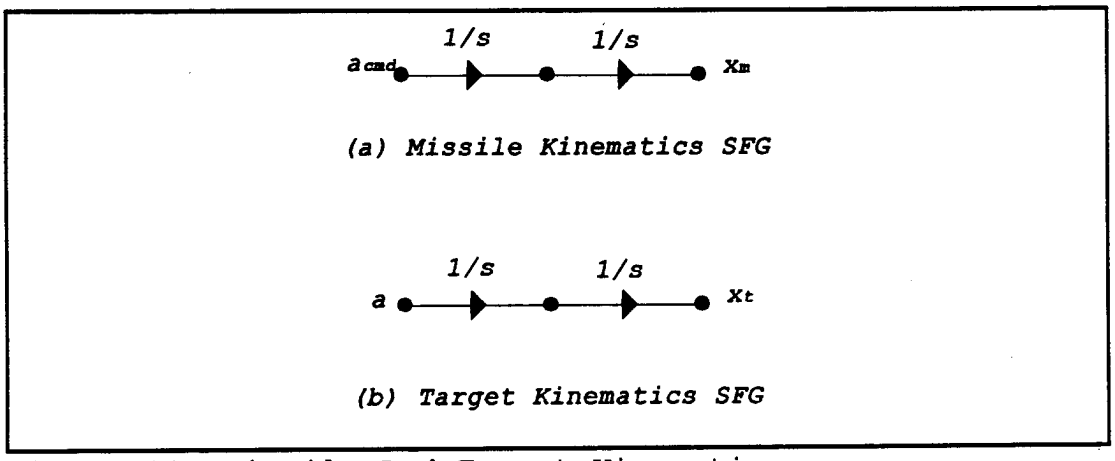

Figure 11. Missile And Target Kinematics

G. KALMAN FILTER DEVELOPMENT

The introduction of noise into the simulation creates a more realistic scenario. The problem is to determine the target's flight path by filtering the noise. This simulation uses an extended Kalman filter to estimate the target's

flight.

The noisy observed target flight is the input to the filter. The cartesian and spherical coordinates of the target are then used in the Kalman iteration to estimate the target's position. The filter is developed to use preprocessed linear pseudomeasurements. These measurements are given by

$$x(kT) = \sqrt{\frac{r^2}{(\tan^2\alpha\tan^2\beta + \tan^2\alpha + \tan^2\beta + 1)}}$$

$$y(kT) = \sqrt{\frac{r^2\tan^2\alpha}{(\tan^2\alpha\tan^2\beta + \tan^2\alpha + \tan^2\beta + 1)}} \qquad (3.32)$$

$$z(kT) = \sqrt{\frac{r^2\tan^2\beta}{(1 + \tan^2\beta)}}$$

where

α = LOS pitch angle

β = LOS yaw angle

The measurement equation then becomes

$$y(kT) = \begin{bmatrix} 1 & 0 & 0 & 0 & 0 & 0 \\ 0 & 0 & 1 & 0 & 0 & 0 \\ 0 & 0 & 0 & 0 & 1 & 0 \end{bmatrix} x(kT) + V_k \qquad (3.33)$$

where V_k = N(0,R), and R = H(kT)$R^*$$H^T$(kT). H(kT) and R^* are given by

$$H(kT) = \begin{bmatrix} \frac{\delta x(r,\alpha,\beta)}{\delta r} & \frac{\delta x(r,\alpha,\beta)}{\delta \alpha} & \frac{\delta x(r,\alpha,\beta)}{\delta \beta} \\ \frac{\delta y(r,\alpha,\beta)}{\delta r} & \frac{\delta y(r,\alpha,\beta)}{\delta \alpha} & \frac{\delta y(r,\alpha,\beta)}{\delta \beta} \\ \frac{\delta z(r,\alpha,\beta)}{\delta r} & \frac{\delta z(r,\alpha,\beta)}{\delta \alpha} & \frac{\delta z(r,\alpha,\beta)}{\delta \beta} \end{bmatrix} \qquad (3.34)$$

$$R^{\cdot} = \begin{bmatrix} \sigma_r^2 & 0 & 0 \\ 0 & \sigma_\alpha^2 & 0 \\ 0 & 0 & \sigma_\beta^2 \end{bmatrix}$$

The discrete time system model then becomes

$$x((k+1)T) = Fx(kT) + W_k$$

$$W_k \approx N(0, Q)$$

$$Q = \begin{bmatrix} \Sigma & 0 & 0 \\ 0 & \Sigma & 0 \\ 0 & 0 & \Sigma \end{bmatrix} \qquad (3.35)$$

$$\Sigma = \begin{bmatrix} \frac{qT^3}{3} & \frac{qT^2}{2} \\ \frac{qT^2}{2} & qT \end{bmatrix}$$

The initial condition for the filter is

$$x(0) \approx N(\hat{x}_0, P_0) \qquad (3.36)$$

The Kalman algorithm is then given by the following set of equations

$$\hat{x}_{k+1/k} = F\hat{x}_{k/k}$$

$$P_{k+1/k} = FP_{k/k}F^T + Q$$

$$K_k = P_{k+1/k}H^T[HP_{k+1/k}H^T + R_k] \qquad (3.37)$$

$$\hat{x}_{k+1/k+1} = \hat{x}_{k+1/k} + K_k[y(kT) - H\hat{x}_{k+1/k}]$$

$$P_{k+1/k+1} = [I-K_kH]P_{k+1/k}[I-K_kH]^T + K_kR_kK_k^T$$

IV. SIMULATION RESULTS

A. OVERVIEW

The proportional navigation and CLOS simulations are tested using three target flight scenarios. In the first scenario the target has constant velocity and level flight in two dimensions. In the second, the target has a constant velocity and level flight in three dimensions. Finally, in the third, noise is added to the three-dimensional scenario.

The Simulink models and associated MATLAB code for the proportional navigation and CLOS simulations are contained in the Appendix.

B. SIMULATION ASSUMPTIONS

The following assumptions are held throughout the simulation:

(1) Acceleration due to gravity does not effect the missile or the target.

(2) The missile is lying in the xy plane at launch.

(3) Missile acceleration is limited to 30g.

(4) The proportional navigation constant is N=6.

C. SIMULATION SCENARIOS

1. Constant Velocity In Two Dimensions

The first scenario is a two-dimensional engagement. The target is flying at a constant altitude with no acceleration. The target parameters are as follows

$$x_t = 30000\ ft$$
$$\dot{x}_t = -3000\ ft/s$$
$$\ddot{x}_t = 0\ ft/s^2$$
$$y_t = 0\ ft$$
$$\dot{y}_t = 0\ ft/s$$
$$\ddot{y}_t = 0\ ft/s^2$$
$$z_t = 1000\ ft$$
$$\dot{z}_t = 0\ ft/s$$
$$\ddot{z}_t = 0\ ft/s^2$$

2. Constant Velocity In Three Dimensions

The next scenario is a three-dimensional engagement. The target is flying at a constant altitude with no acceleration. The target parameters are as follows

$$x_t = 60000\ ft$$
$$\dot{x}_t = -2121\ ft/s$$
$$\ddot{x}_t = 0\ ft/s^2$$
$$y_t = 10000\ ft$$
$$\dot{y}_t = -2121\ ft/s$$
$$\ddot{y}_t = 0\ ft/s^2$$
$$z_t = 1000\ ft$$
$$\dot{z}_t = 0\ ft/s$$
$$\ddot{z}_t = 0\ ft/s^2$$

3. Three-Dimensional Simulation With Radar Noise

The final simulation uses the same target parameters as the three-dimensional constant velocity simulation. White noise is added to the target flight. This simulates received noise in the target's radar return. The noise has the following characteristics

$$\sigma_r = 15\ ft$$
$$\sigma_{yaw} = 1^\circ$$
$$\sigma_{pitch} = 1^\circ$$

D. RESULTS AND SIMULATION COMPARISON

Figure 12 indicates the missile leads the target. This is attributed to the slow missile autopilot time constant (τ_{AP}=1 sec) and the target's speed advantage of mach 3 to mach 2 over the missile. This problem is exaggerated in figures 12 and 13 since the z scale is twenty times the x scale. It was determined by considering the z acceleration profile in figure 16, the z velocity profile in figure 19, and the z position profile in figure 12, that this effect was caused by the autopilot.

Figure 14 shows the rate of change of σ is positive for approximately 1 second; thereafter it is negative but, for 2 seconds the missile has a positive commanded acceleration. Figures 15 and 16 show the missile's acceleration variations. Figures 17, 18 and 19 show the missile's velocity variations.

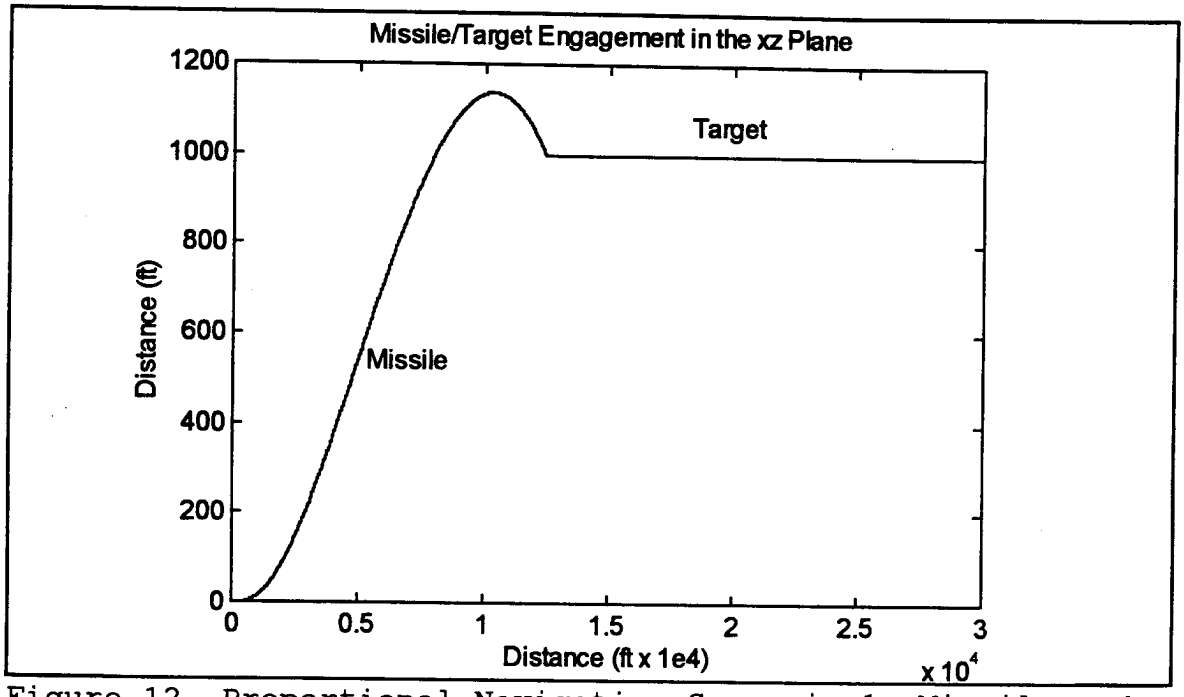

Figure 12. Proportional Navigation Scenario 1. Missile and Target Trajectories in the xz Plane.

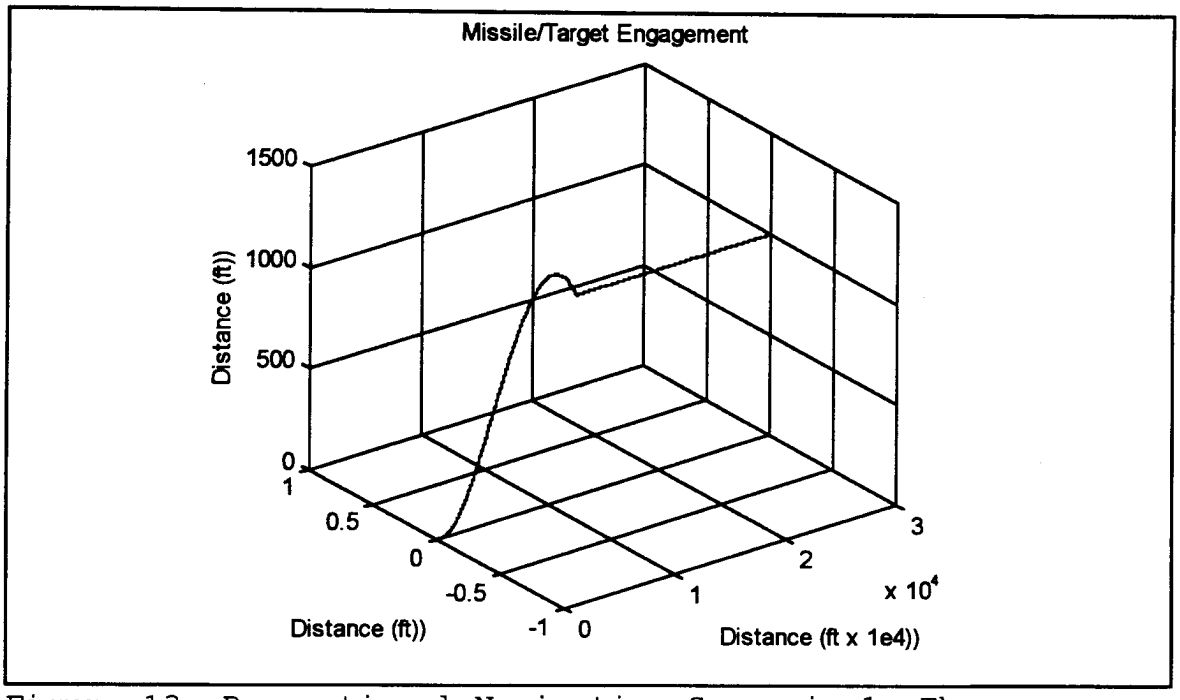

Figure 13. Proportional Navigation Scenario 1. Three-Dimensional Engagement Plot.

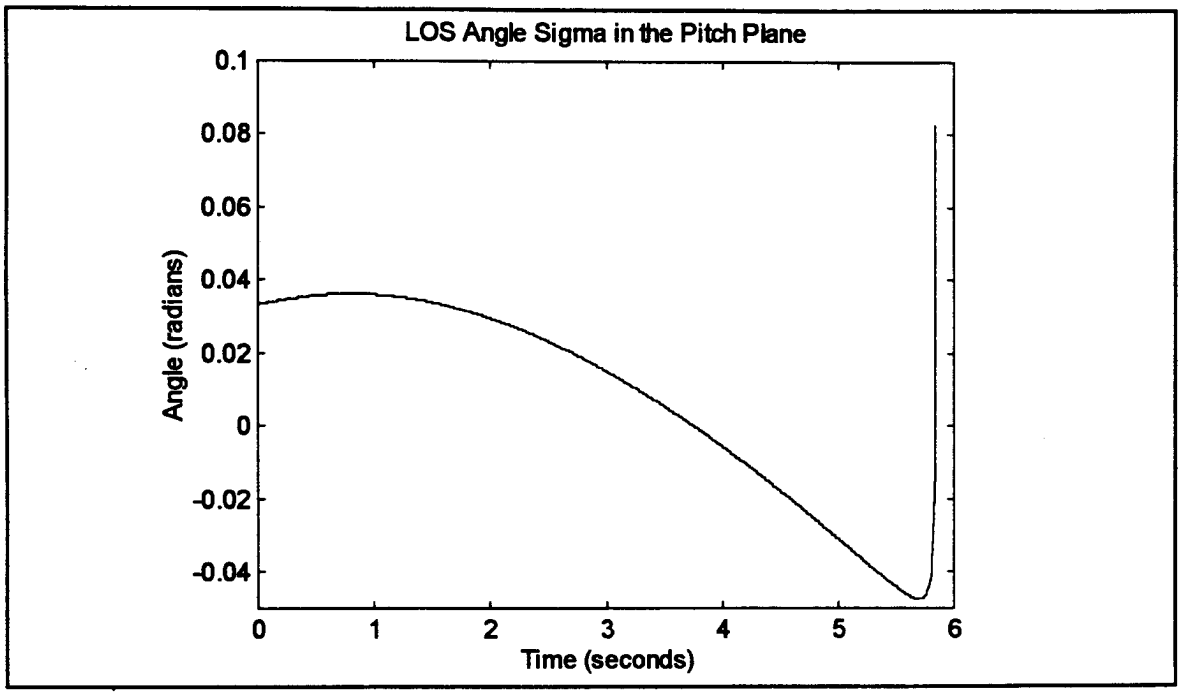

Figure 14. Proportional Navigation Scenario 1. LOS Angle σ_{pitch}.

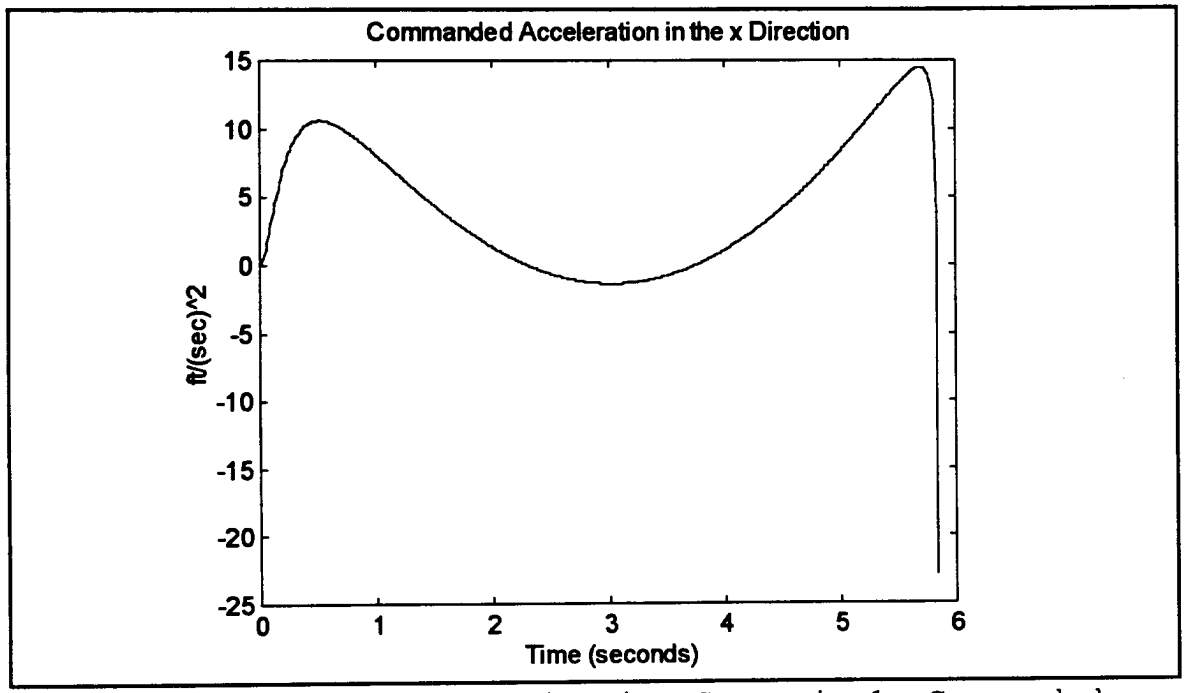

Figure 15. Proportional Navigation Scenario 1. Commanded Acceleration in the x Direction.

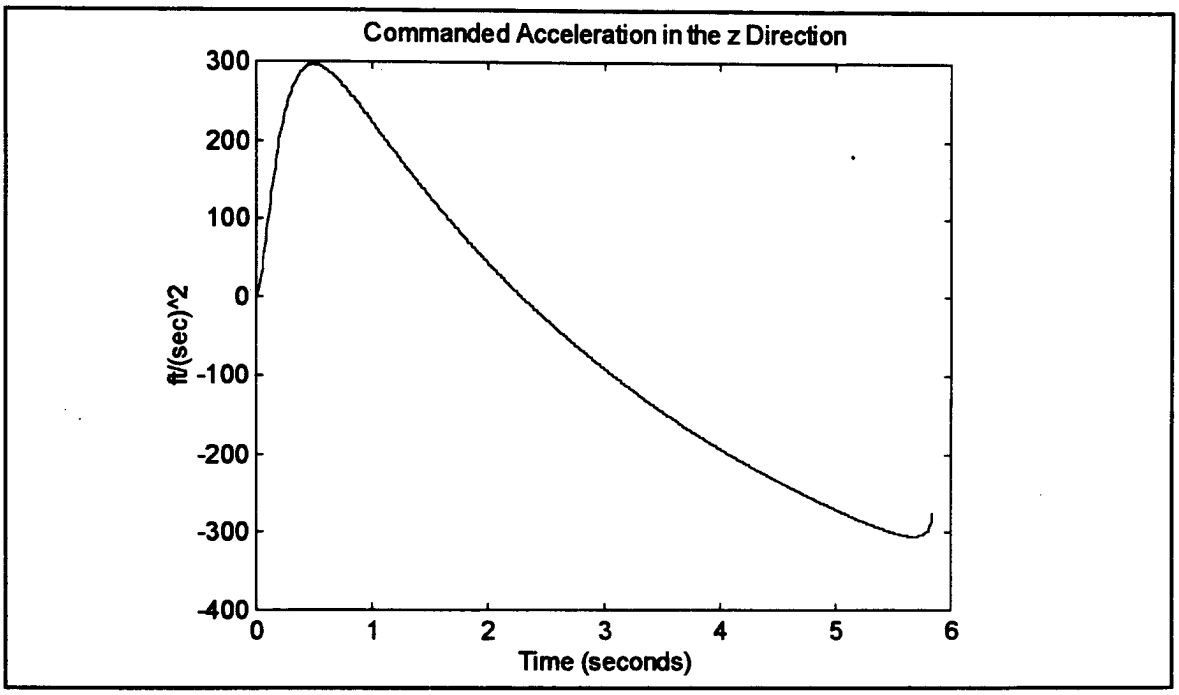

Figure 16. Proportional Navigation Scenario 1. Commanded Acceleration in the z Direction.

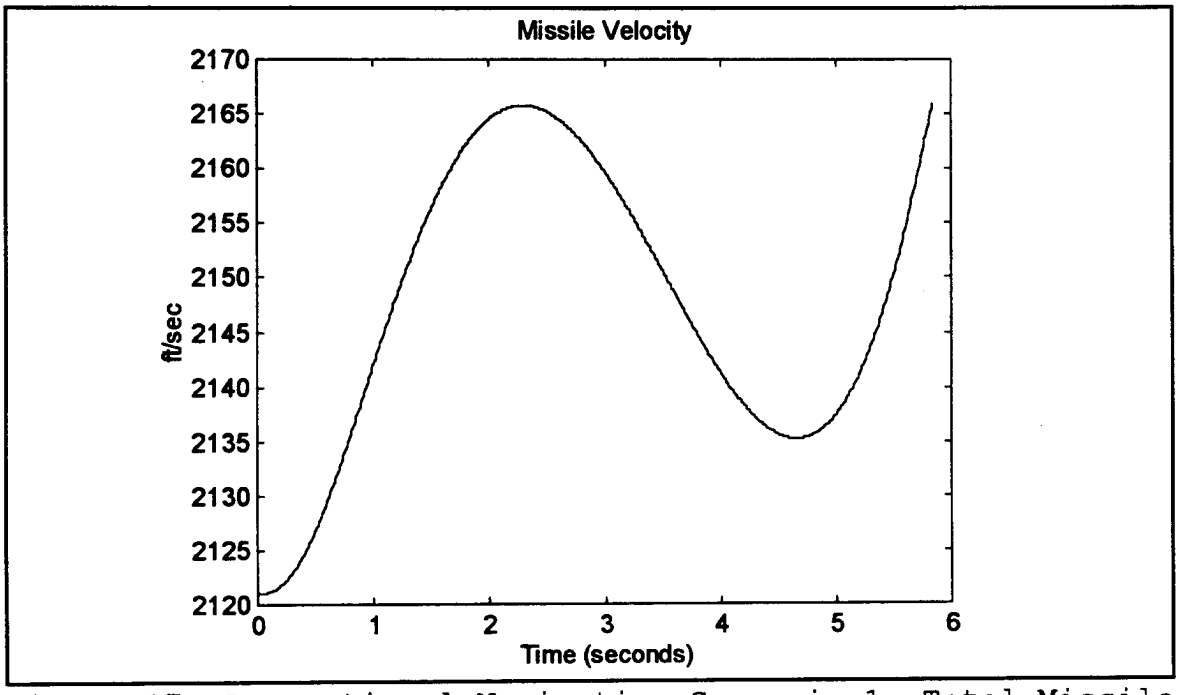

Figure 17. Proportional Navigation Scenario 1. Total Missile Velocity.

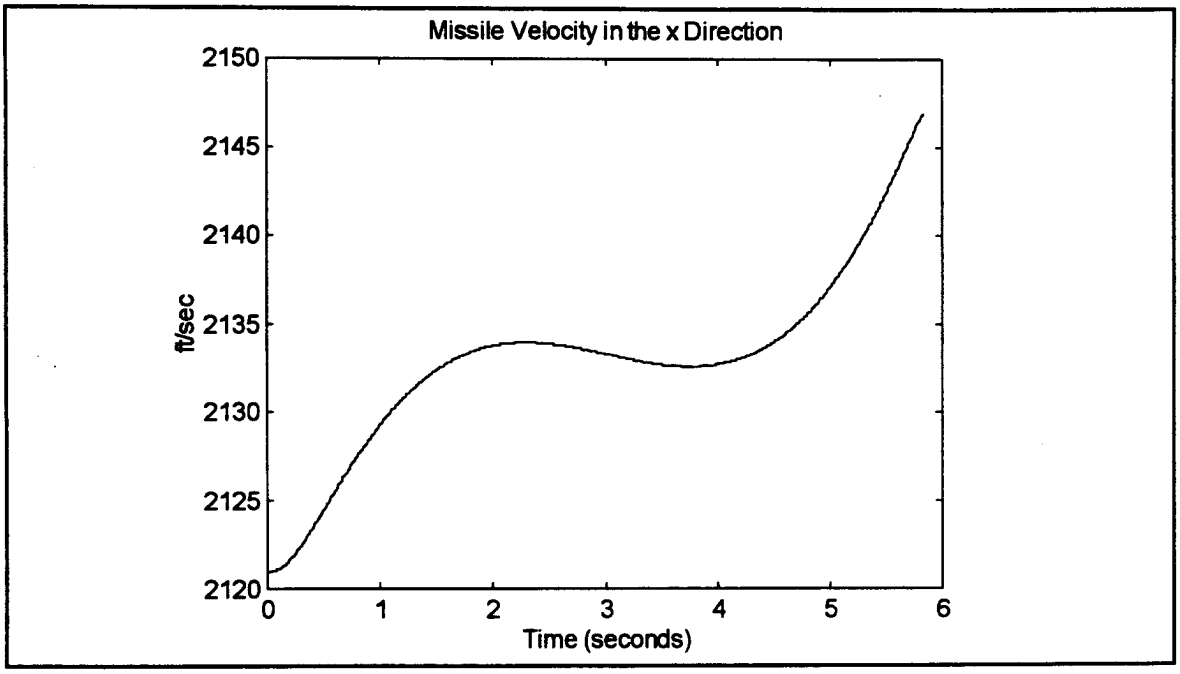

Figure 18. Proportional Navigation Scenario 1. Missile Velocity in the x Direction.

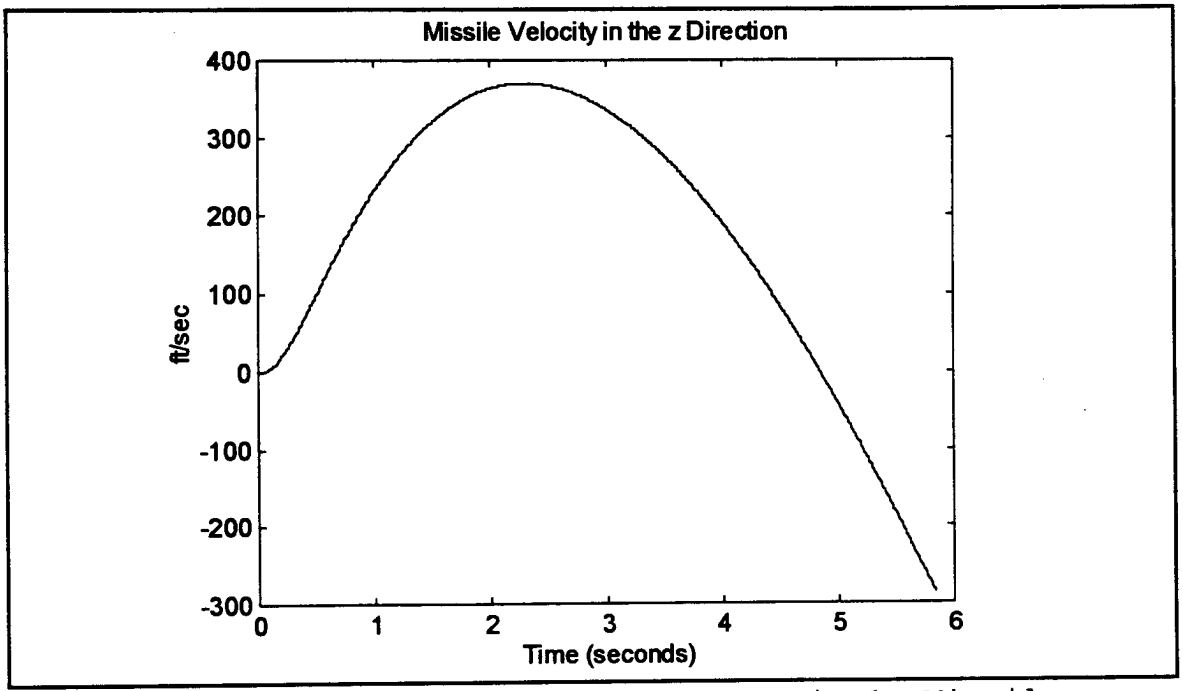

Figure 19. Proportional Navigation Scenario 1. Missile Velocity in the z Direction.

Plots for the other scenarios are given in the Appendix. The following table summarizes the missile's closest point of approach (CPA), and the time of the CPA for each simulation.

Scenario	Simulation	CPA	Time of CPA
1	Prop Nav	4.13 ft	5.89 s
	CLOS	1.39 ft	7.18 s
2	Prop Nav	14.94 ft	14.72 s
	CLOS	1.24 ft	19.51 s
3	Prop Nav	27.15 ft	14.5 s
	CLOS	267.79 ft	22.34 s

Table 1. Missile Miss Distance Summary

Overall, the proportional navigation missile achieves a quicker target intercept time. The miss distances for each missile are very close, except when noise is added. The CLOS missile degrades significantly in the presence of noise.

The proportional navigation missile is a superior missile. The CLOS missile is unable to give satisfactory results when sensor noise is added to the simulation. For very short range intercept scenarios, where sensor noise is negligible, the missile will perform well. The proportional navigation missile will perform well for any engagement scenario. This fact makes proportional navigation preferable for missile guidance.

V. CONCLUSIONS AND RECOMMENDATIONS

A. CONCLUSIONS

The simulation provides insight in chosing the proper type of missile guidance. The two types of guidance explored both give acceptable miss distances without sensor noise. However, when sensor noise is present the proportional navigation missile outperformed the CLOS missile.

The presence of an on board seeker gives the proportional navigation missile an advantage when dealing with sensor noise. Since the sensor is on the missile as it closes the target, the sensor noise will have less of an effect on the detection of the target. The CLOS missile is guided from a stationary radar at the launch site. The error incurred from sensor noise does not decrease as the missile approaches the target. To overcome this problem the CLOS missile will require a very sophisticated tracking radar that has very little sensor noise.

The addition of noise to the engagement provides a more realistic scenario for the missile control problem. Developing a noise filter and adjusting the missile characteristics to adapt to the noise created a unique and educational challenge. The increased realism reinforced the fact that actual missile control developement is a compromise of design requirements.

B. RECOMMENDATIONS

The simulation can be taken to several different levels. The target flight can be modified for different engagement scenarios. A manuevering target would provide another level of realism to the engagement.

An adjoint model could be built for each simulation.

This would aid in the miss distance analysis for the two missiles.

Finally, different noise filters can be developed and tested. The miss distance will be decreased if better noise filtering is achieved during the simulation.

APPENDIX

A. COMMAND GUIDED MISSILE PLOTS FOR SCENARIO 1

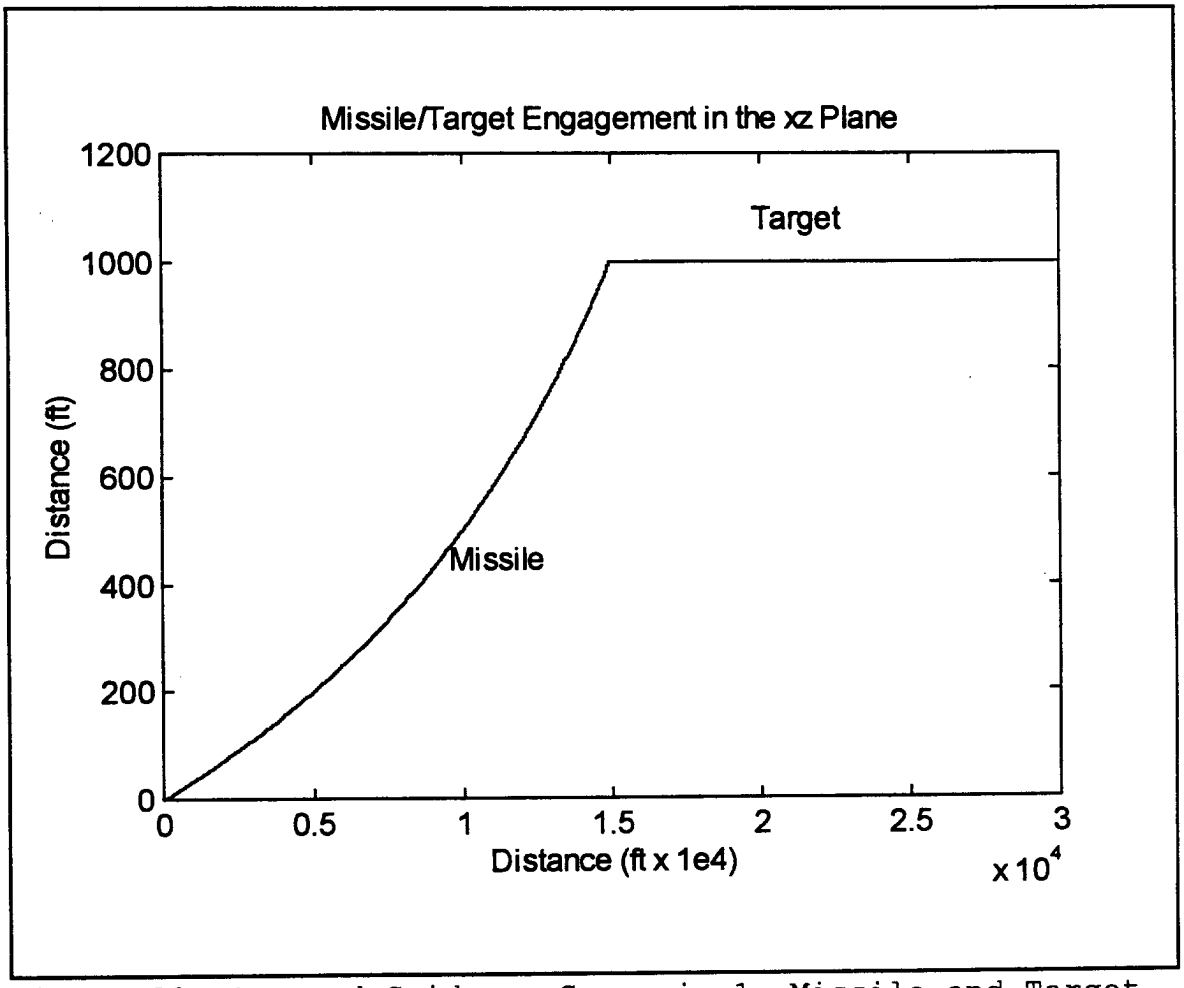

Figure 20. Command Guidance Scenario 1. Missile and Target Trajectories in the xz Plane.

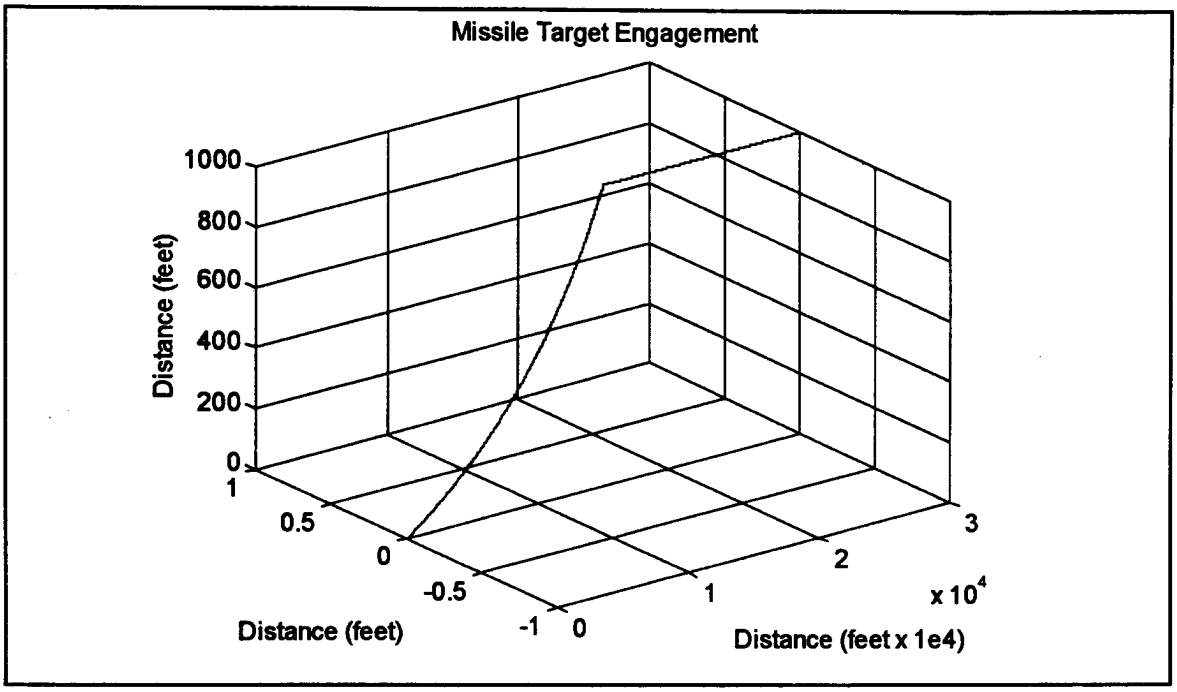

Figure 21. Command Guidance Scenario 1. Three- Dimensional Plot.

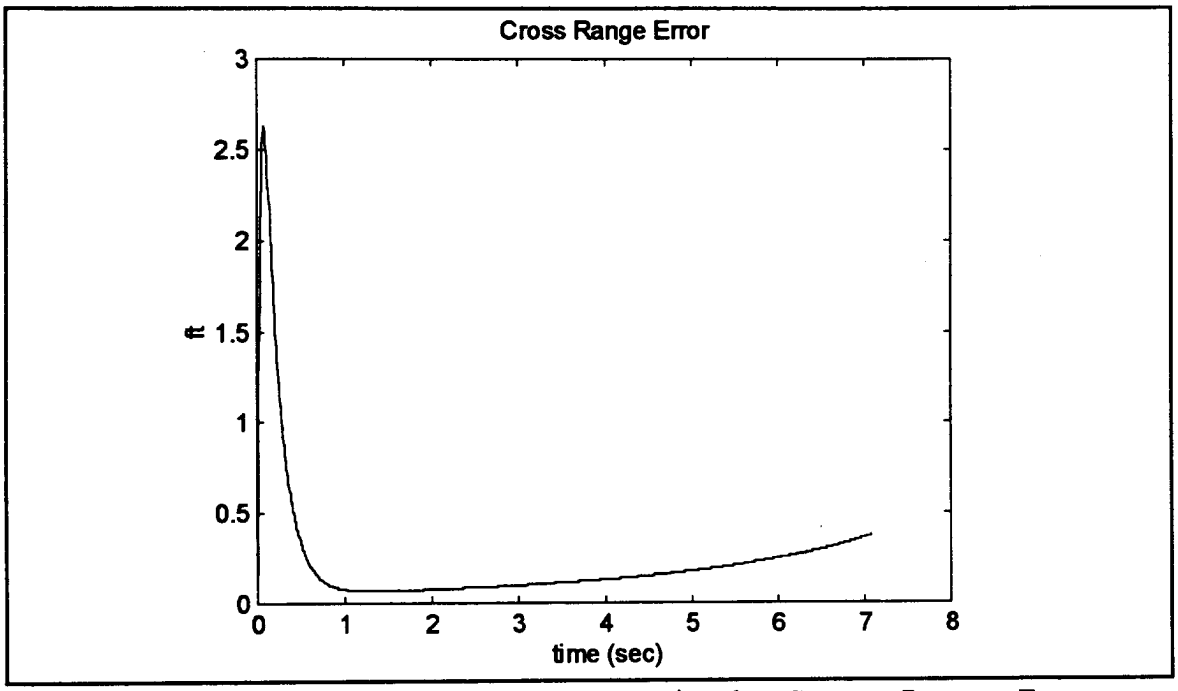

Figure 22. Command Guidance Scenario 1. Cross Range Error.

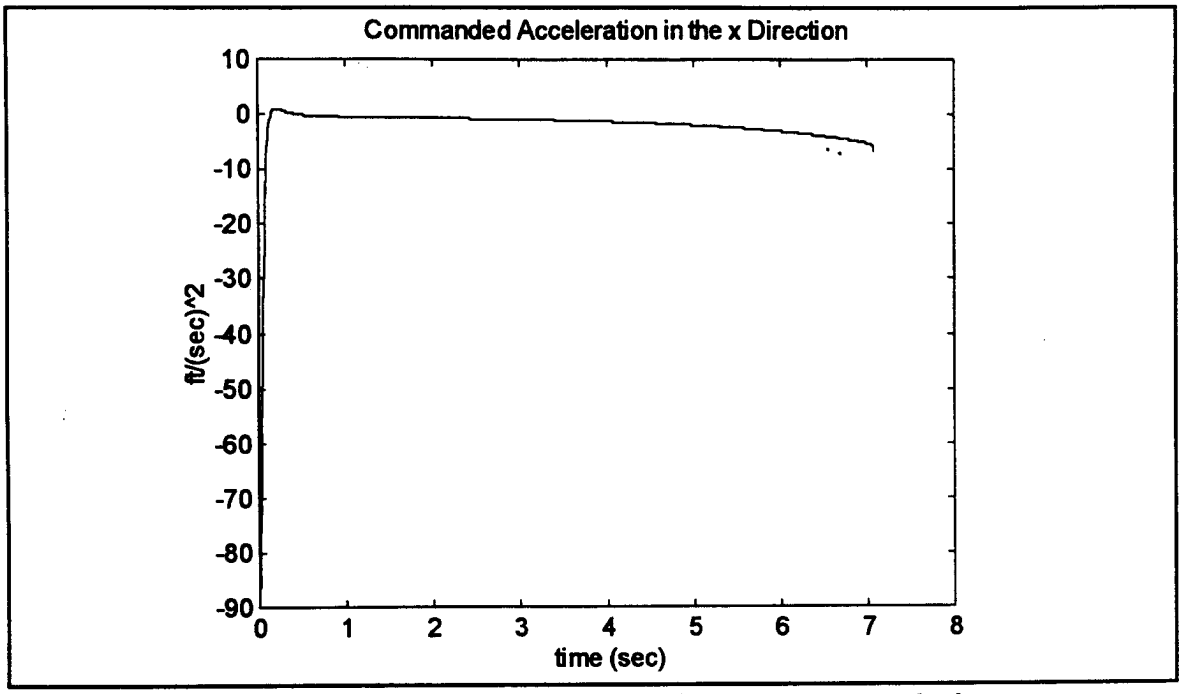

Figure 23. Command Guidance Scenario 1. Commanded Acceleration in the x Direction.

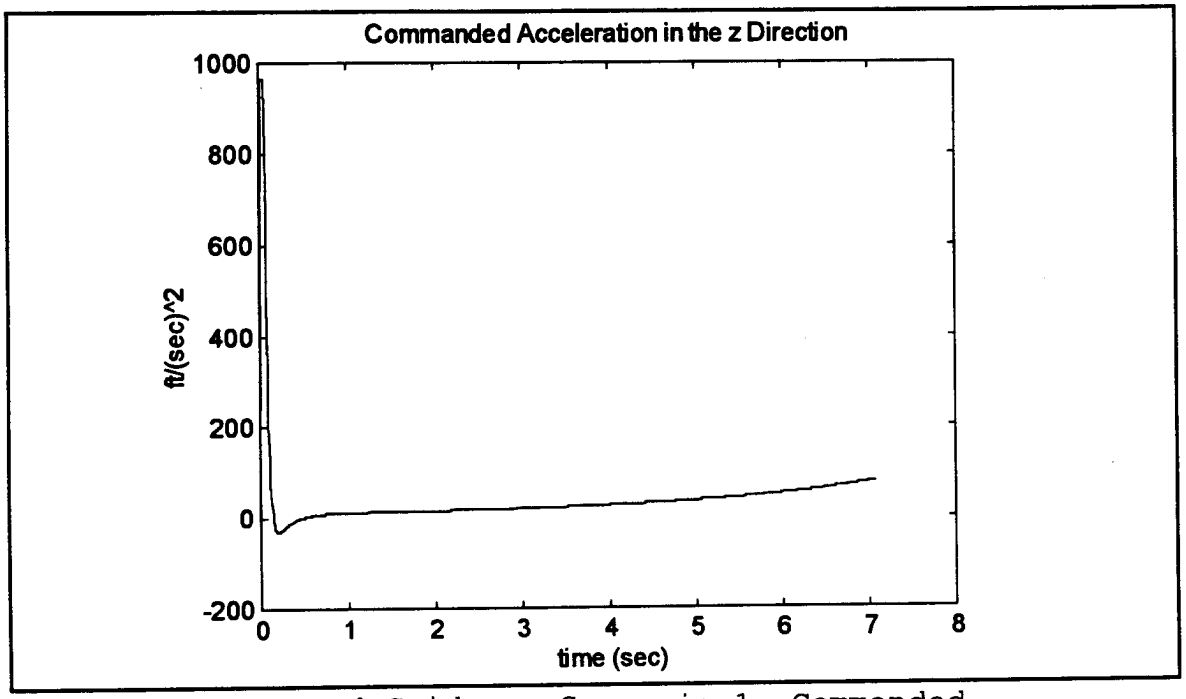

Figure 24. Command Guidance Scenario 1. Commanded Acceleration in the z Direction.

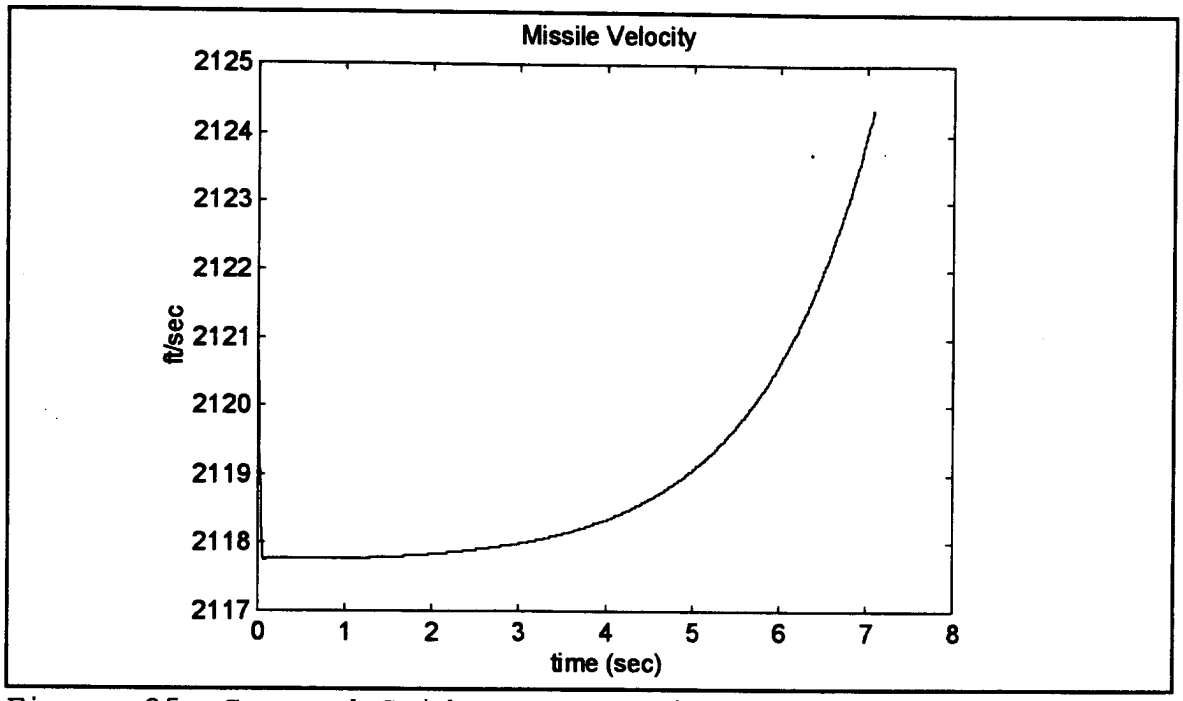

Figure 25. Command Guidance Scenario 1. Total Missile Velocity.

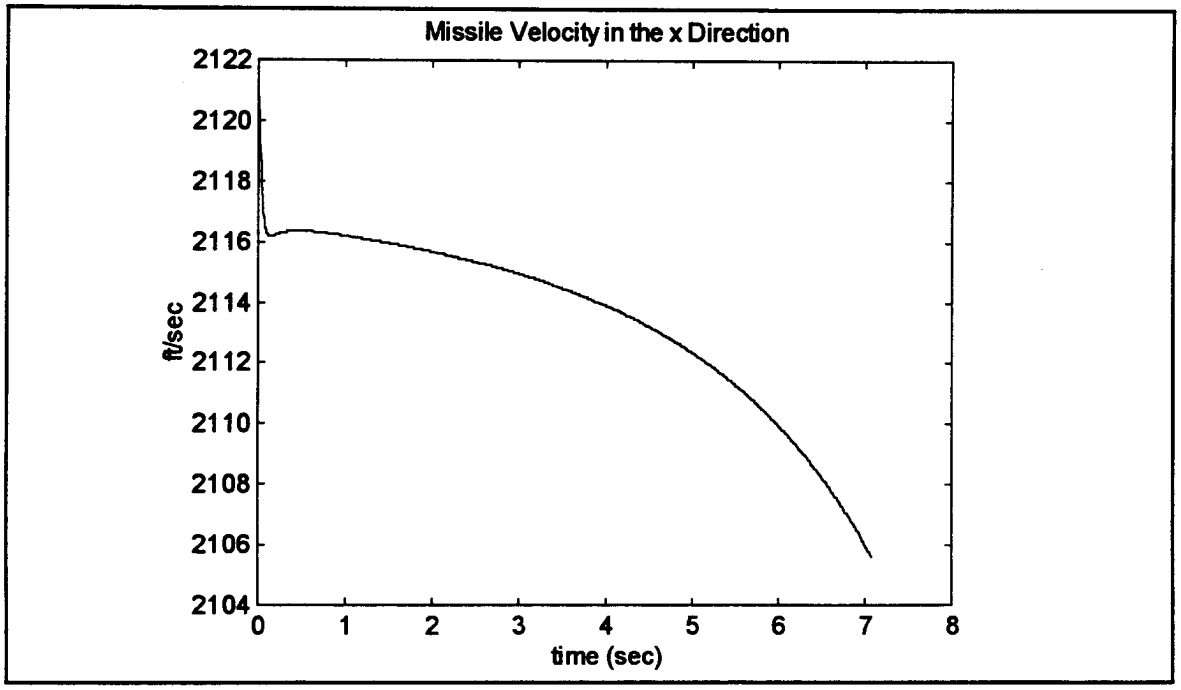

Figure 26. Command Guidance Scenario 1. Missile Velocity in the x Direction.

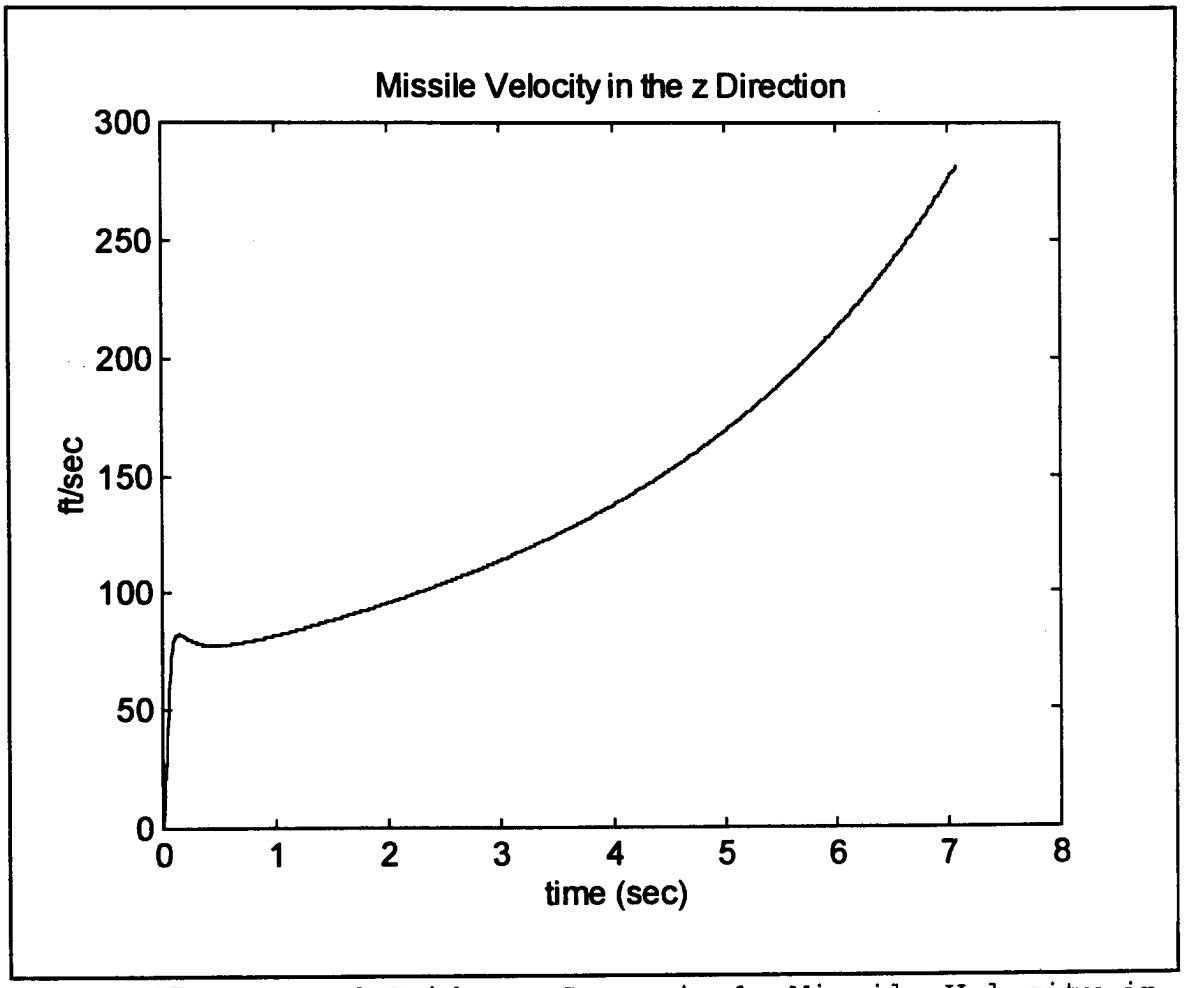

Figure 27. Command Guidance Scenario 1. Missile Velocity in the z Direction.

B. PROPORTIONAL NAVIGATION MISSILE PLOTS FOR SCENARIO 2

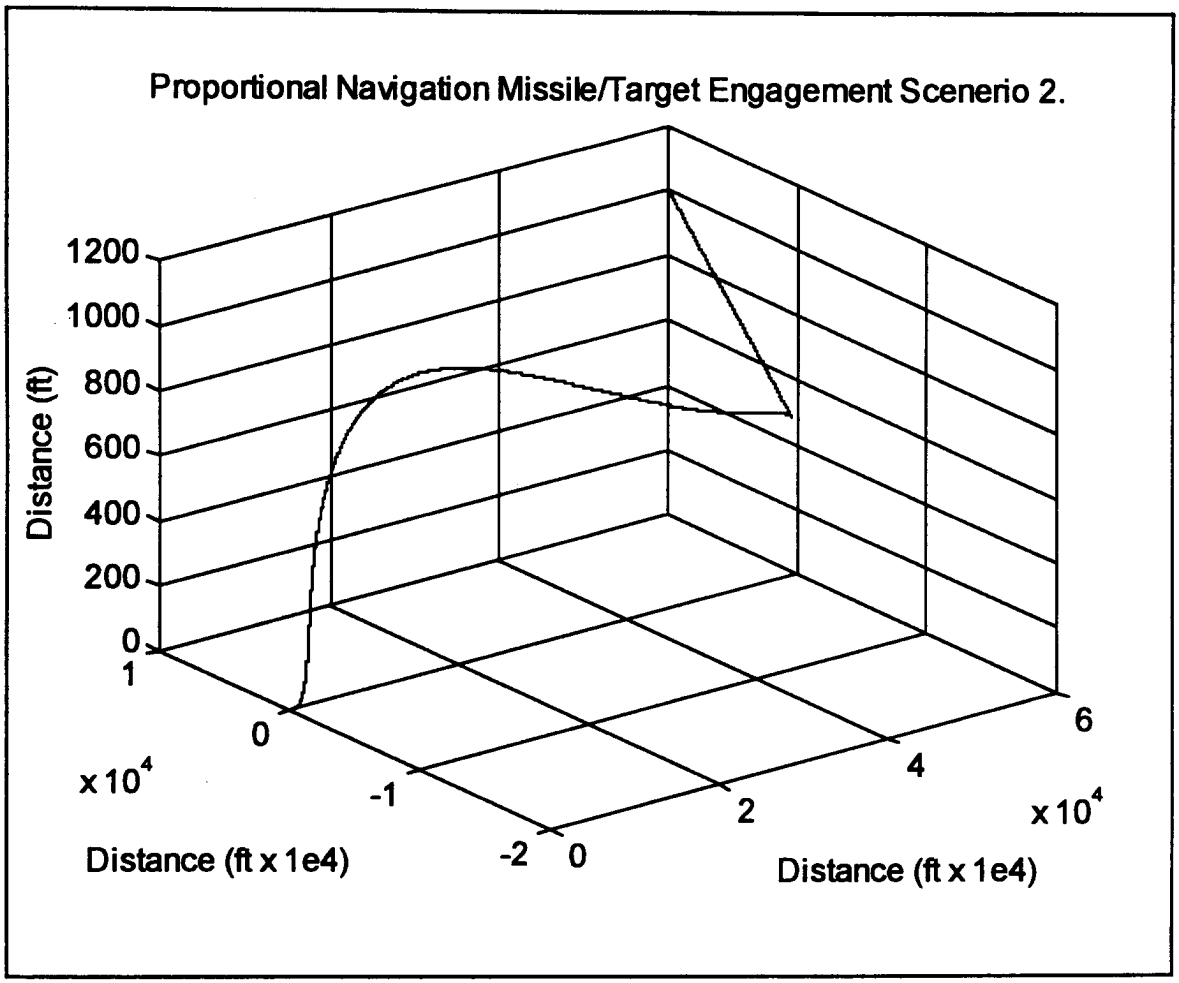

Figure 28. Proportional Navigation Scenario 2. Missile and Target Trajectories in Three Dimensions.

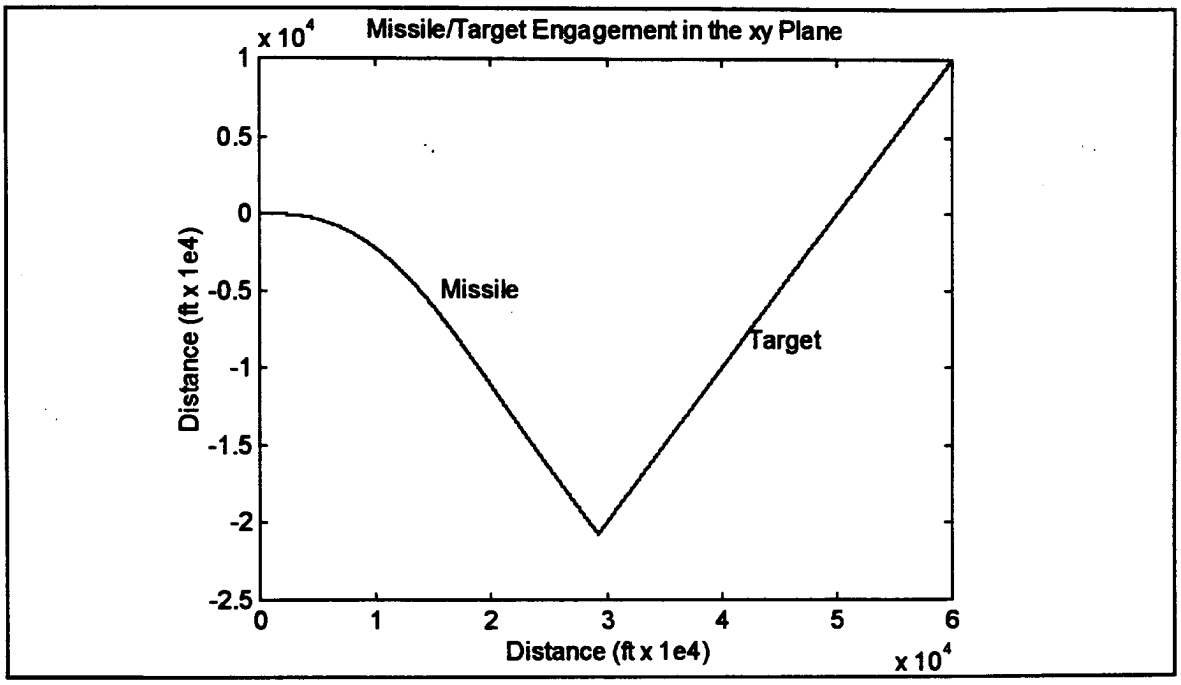

Figure 29. Proportional Navigation Scenario 2. Missile Target Trajectories in the xy Plane.

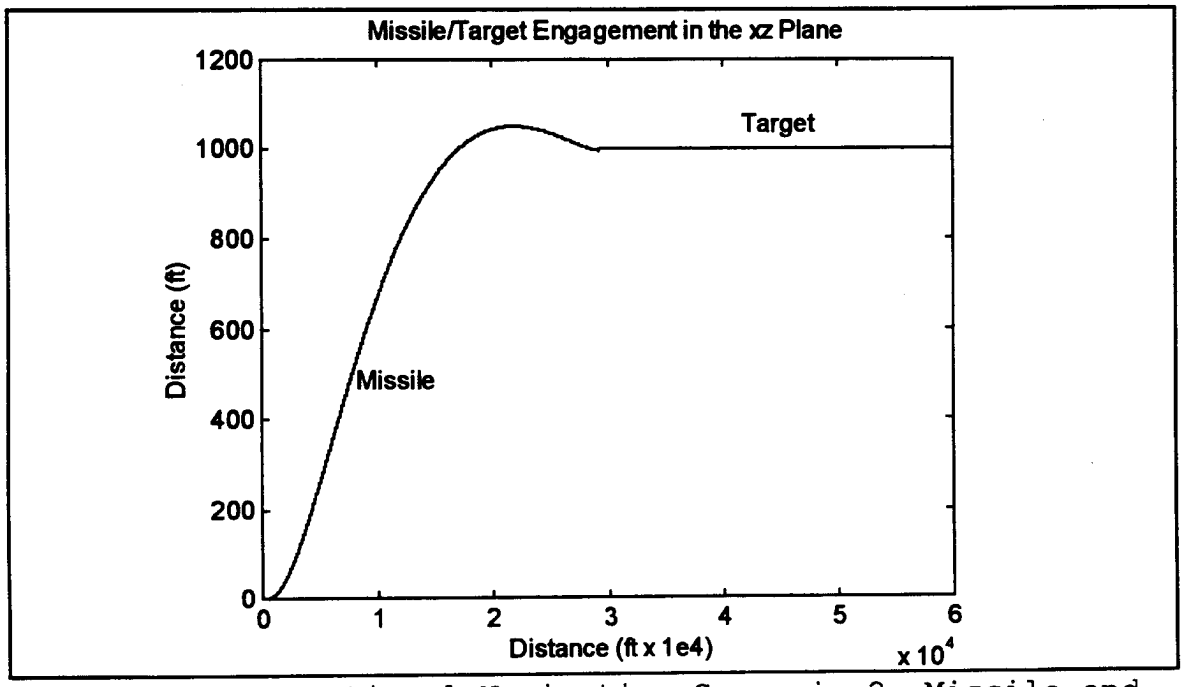

Figure 30. Proportional Navigation Scenario 2. Missile and Target Trajectories in the xz Plane.

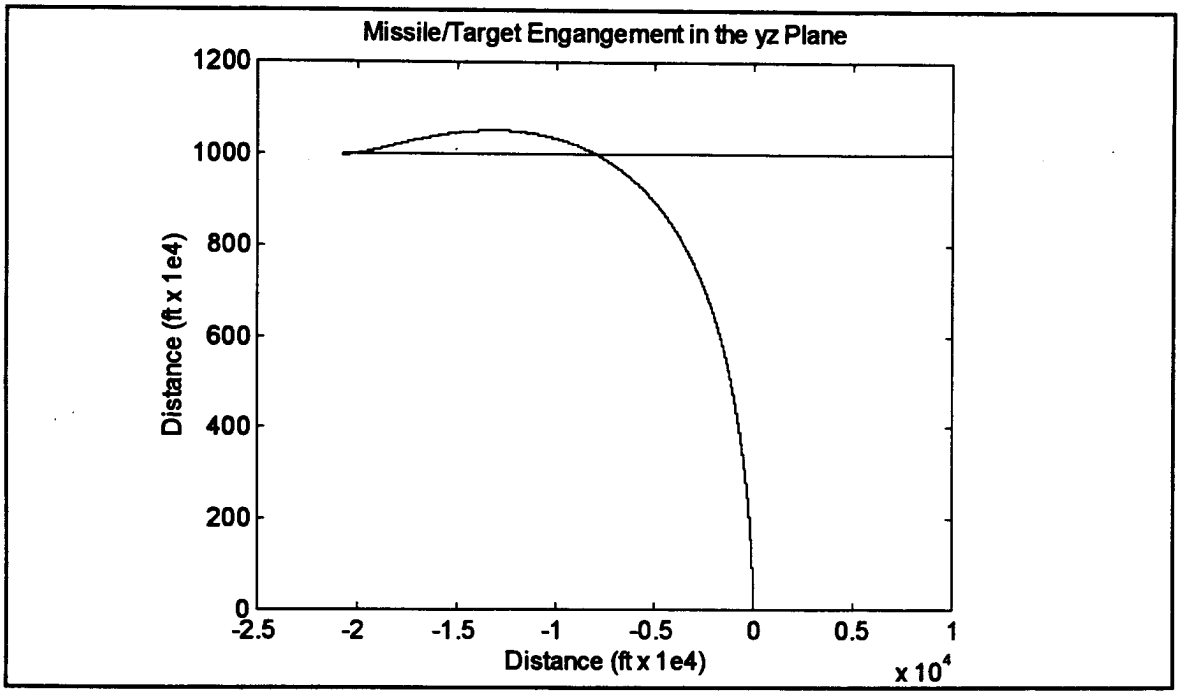

Figure 31. Proportional Navigation Scenario 2. Missile Target Trajectories in the yz Plane.

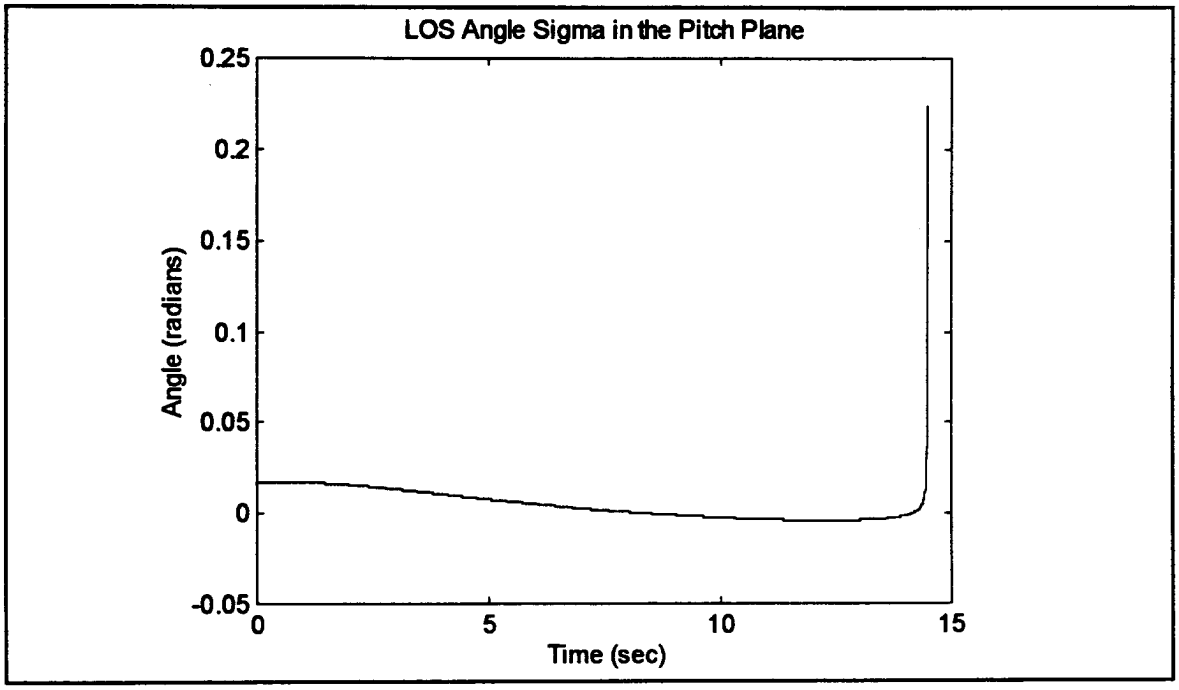

Figure 32. Proportional Navigation Scenario 2. LOS Angle σ_{pitch}.

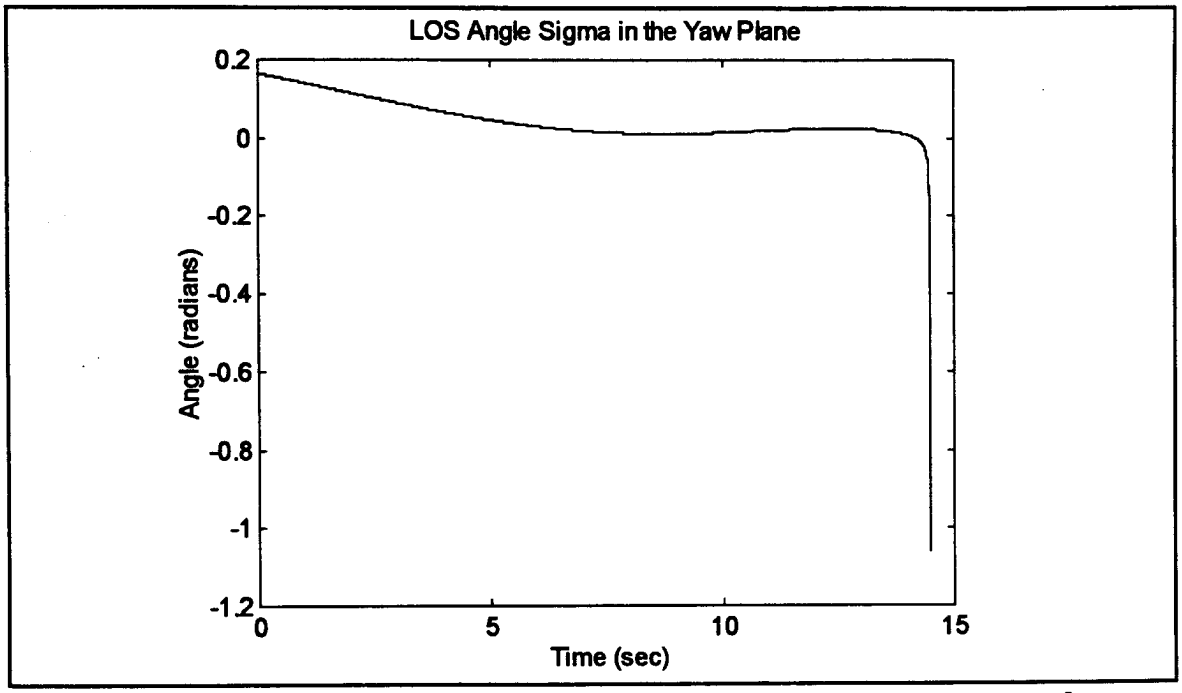

Figure 33. Proportional Navigation Scenario 2. LOS Angle σ_{yaw}.

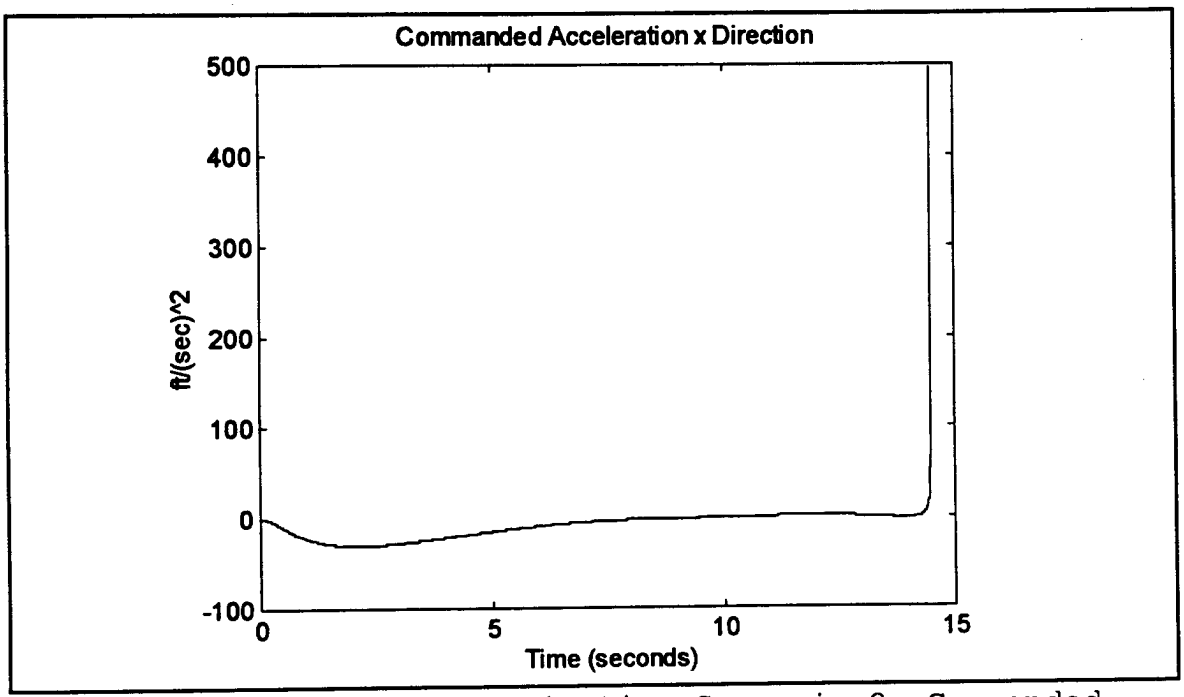

Figure 34. Proportional Navigation Scenario 2. Commanded Acceleration in the x Direction.

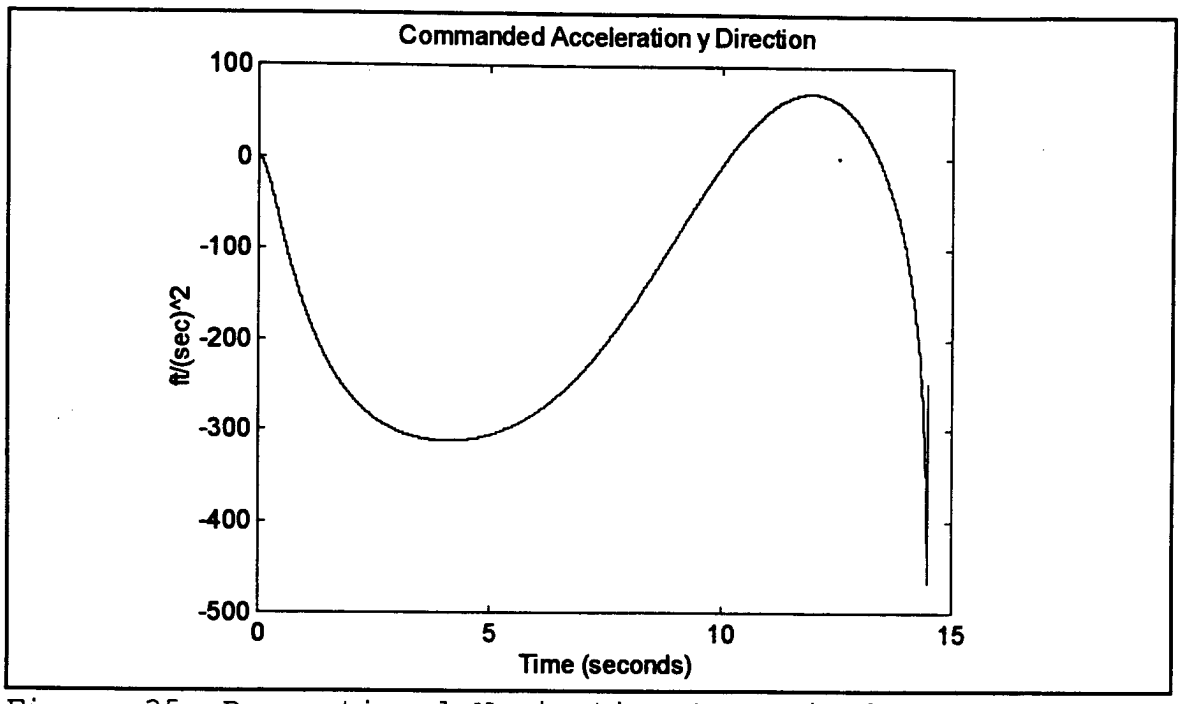

Figure 35. Proportional Navigation Scenario 2. Commanded Acceleration in the y Direction.

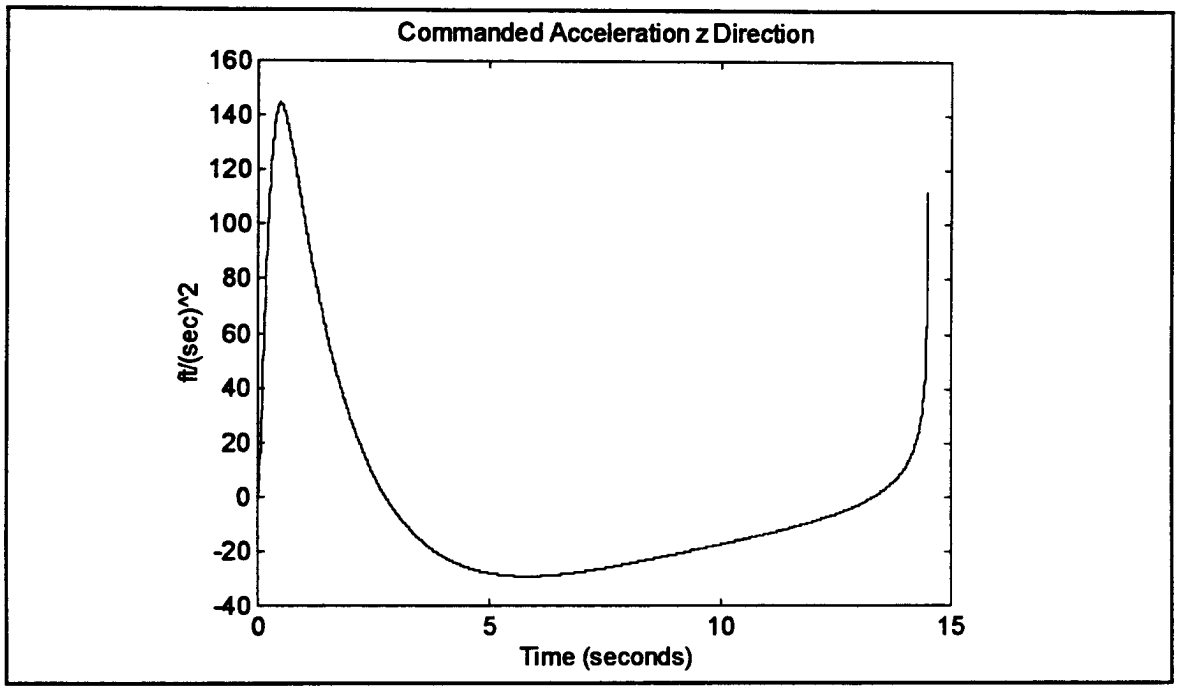

Figure 36. Proportional Navigation Scenario 2. Commanded Acceleration in the z Direction.

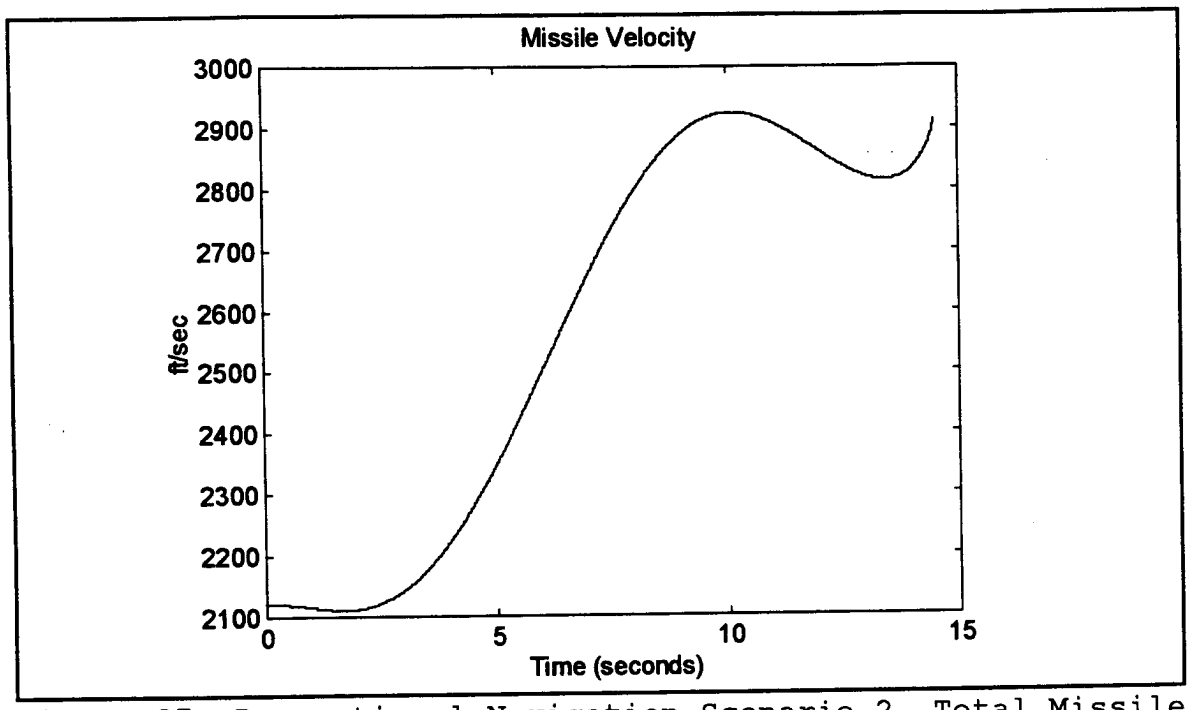

Figure 37. Proportional Navigation Scenario 2. Total Missile Velocity.

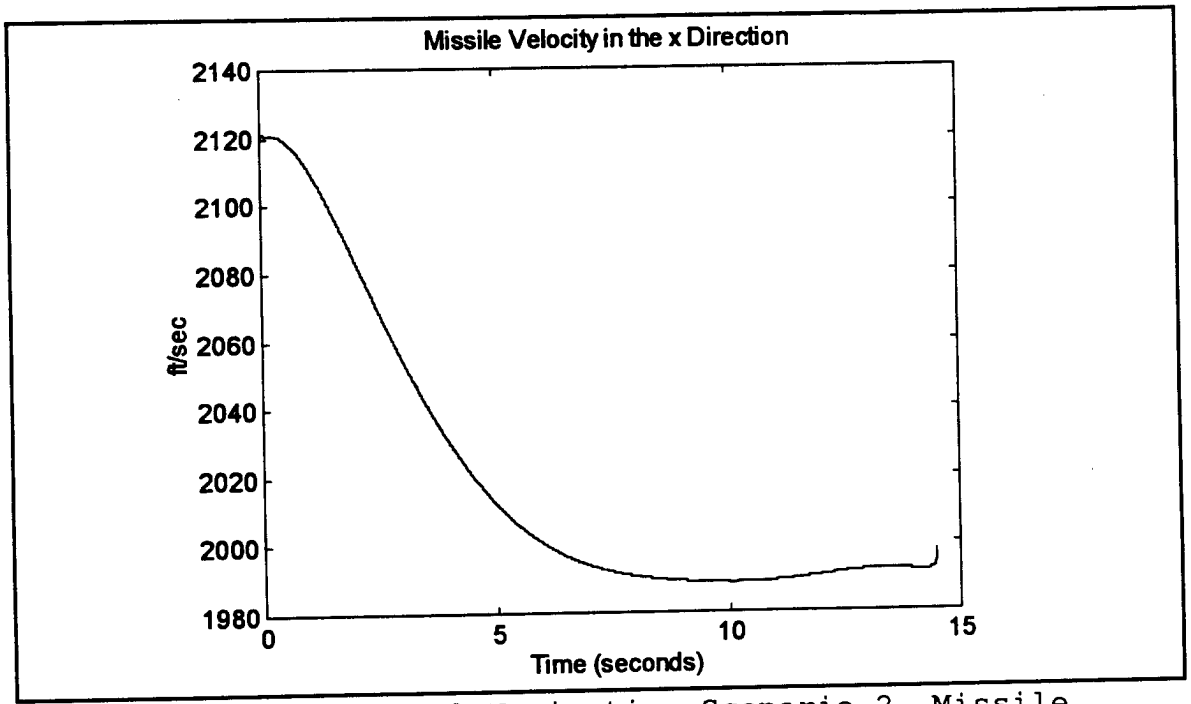

Figure 38. Proportional Navigation Scenario 2. Missile Velocity in the x Direction.

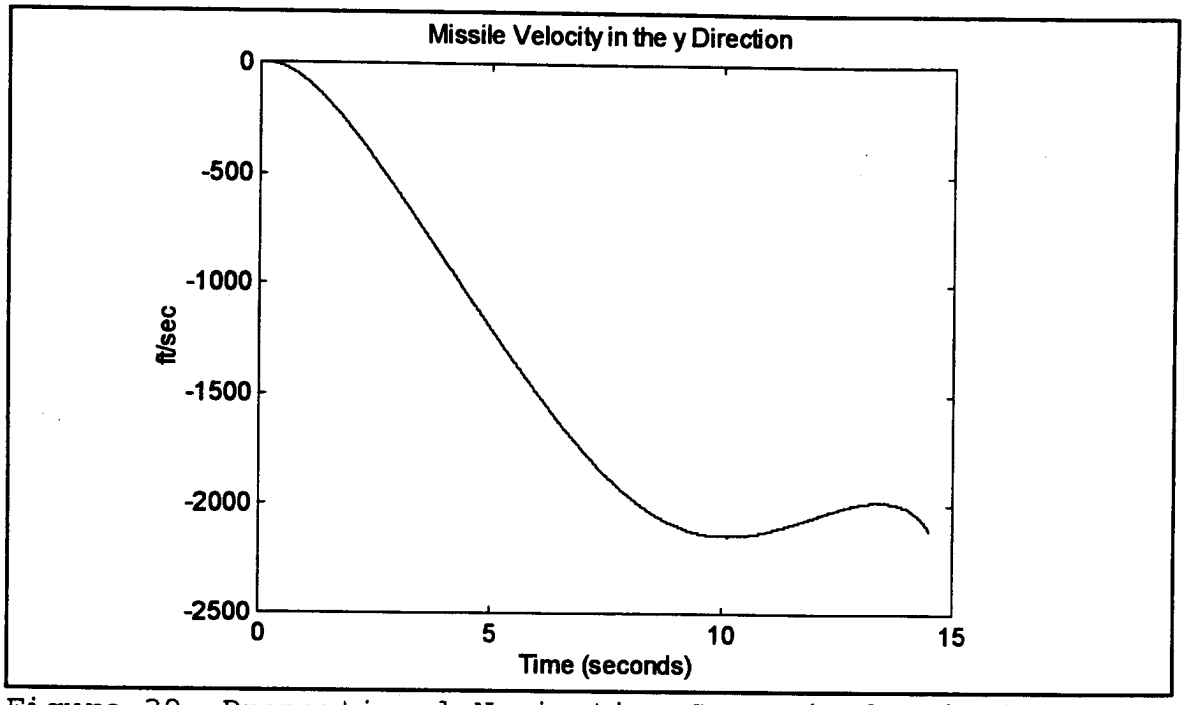

Figure 39. Proportional Navigation Scenario 2. Missile Velocity in the y Direction.

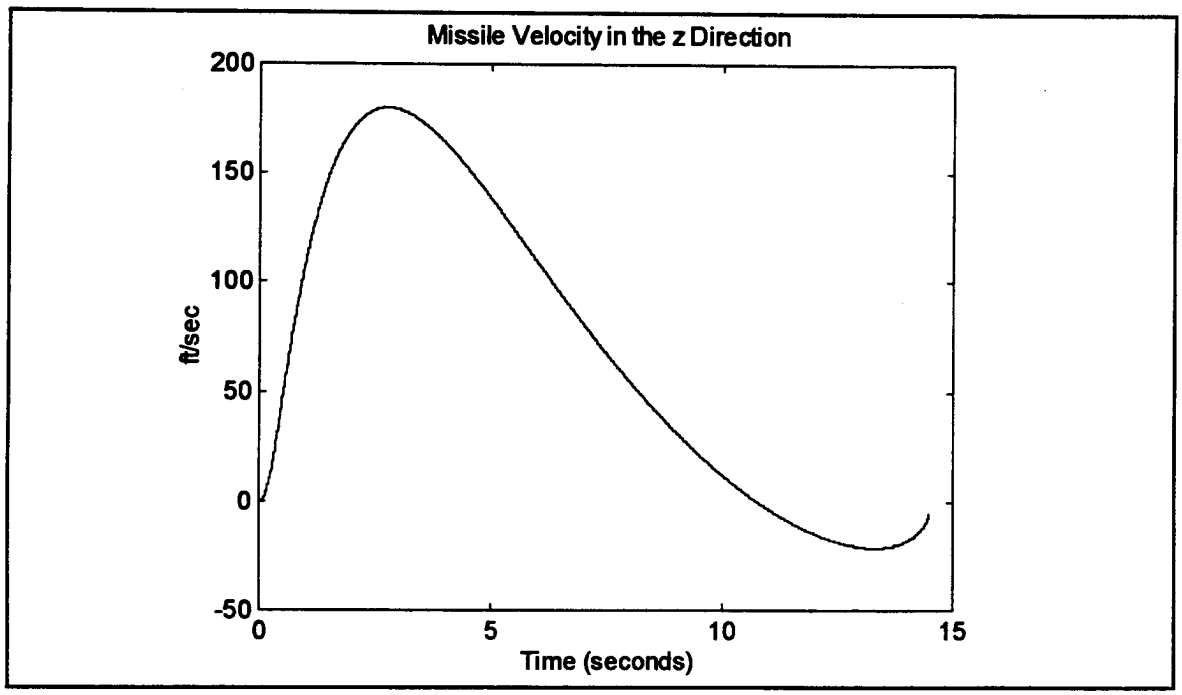

Figure 40. Proportional Navigation Scenario 2. Missile Velocity in the z Direction.

C. COMMAND GUIDED MISSILE PLOTS FOR SCENARIO 2

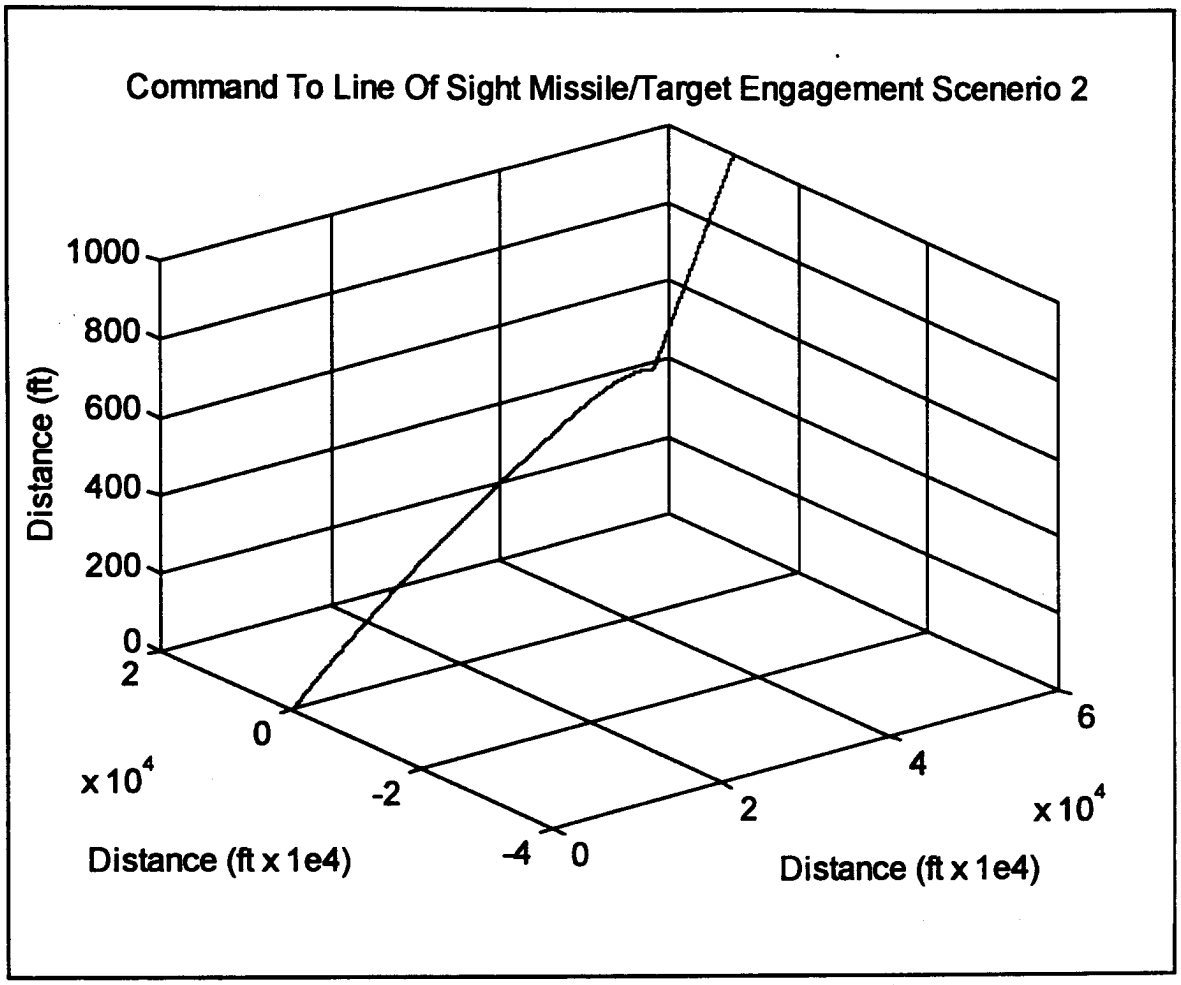

Figure 41. Command Guidance Scenario 2. Missile Target Engagement.

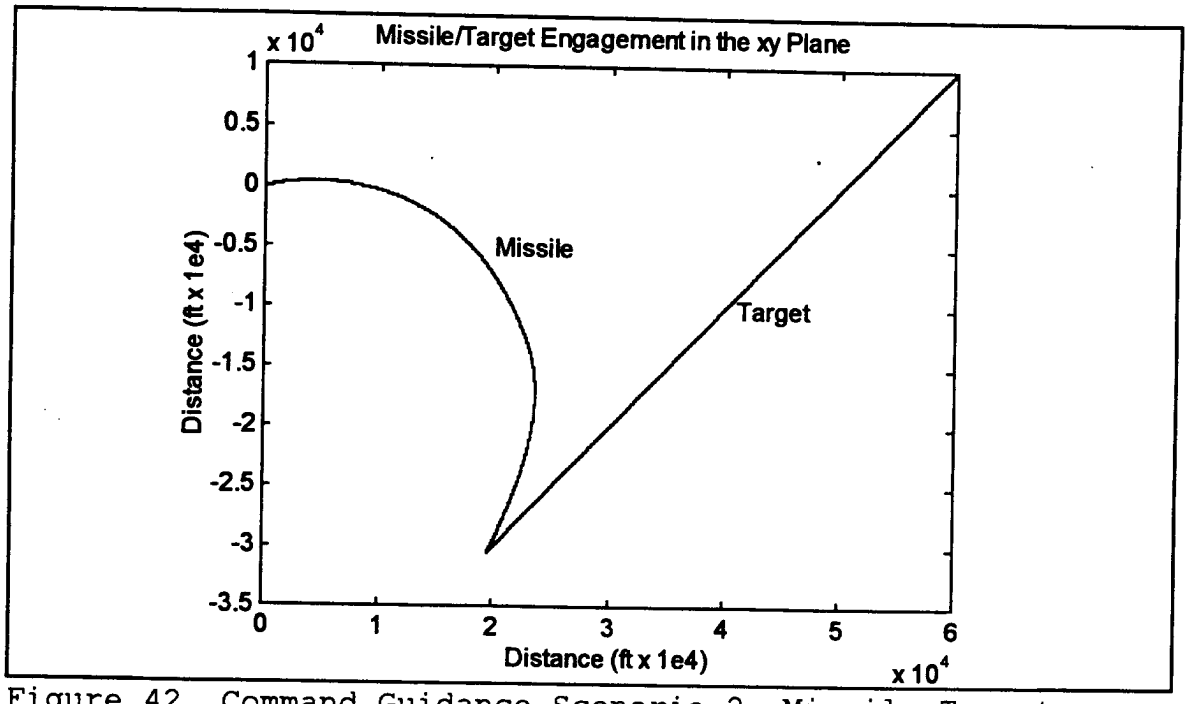

Figure 42. Command Guidance Scenario 2. Missile Target Trajectories in the xy Plane.

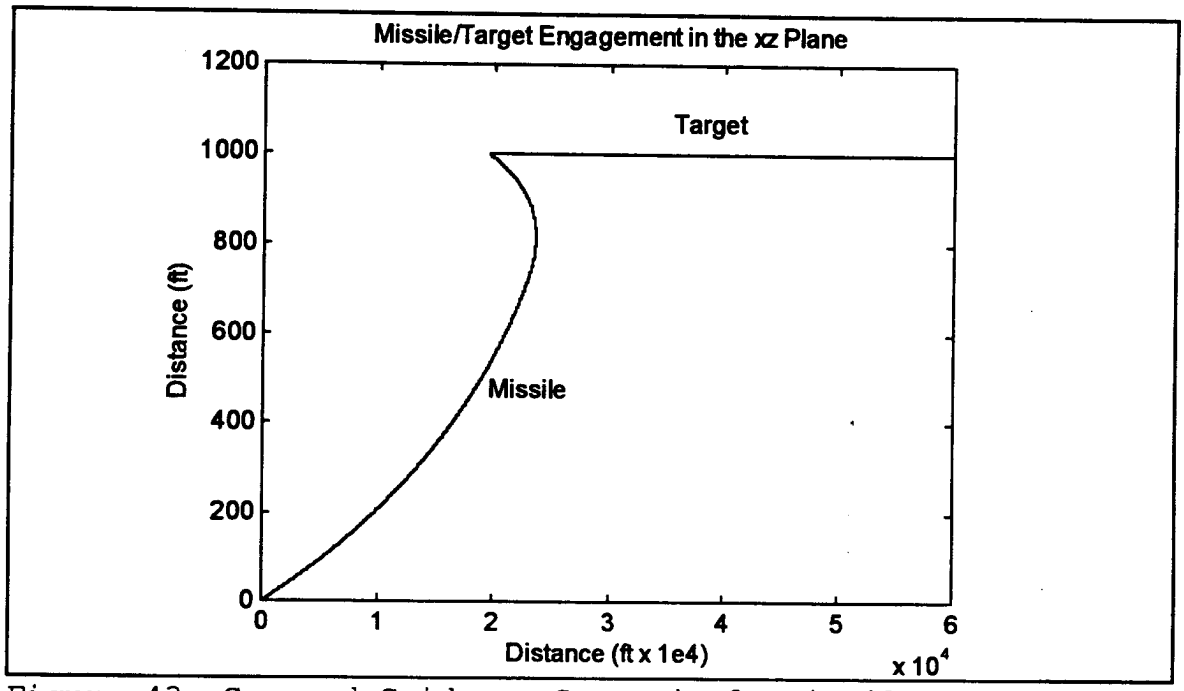

Figure 43. Command Guidance Scenario 2. Missile Target Trajectories in the xz Plane.

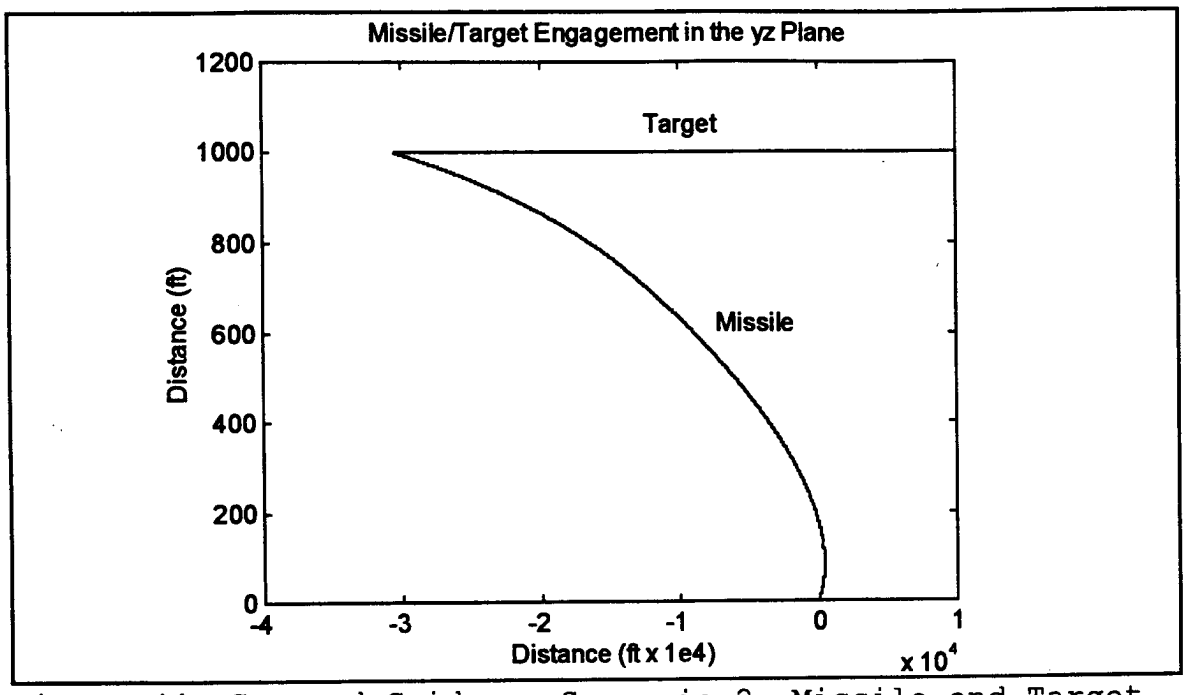

Figure 44. Command Guidance Scenario 2. Missile and Target Trajectories in the yz Plane.

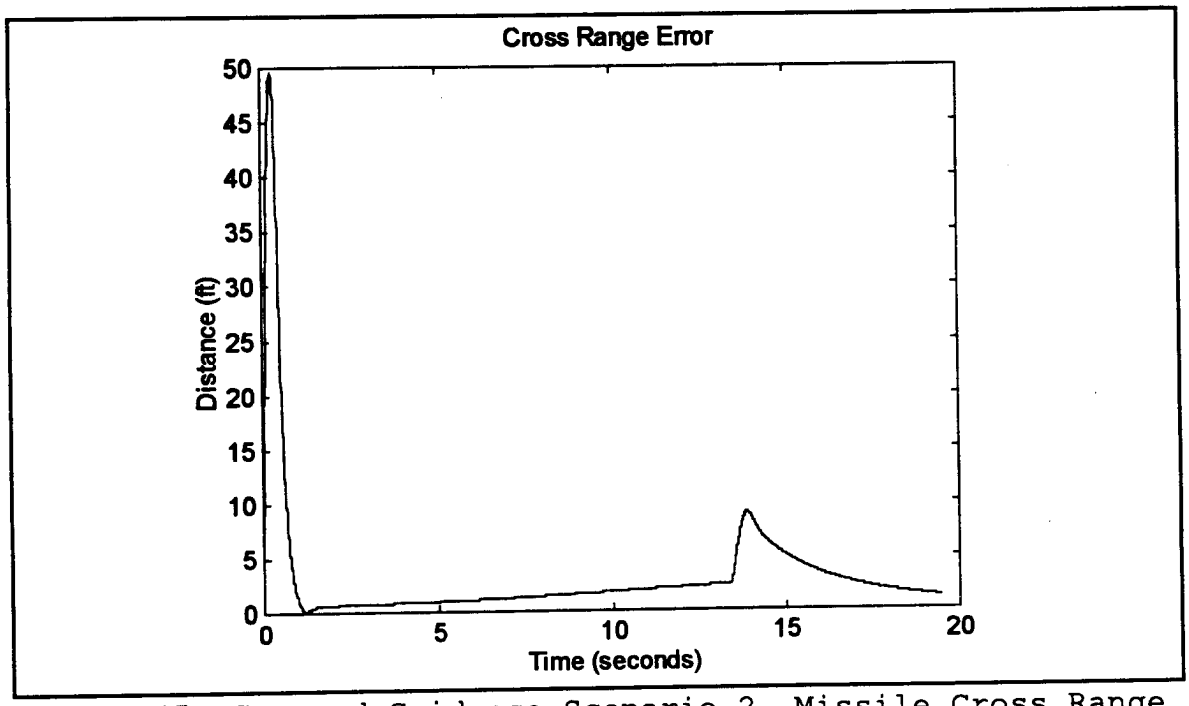

Figure 45. Command Guidance Scenario 2. Missile Cross Range Error.

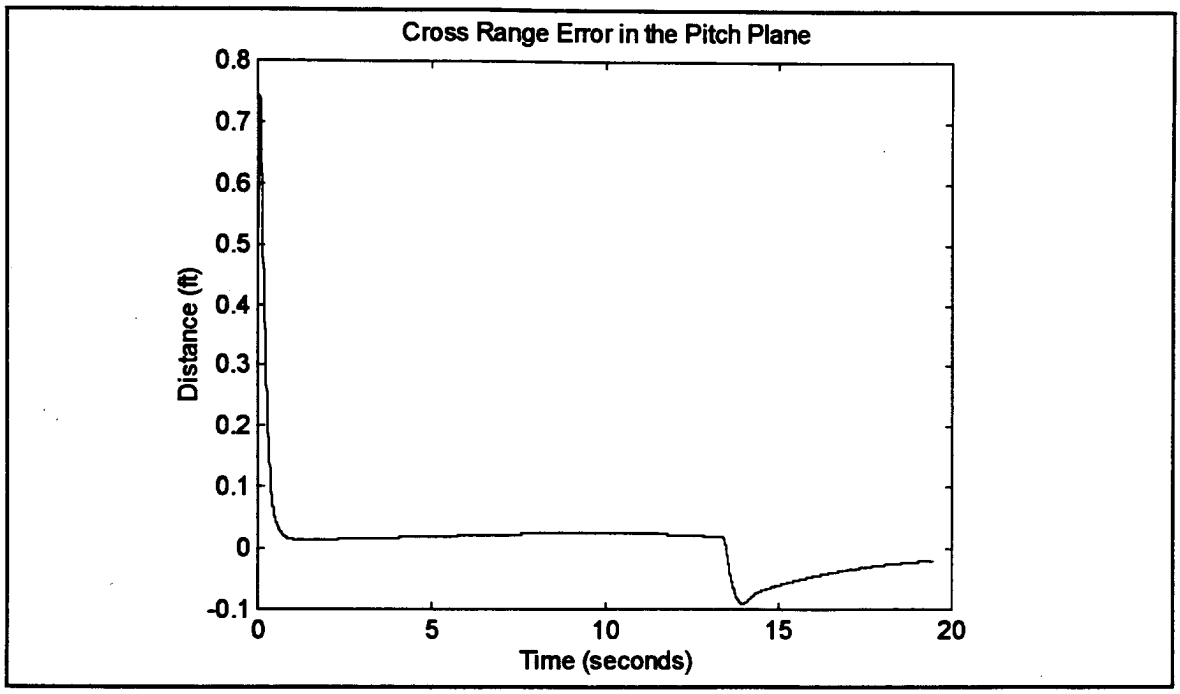

Figure 46. Command Guidance Scenario 2. Cross Range Error in the Pitch Plane.

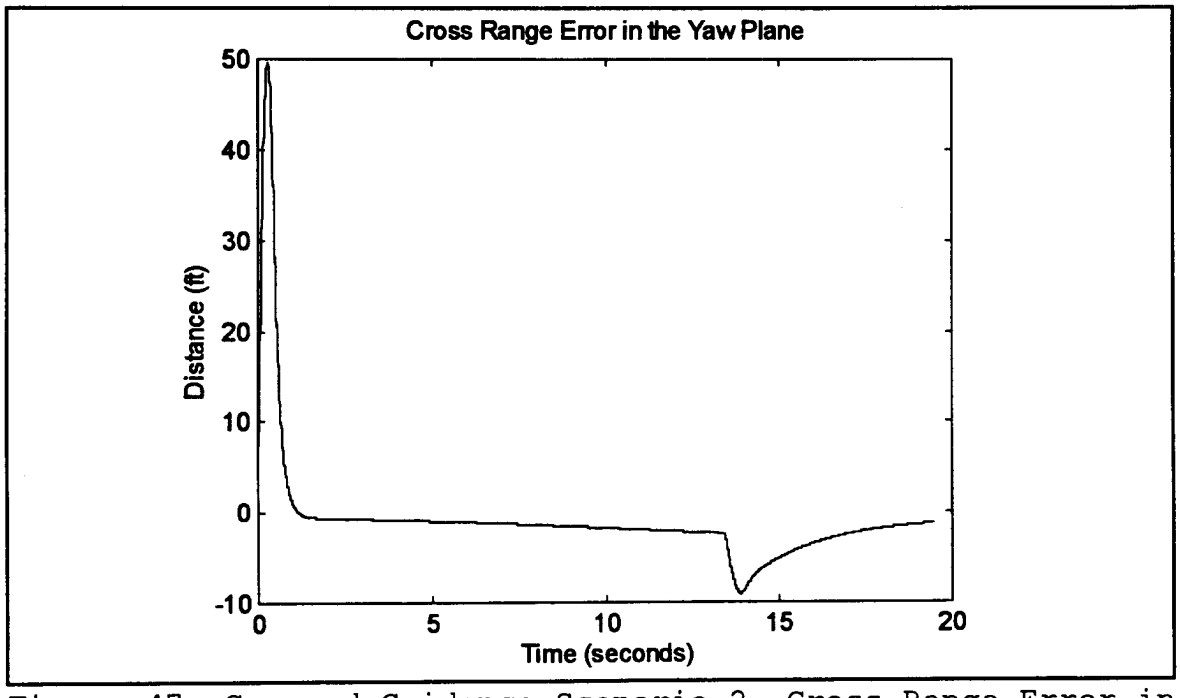

Figure 47. Command Guidance Scenario 2. Cross Range Error in the Yaw Plane.

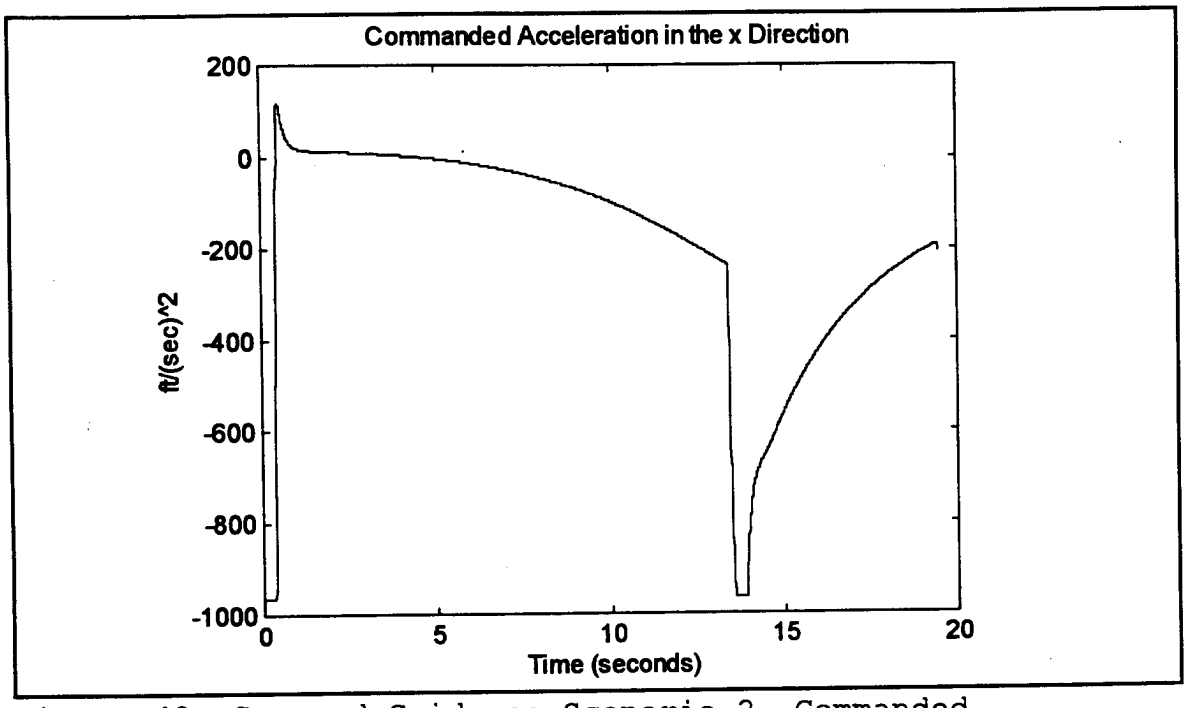

Figure 48. Command Guidance Scenario 2. Commanded Acceleration in the x Direction.

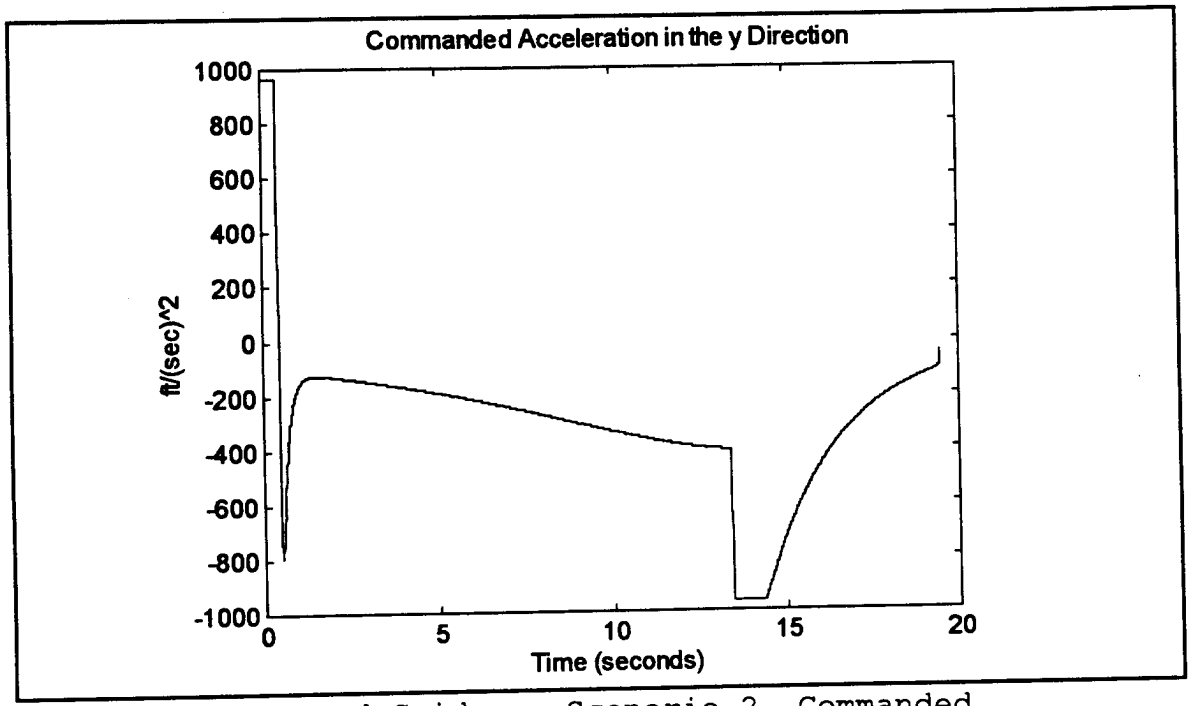

Figure 49. Command Guidance Scenario 2. Commanded Acceleration in the y Direction.

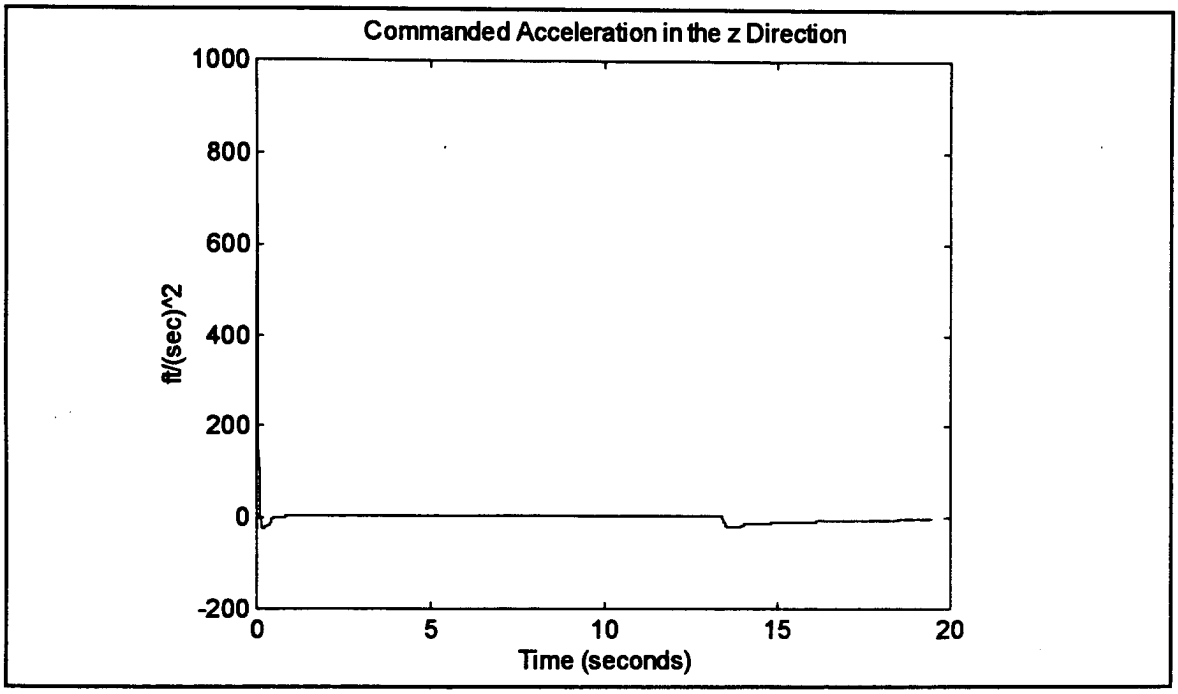

Figure 50. Command Guidance Scenario 2. Commanded Acceleration in the z Direction.

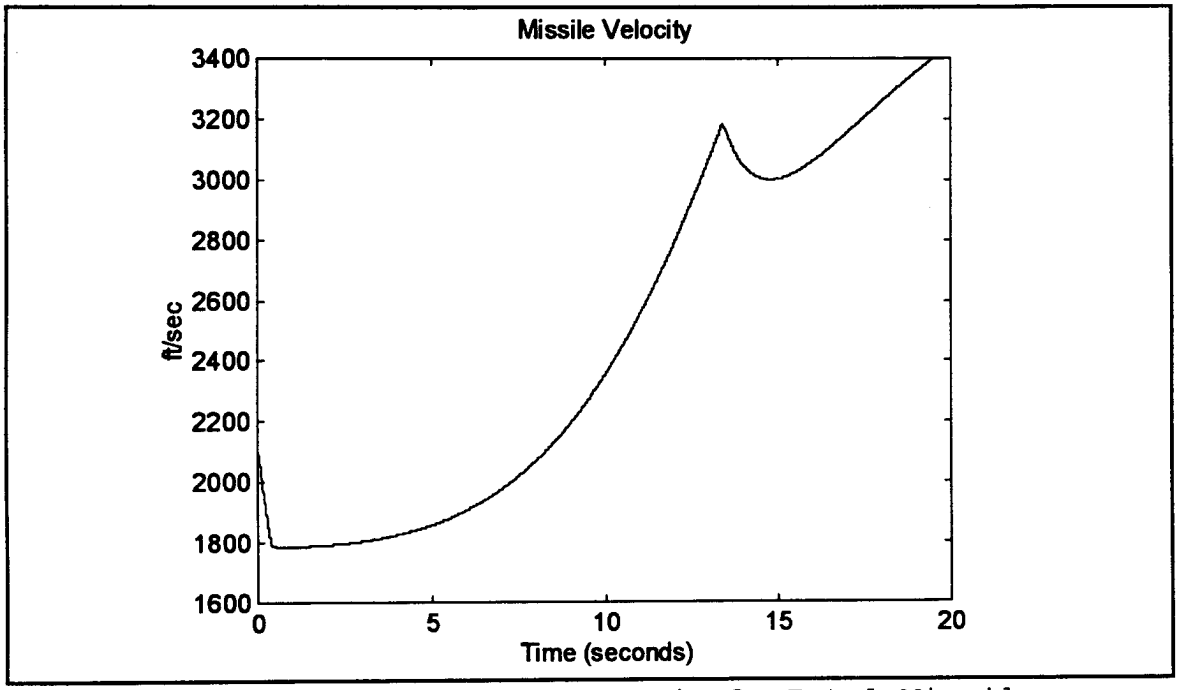

Figure 51. Command Guidance Scenario 2. Total Missile Velocity.

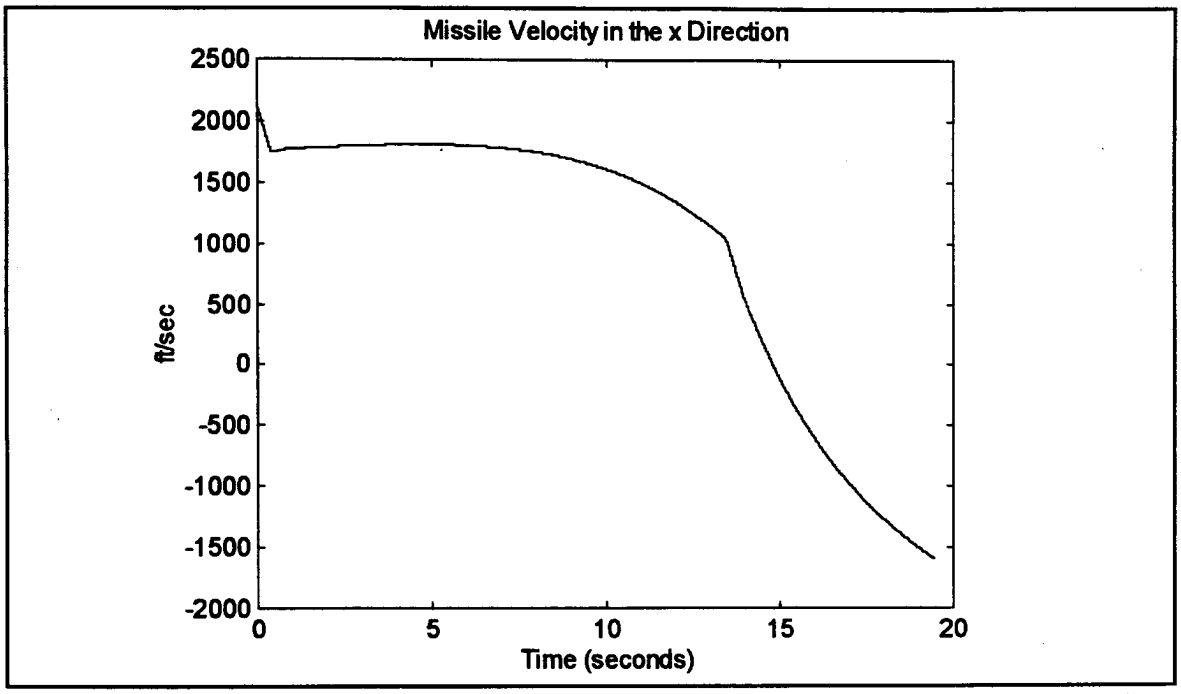

Figure 52. Command Guidance Scenario 2. Missile Velocity in the x Direction.

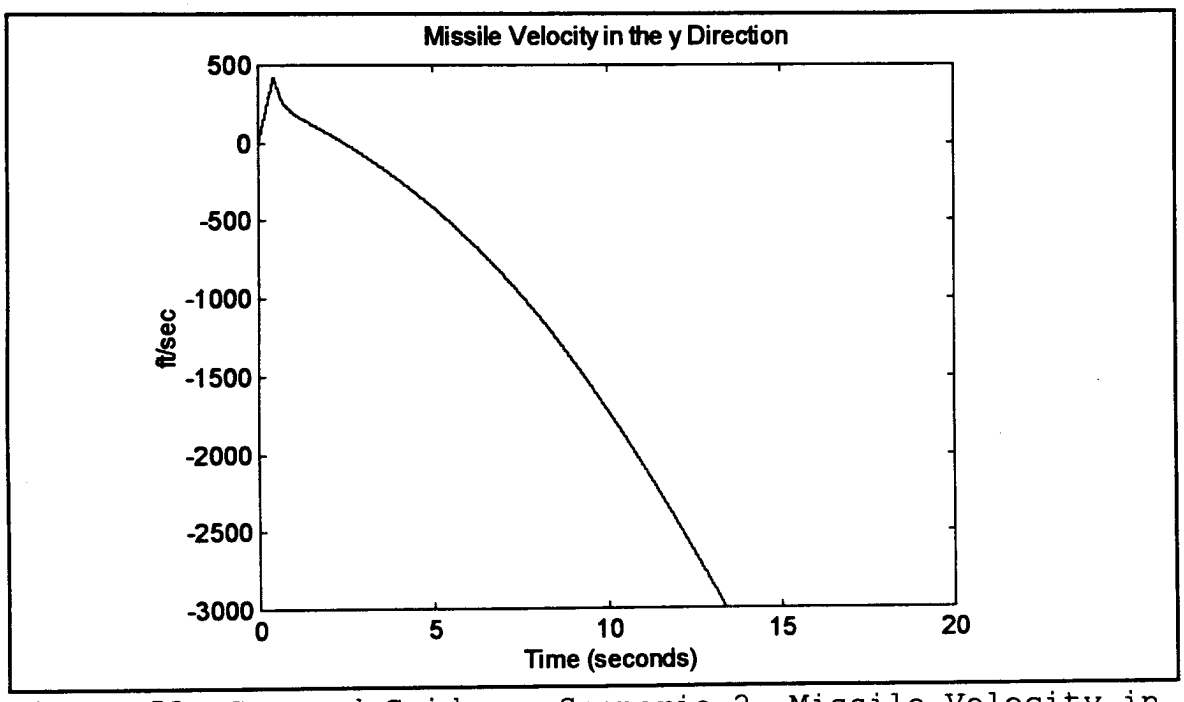

Figure 53. Command Guidance Scenario 2. Missile Velocity in the y Direction.

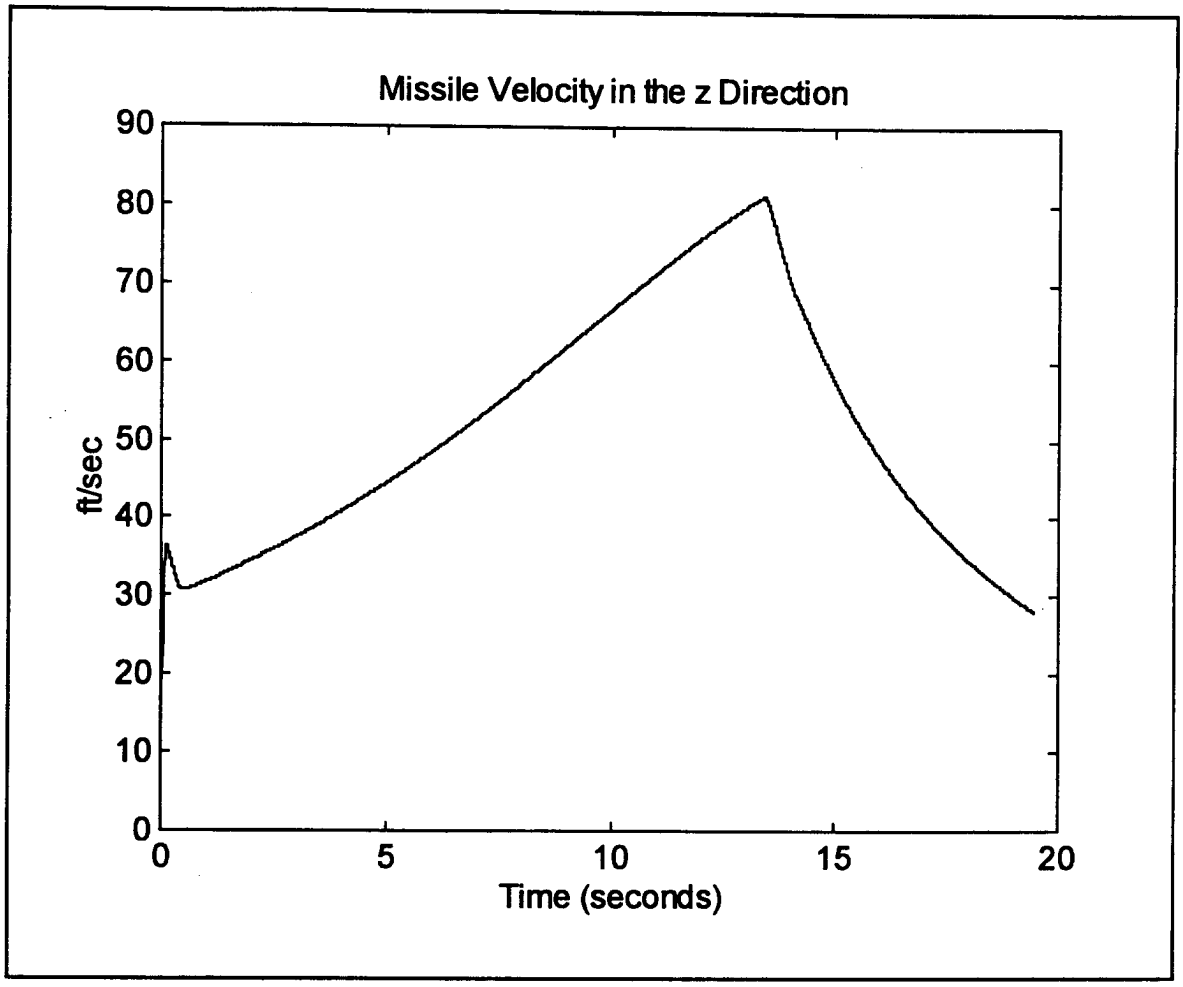

Figure 54. Command To Line Sight Scenario 2. Missile Velocity in the z Direction.

D. PROPORTIONAL NAVIGATION MISSILE PLOTS FOR SCENARIO 3

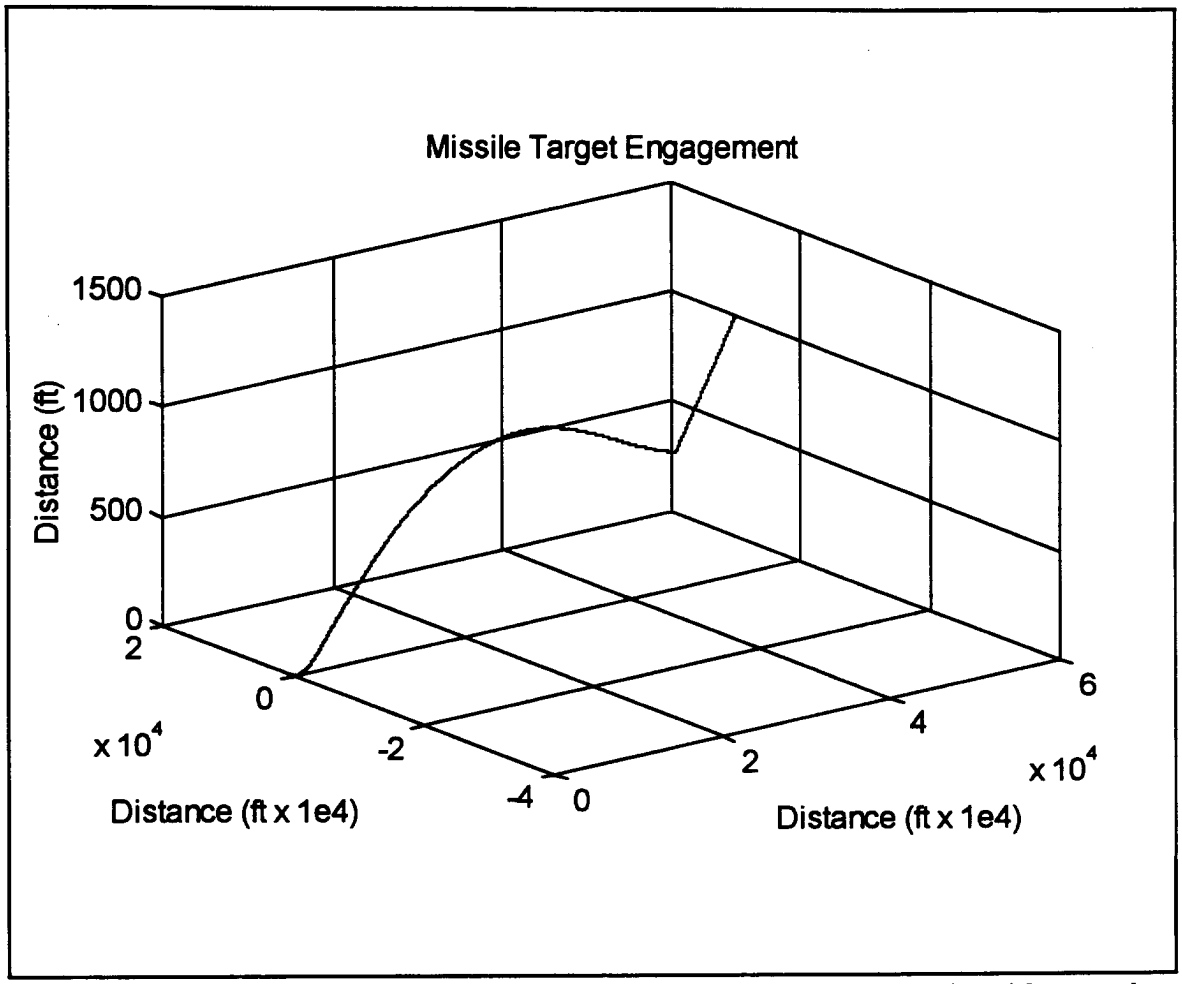

Figure 55. Proportional Navigation Scenario 3. Missile and Actual Target Trajectory.

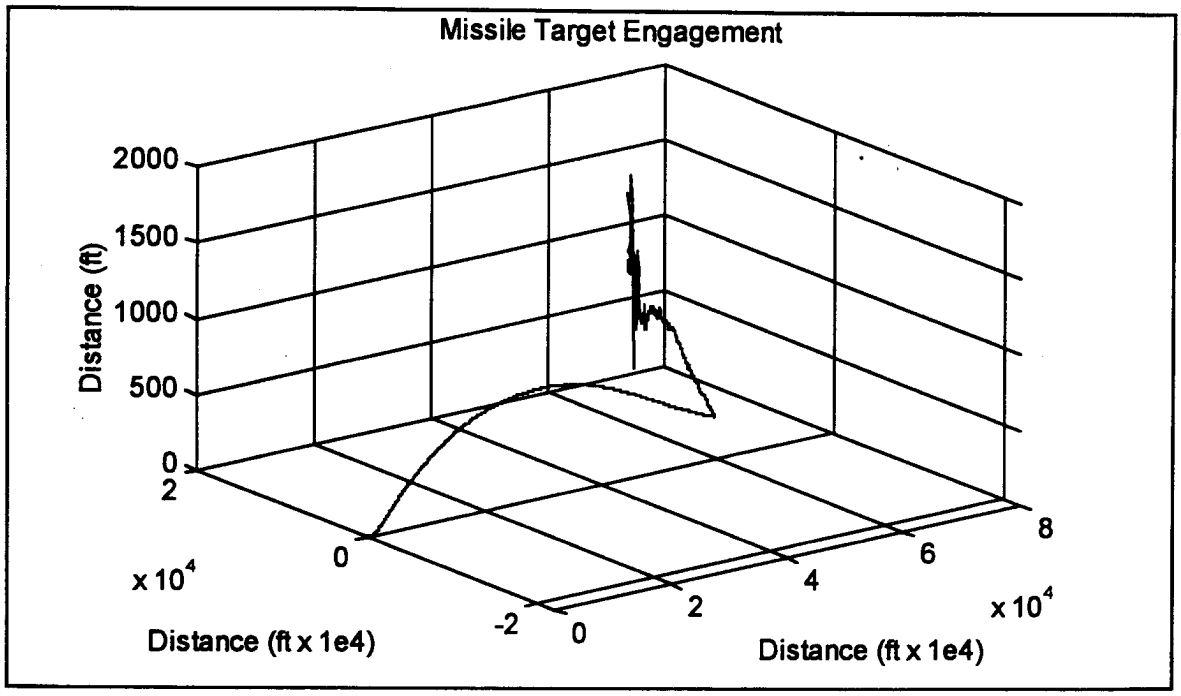

Figure 56. Proportional Navigation Scenario 3. Missile and Filtered Target Trajectory.

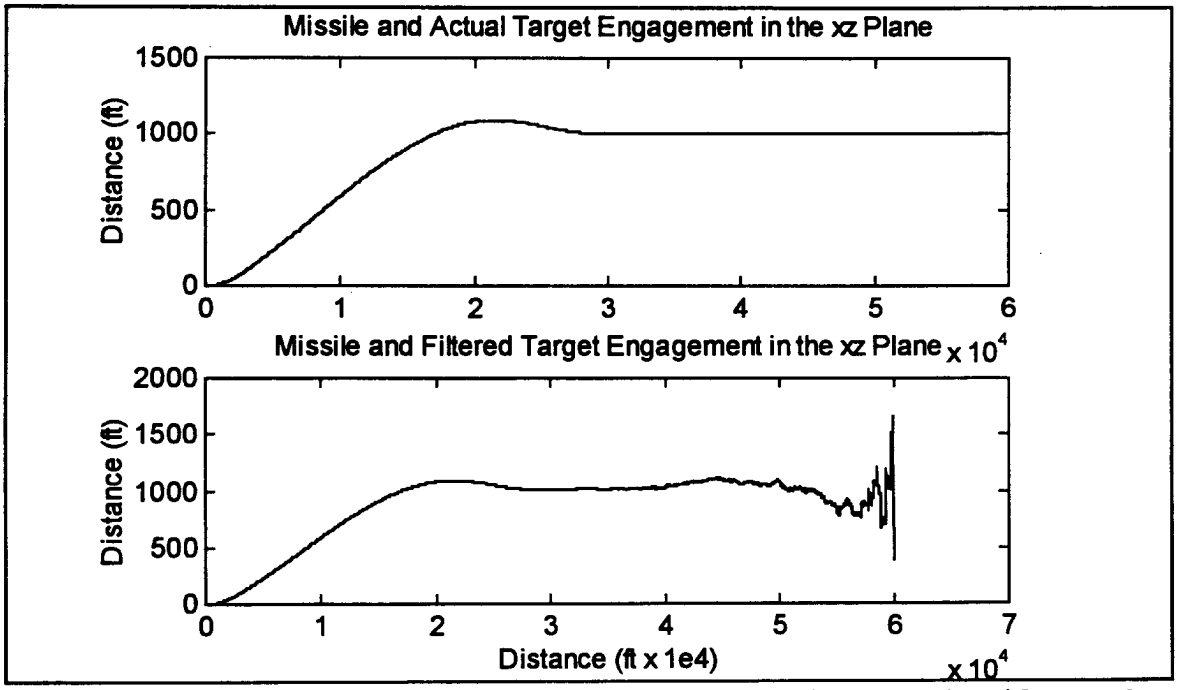

Figure 57. Proportional Navigation Scenario 3. Missile and Target Trajectories in the xz Plane.

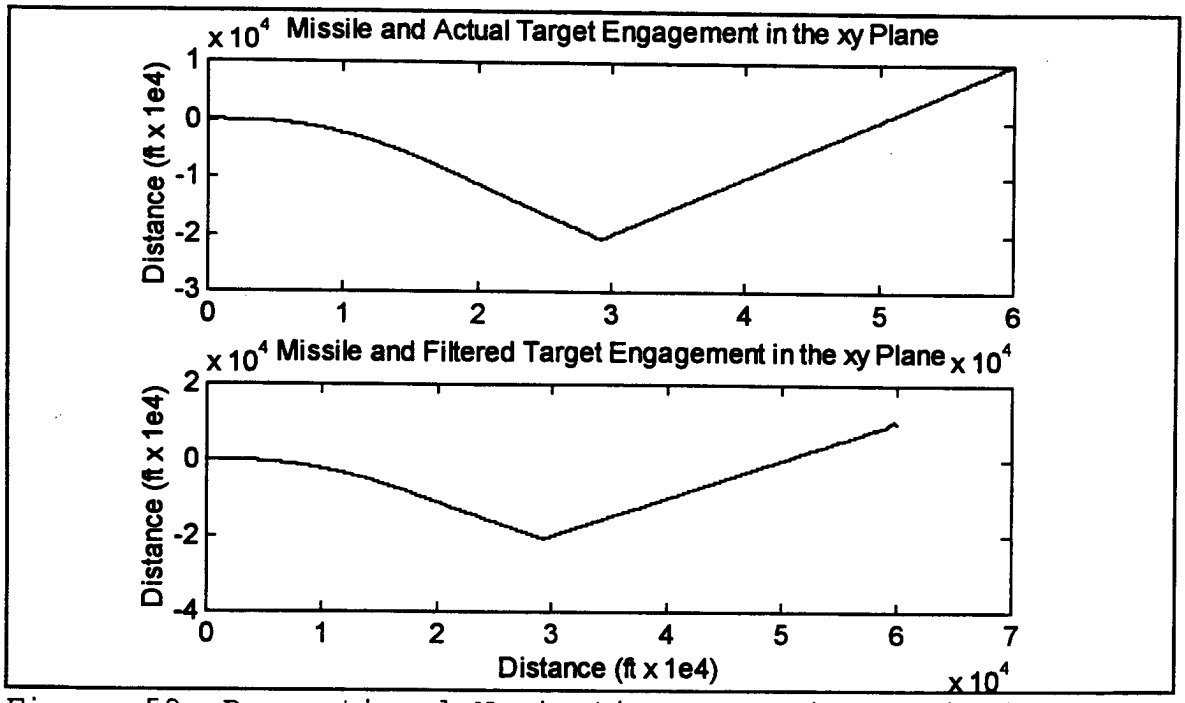

Figure 58. Proportional Navigation Scenario 3. Missile and Target Trajectories in the xy Plane.

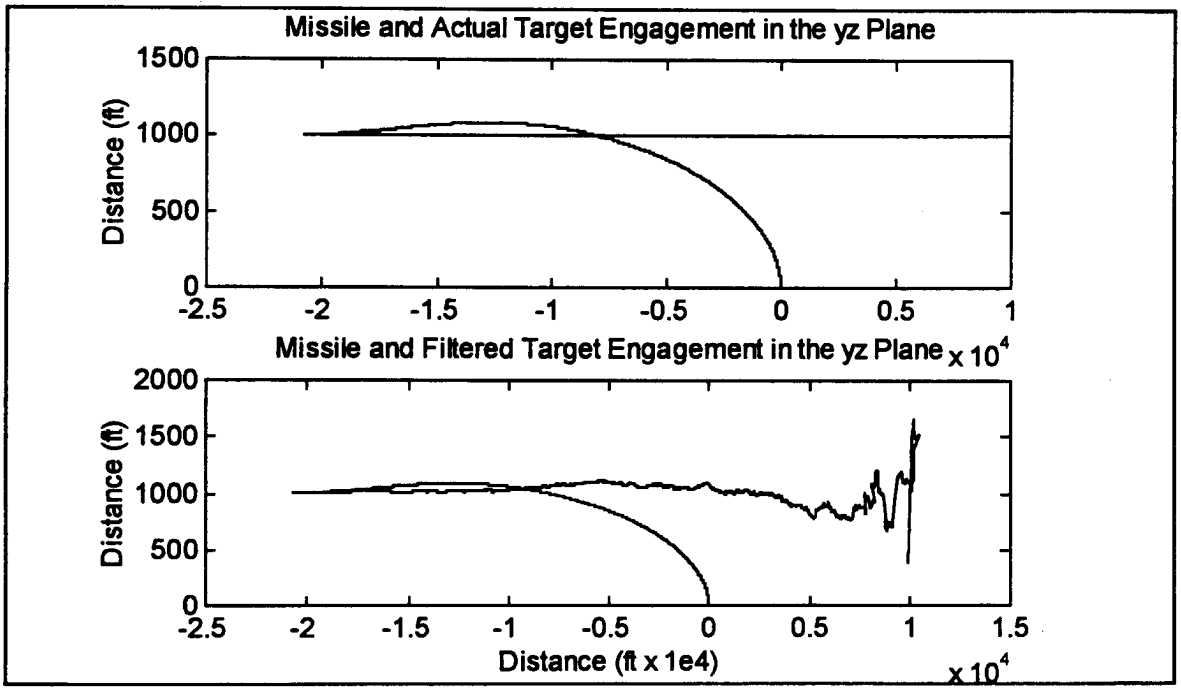

Figure 59. Proportional Navigation Scenario 3. Missile and Target Trajectories in the yz Plane.

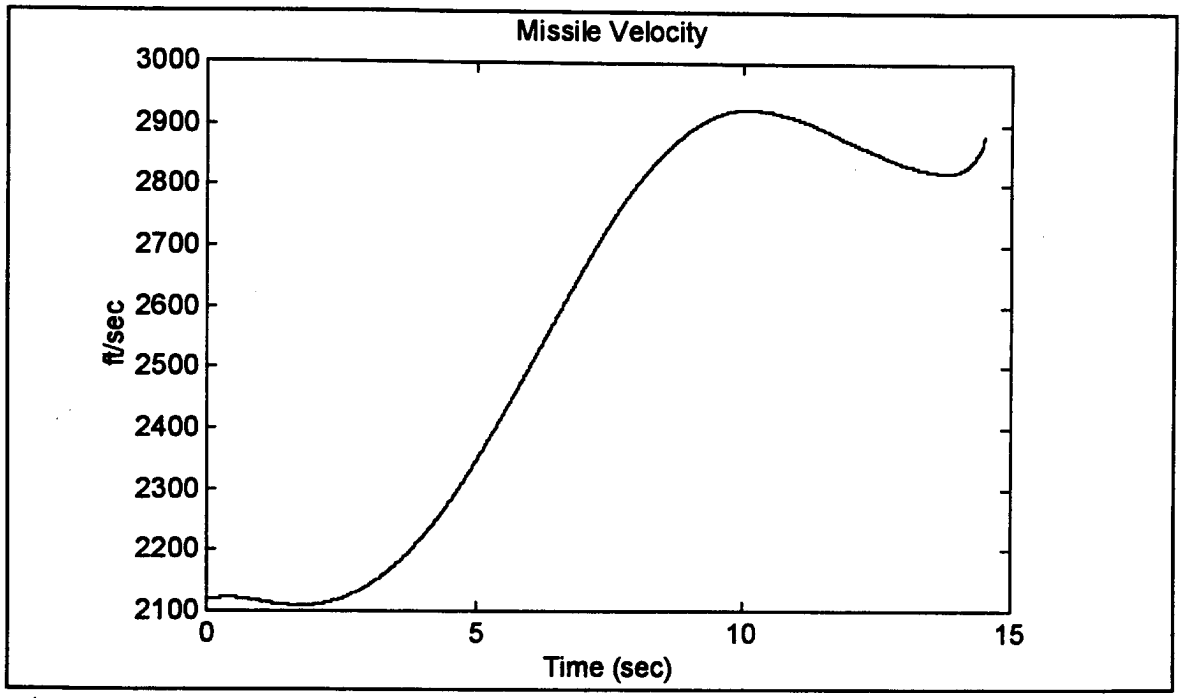

Figure 60. Proportional Navigation Scenario 3. Total Missile Velocity.

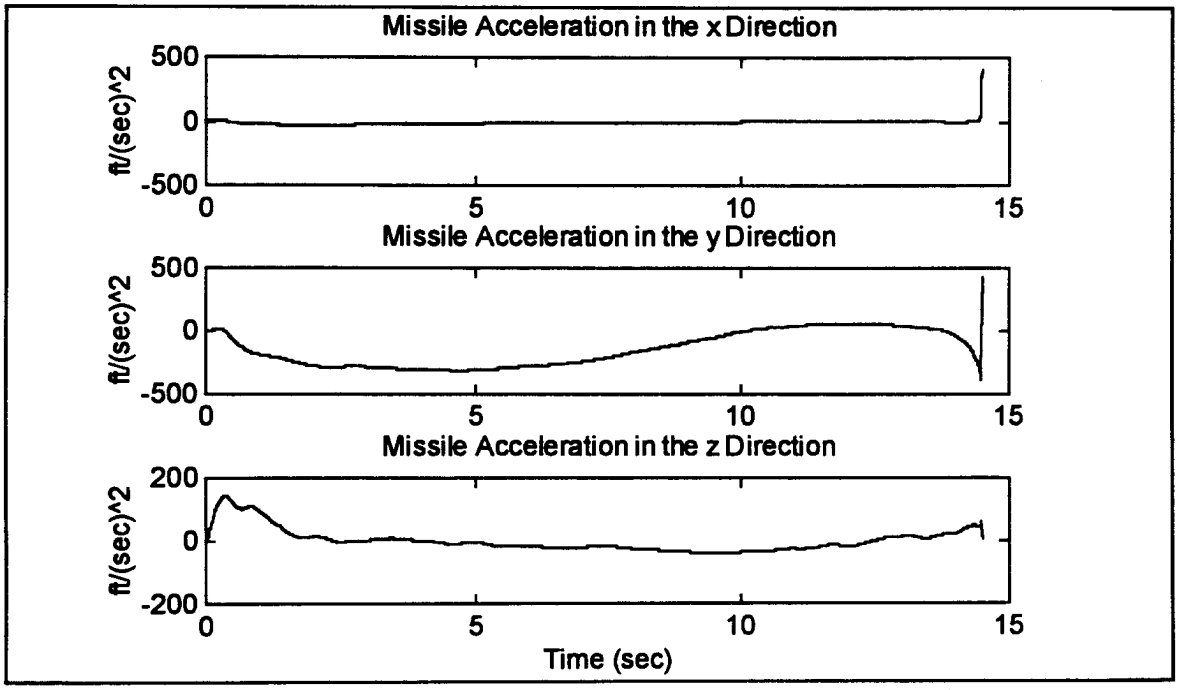

Figure 61. Proportional Navigation Scenario 3. Missile Accelerations.

E. COMMAND GUIDED MISSILE PLOTS FOR SCENARIO 3

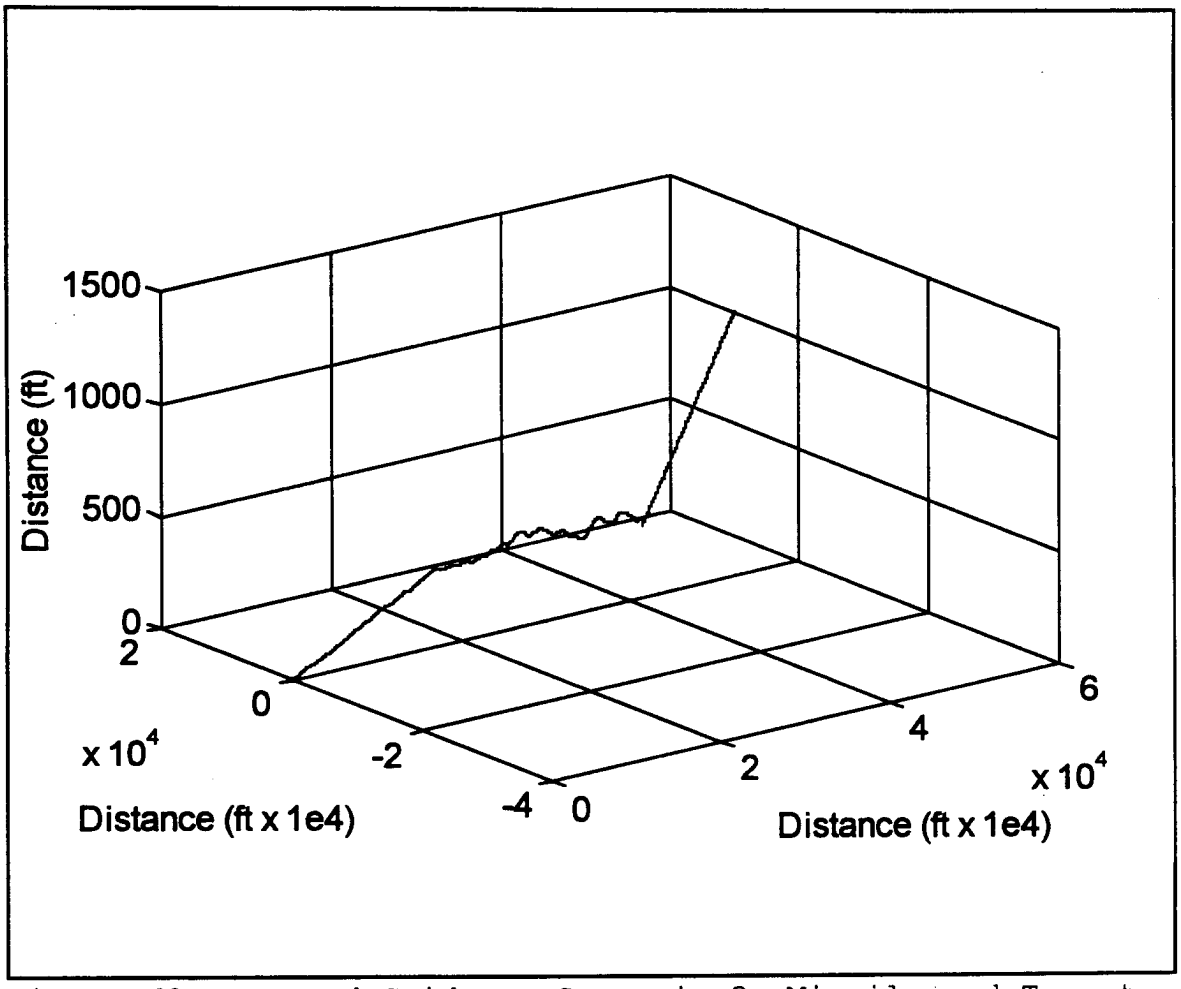

Figure 62. Command Guidance Scenario 3. Missile and Target Trajectory.

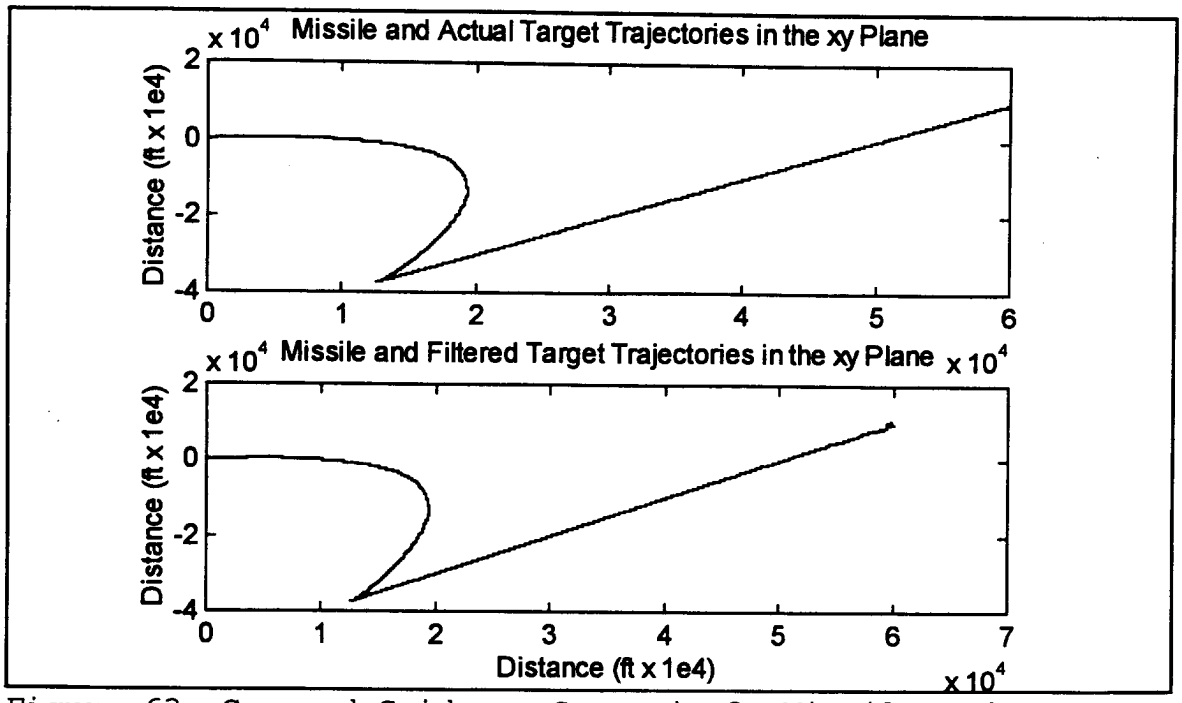

Figure 63. Command Guidance Scenario 3. Missile and Target Trajectories in the xy Plane.

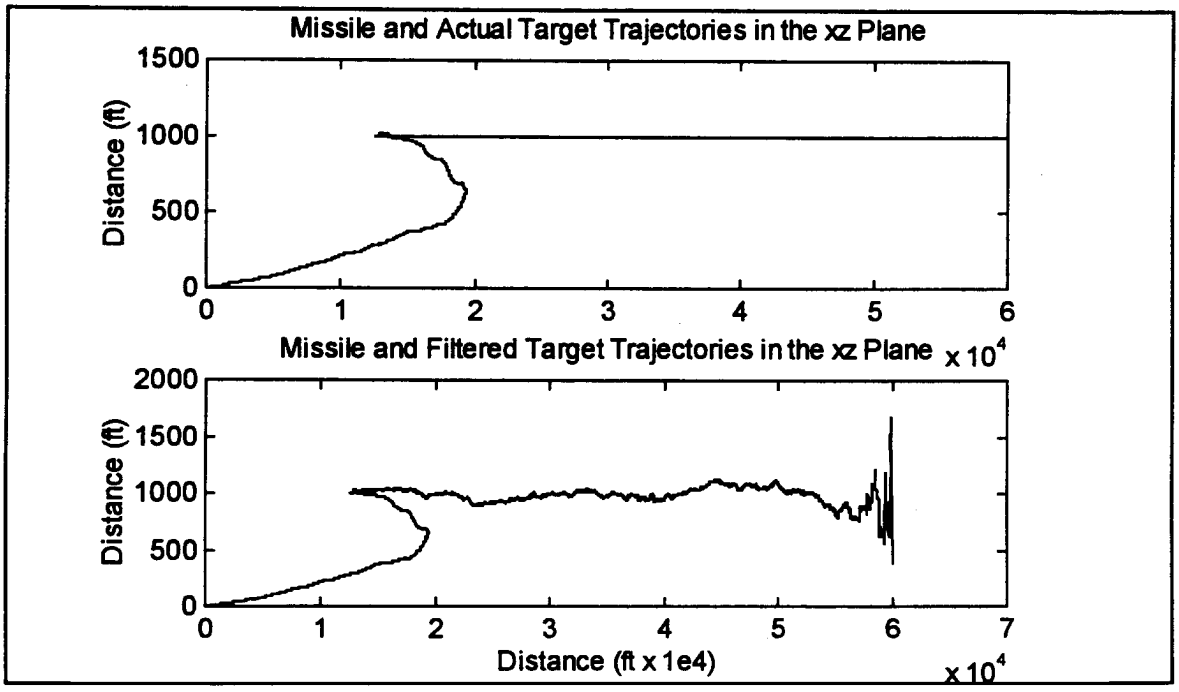

Figure 64. Command Guidance Scenario 3. Missile and Target Trajectories in the xz Plane.

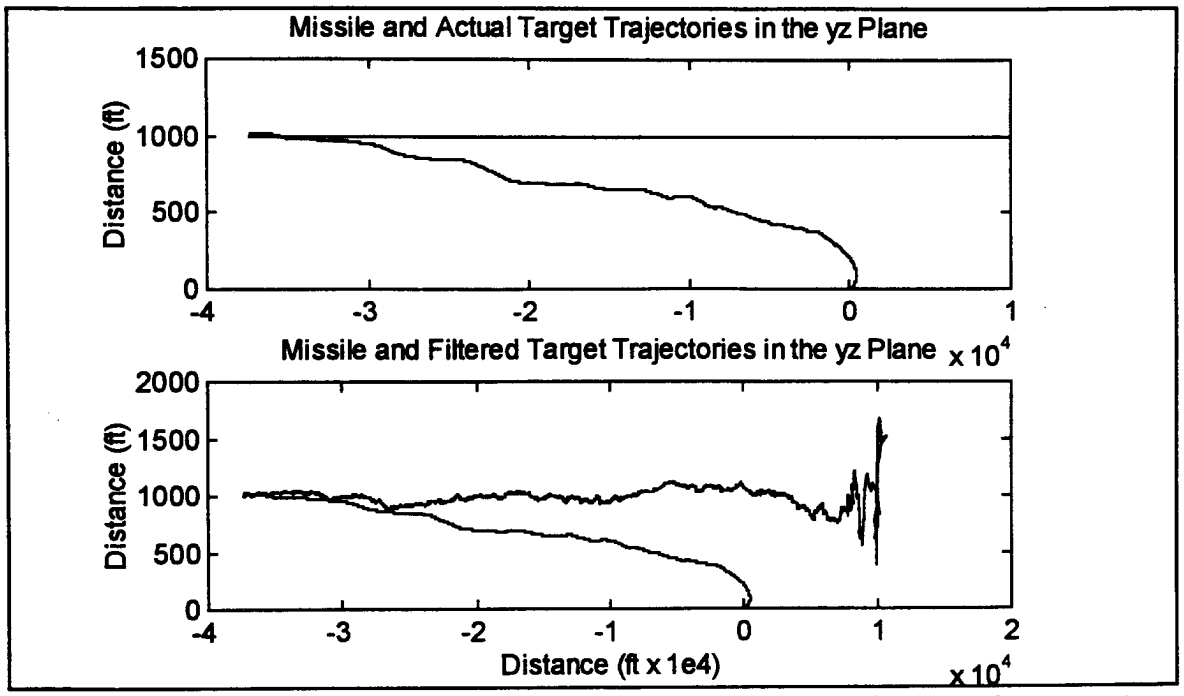

Figure 65. Command Guidance Scenario 3. Missile and Target Trajectories in the yz Plane.

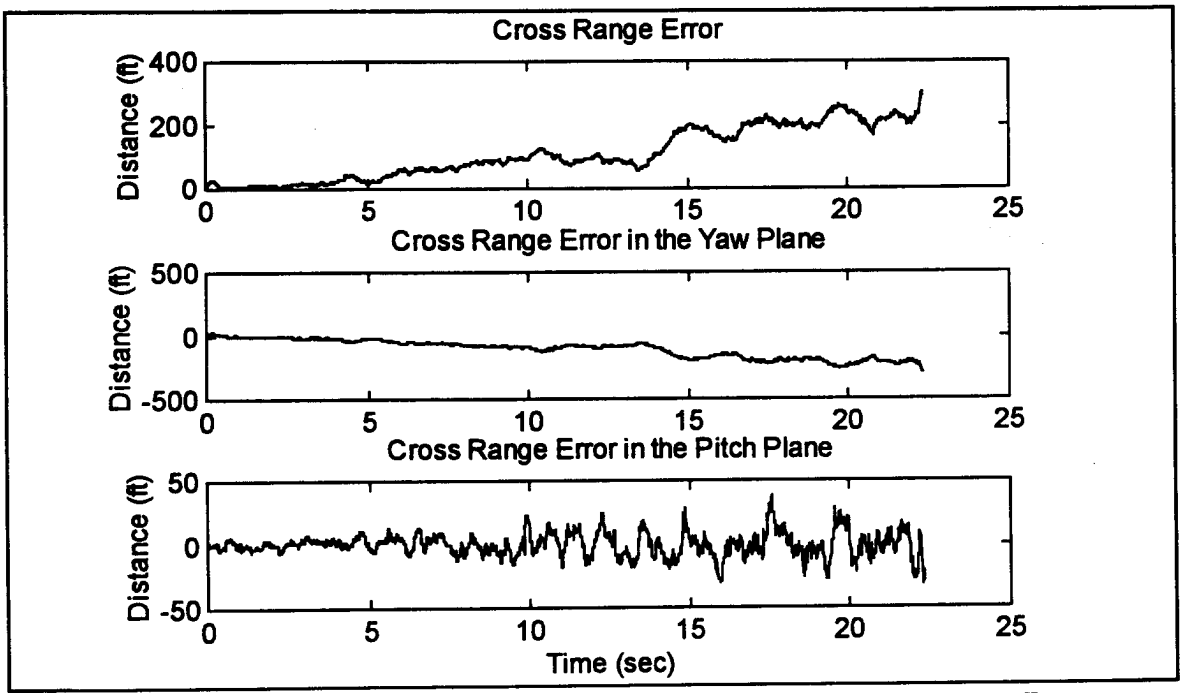

Figure 66. Command Guidance Scenario 3. Cross Range Error.

F. PROPORTIONAL NAVIGATION SIMULINK MODEL

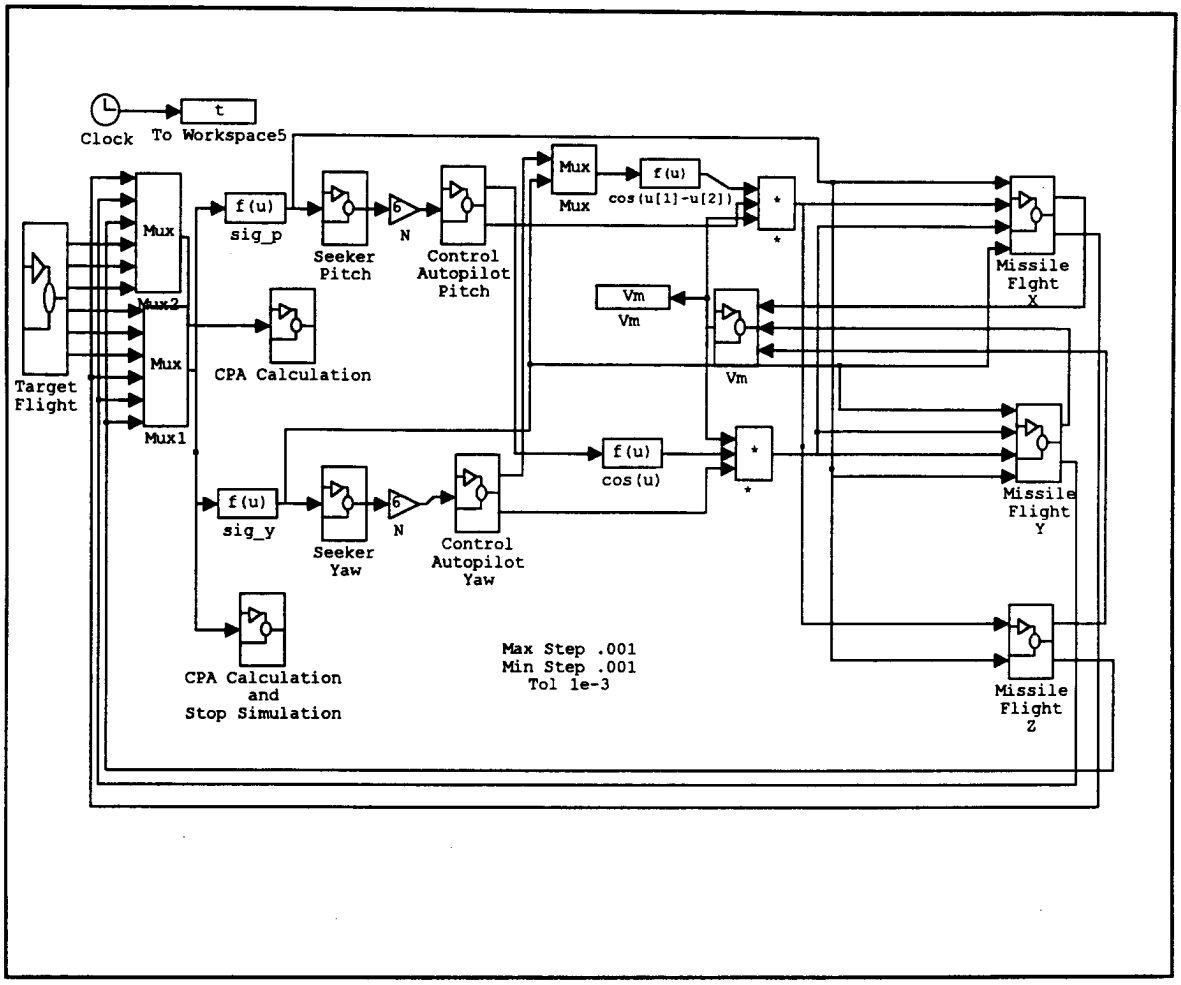

Figure 67. Proportional Navigation Missile Model.

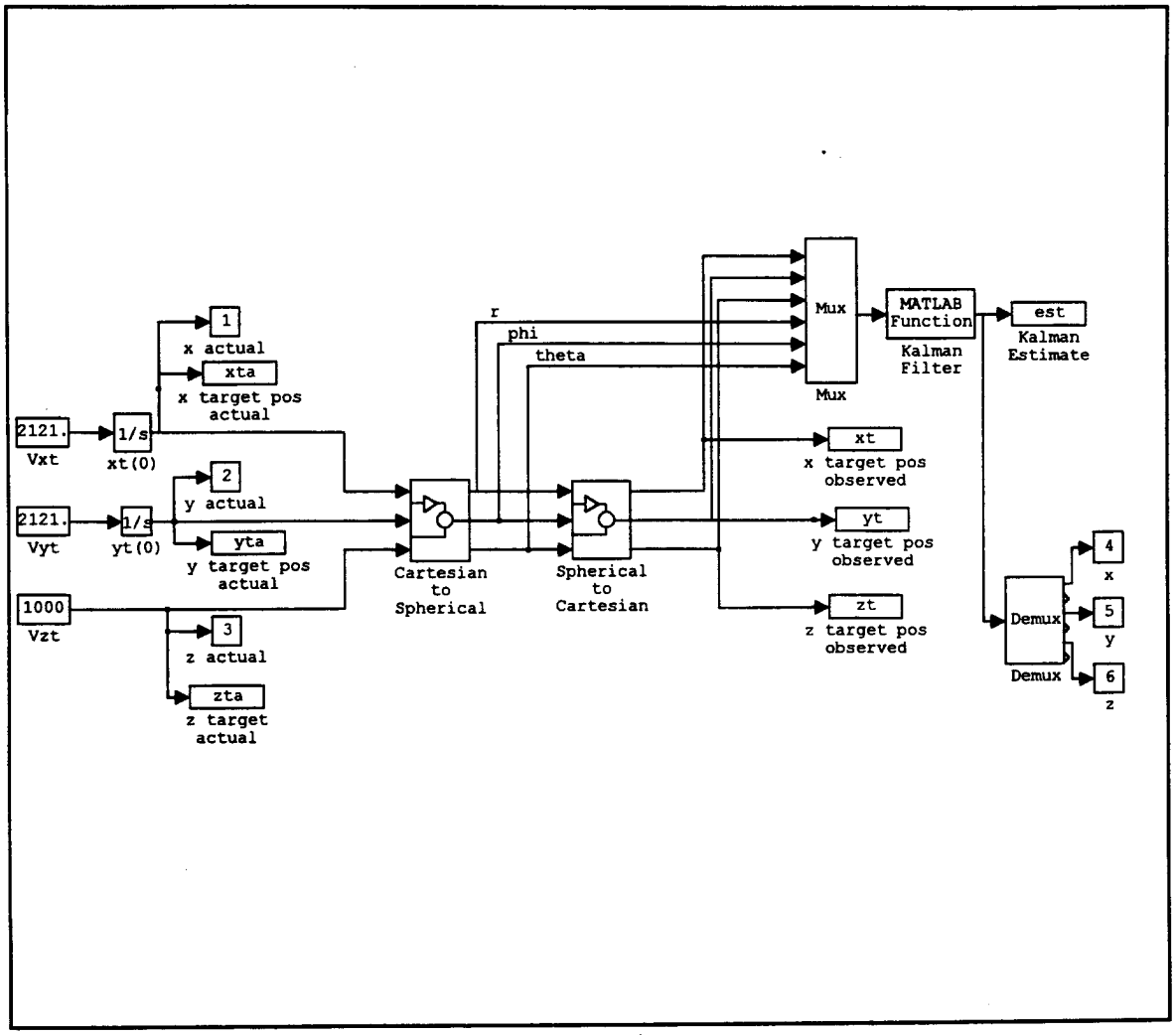

Figure 68. Target Flight with Noise.

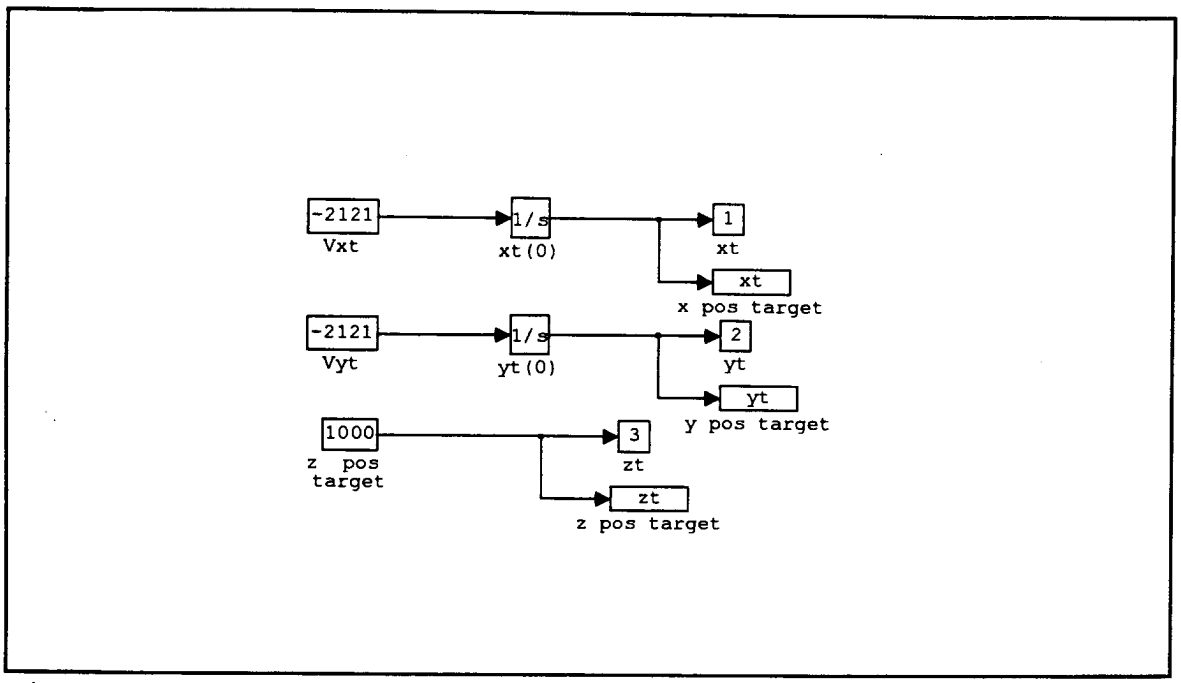

Figure 69. Target Flight without noise.

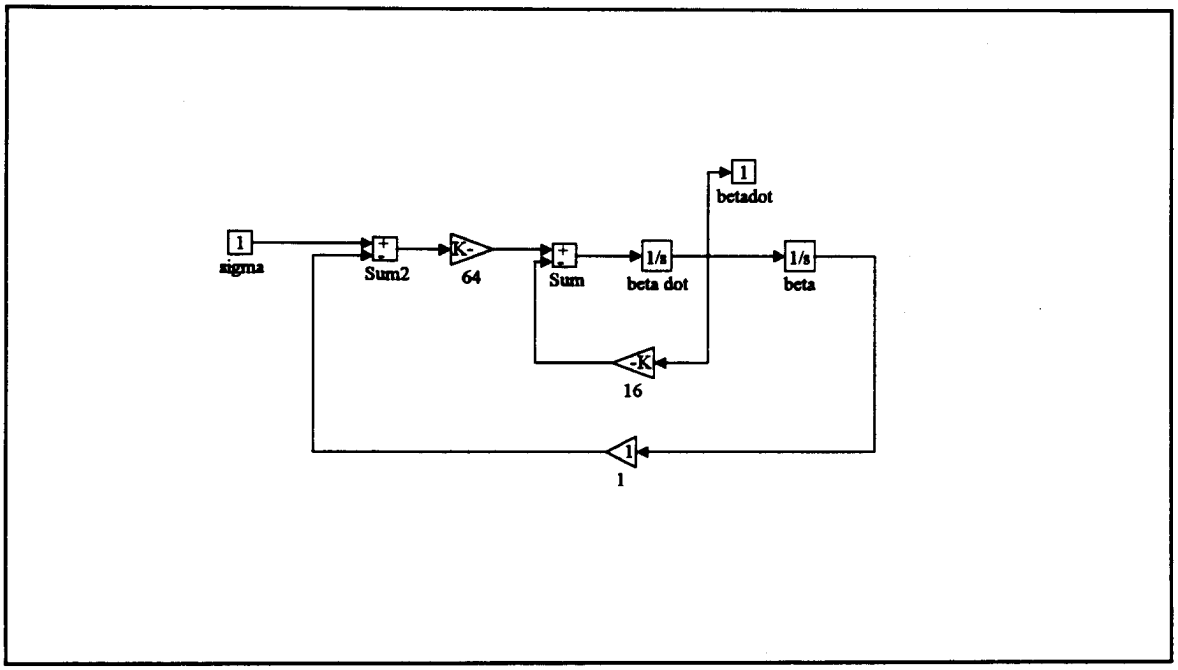

Figure 70. Proportional Navigation Pitch and Yaw Seeker.

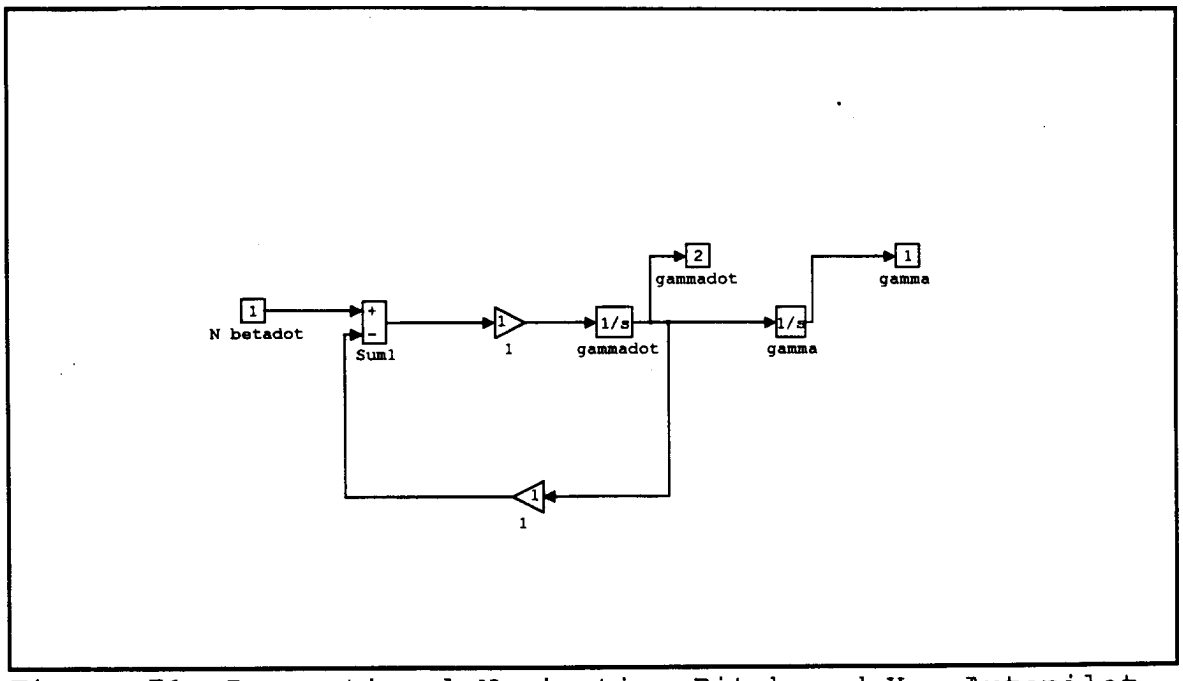

Figure 71. Proportional Navigation Pitch and Yaw Autopilot.

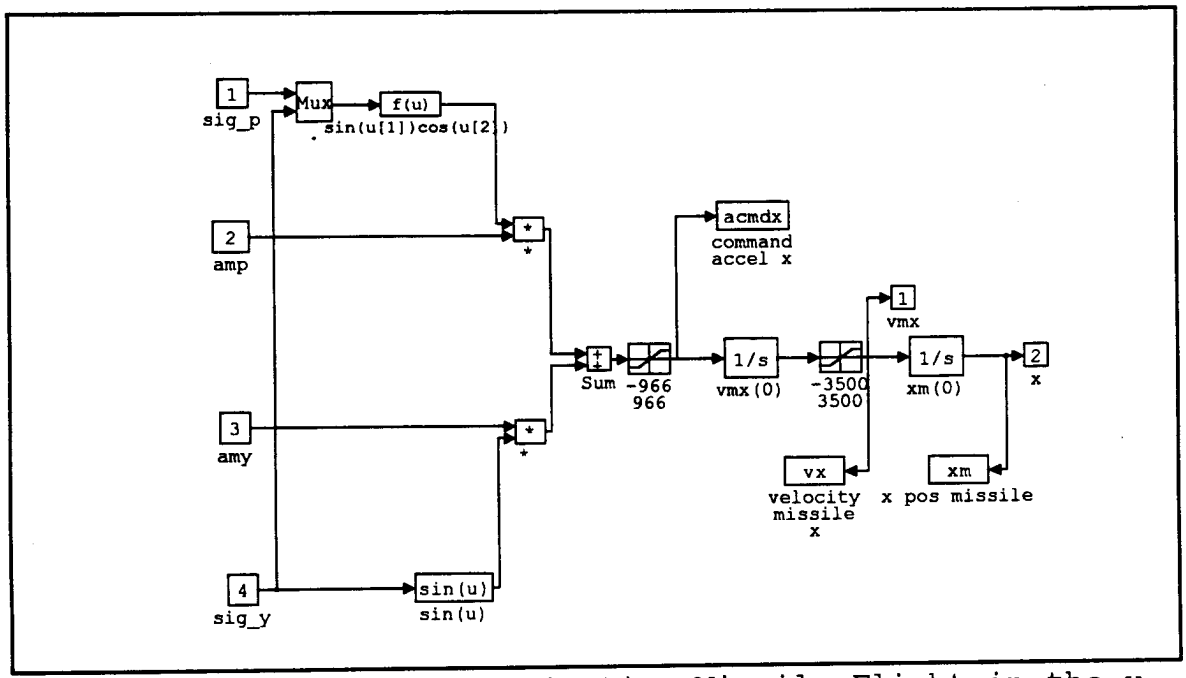

Figure 72. Proportional Navigation Missile Flight in the x Direction.

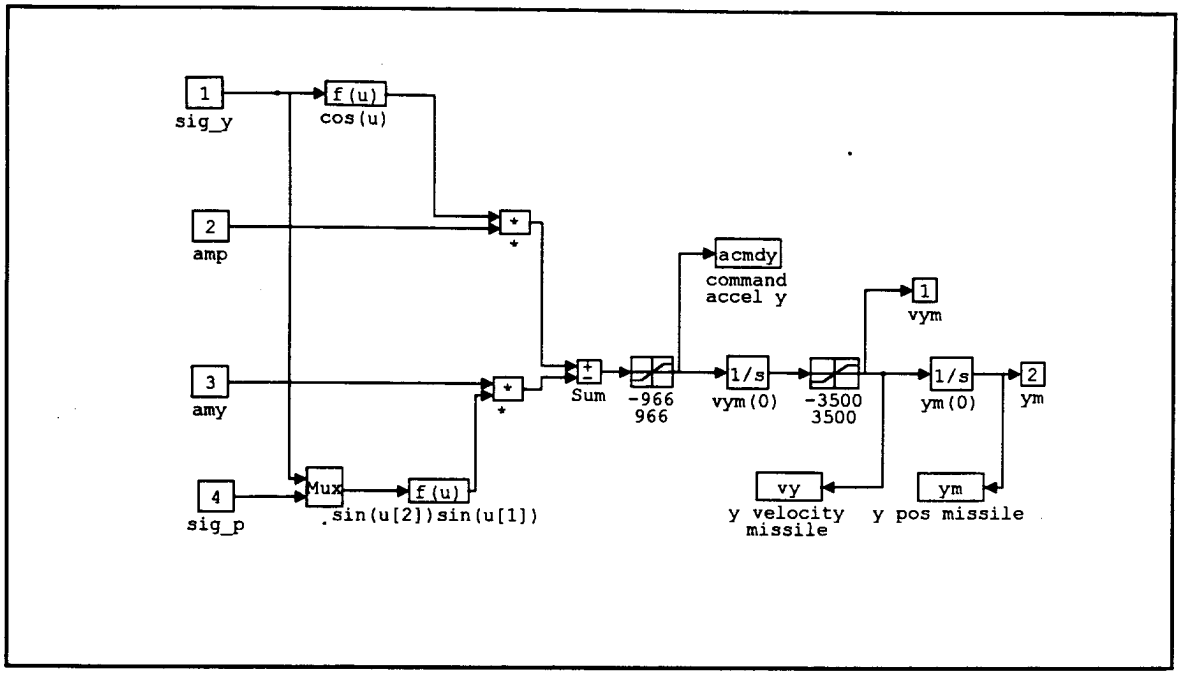

Figure 73. Proportional Navigation Missile Flight in the y Direction.

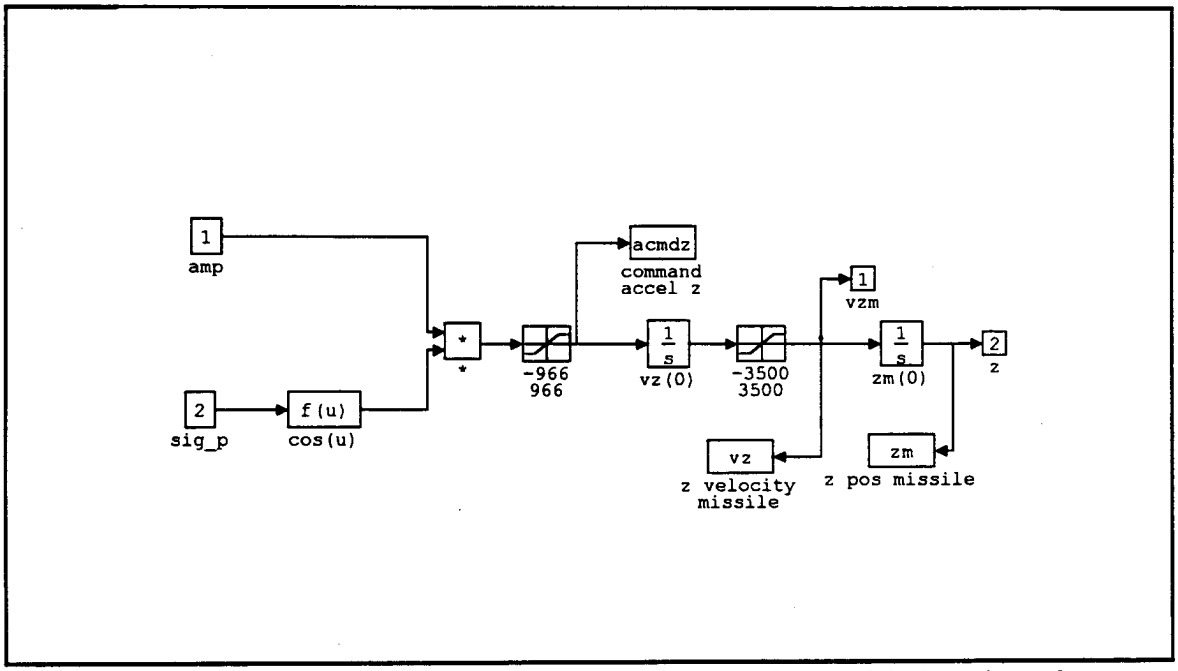

Figure 74. Proportional Navigation Missile Flight in the z Direction.

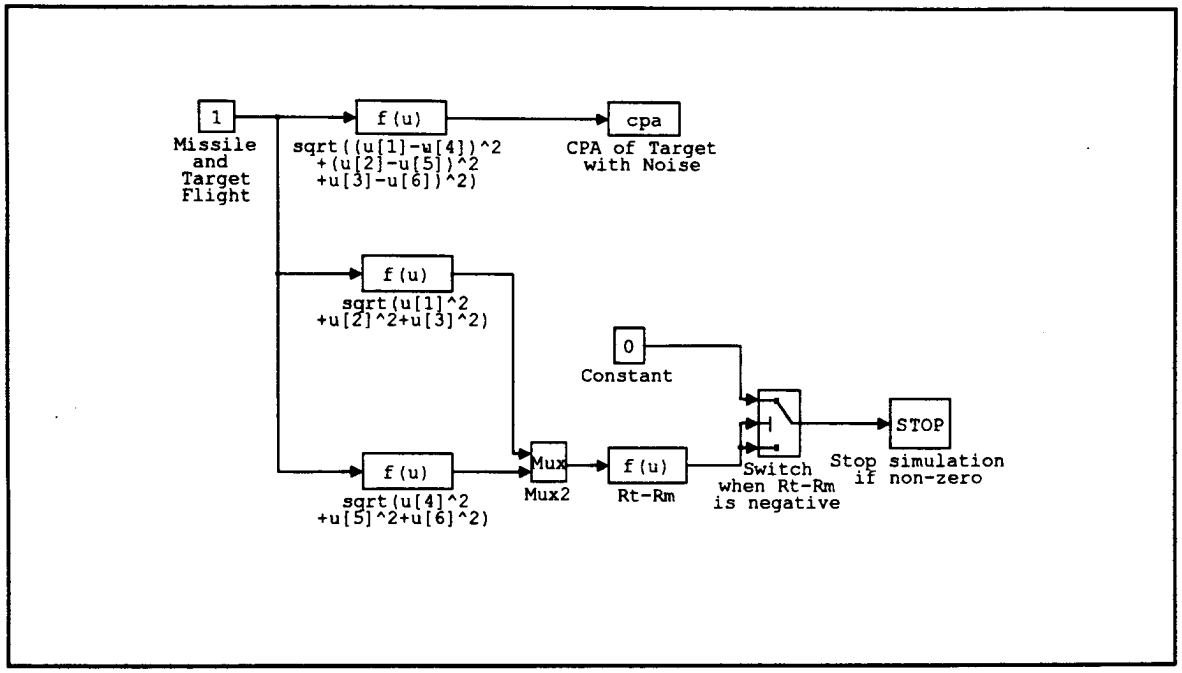

Figure 75. Proportional Navigation CPA and Stop Simulation Calculation.

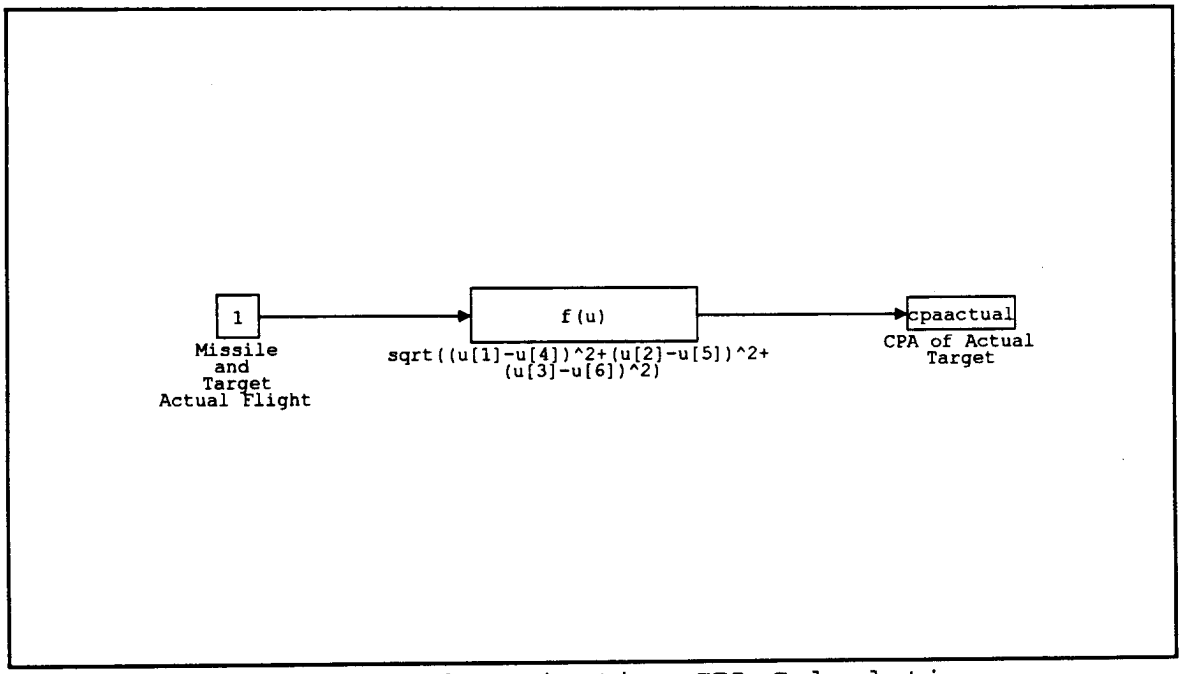

Figure 76. Proportional Navigation CPA Calculation.

G. COMMAND GUIDANCE SIMULINK MODEL

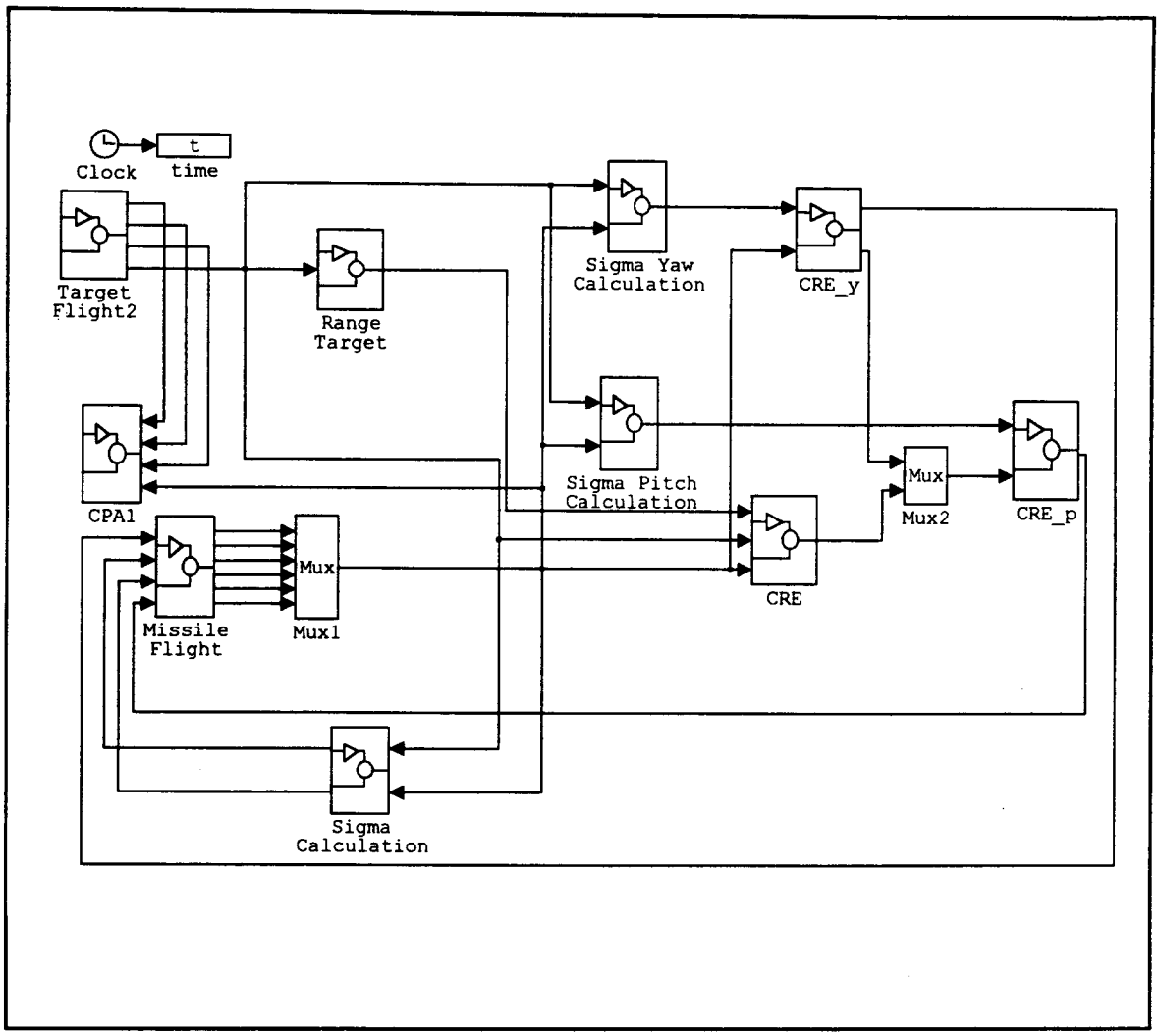

Figure 77. Command Guidance Missile Model.

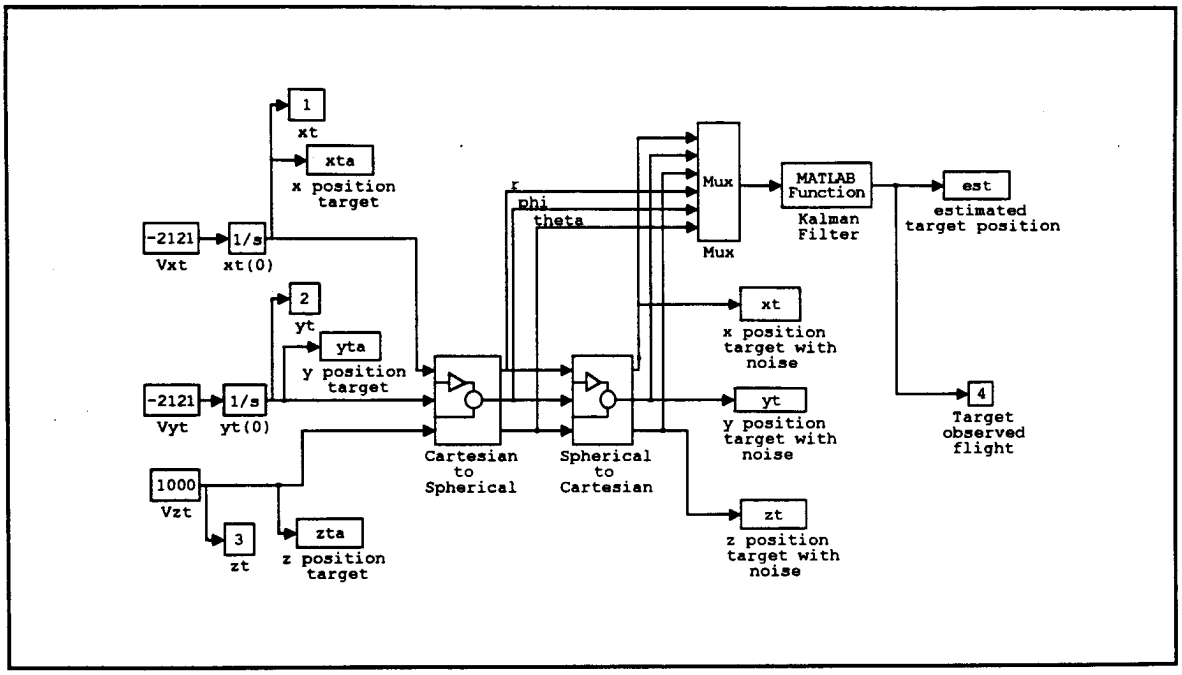

Figure 78. Command Guidance Target Flight with Noise.

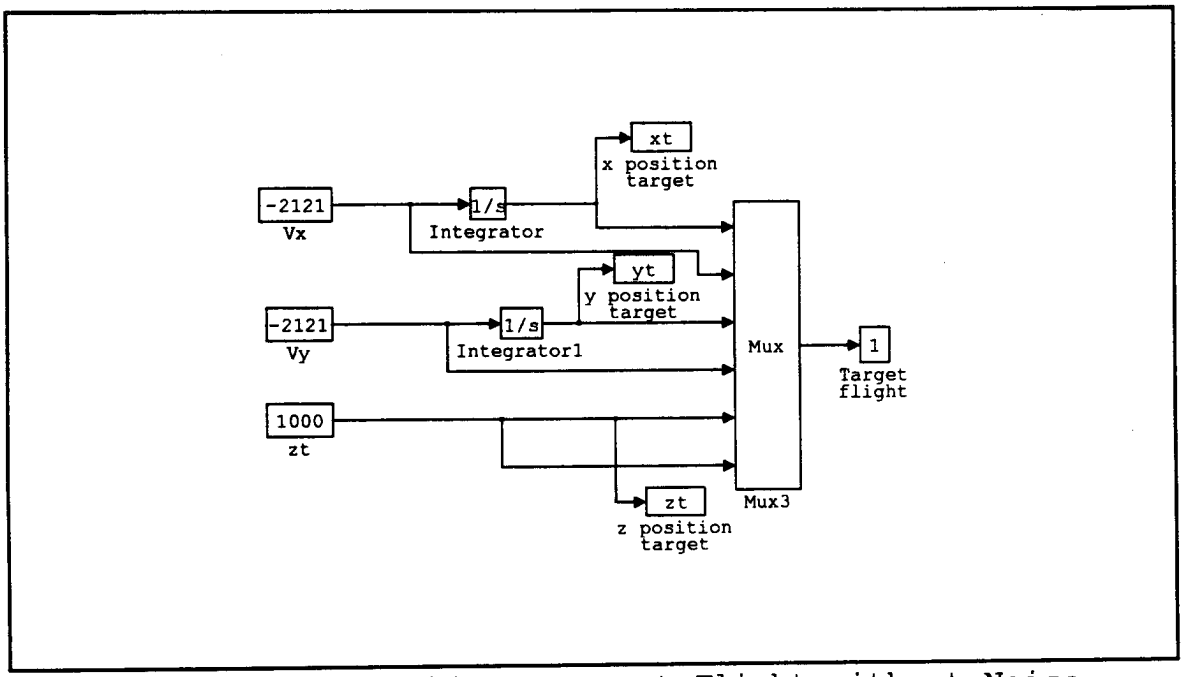

Figure 79. Command Guidance Target Flight without Noise.

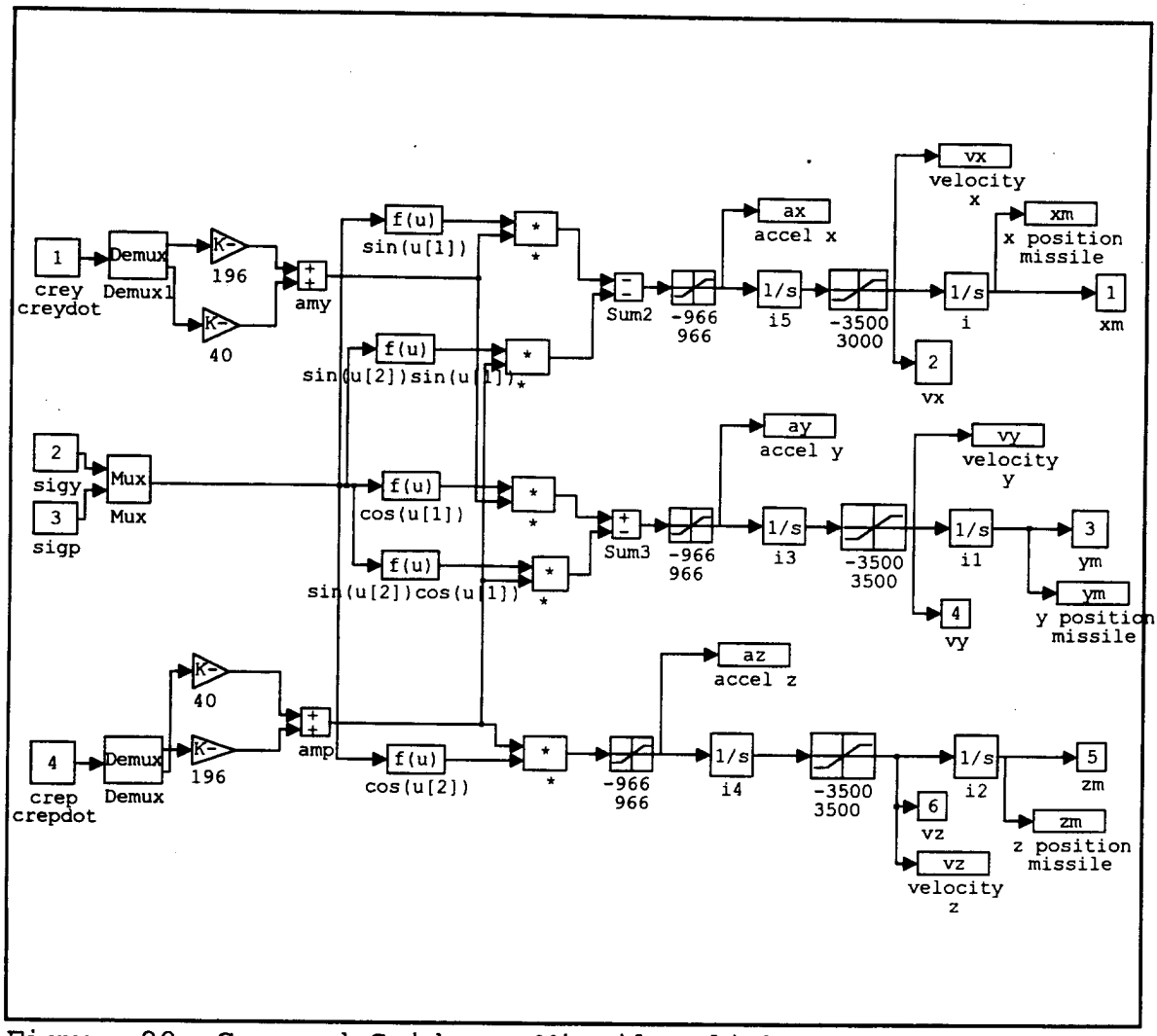

Figure 80. Command Guidance Missile Flight.

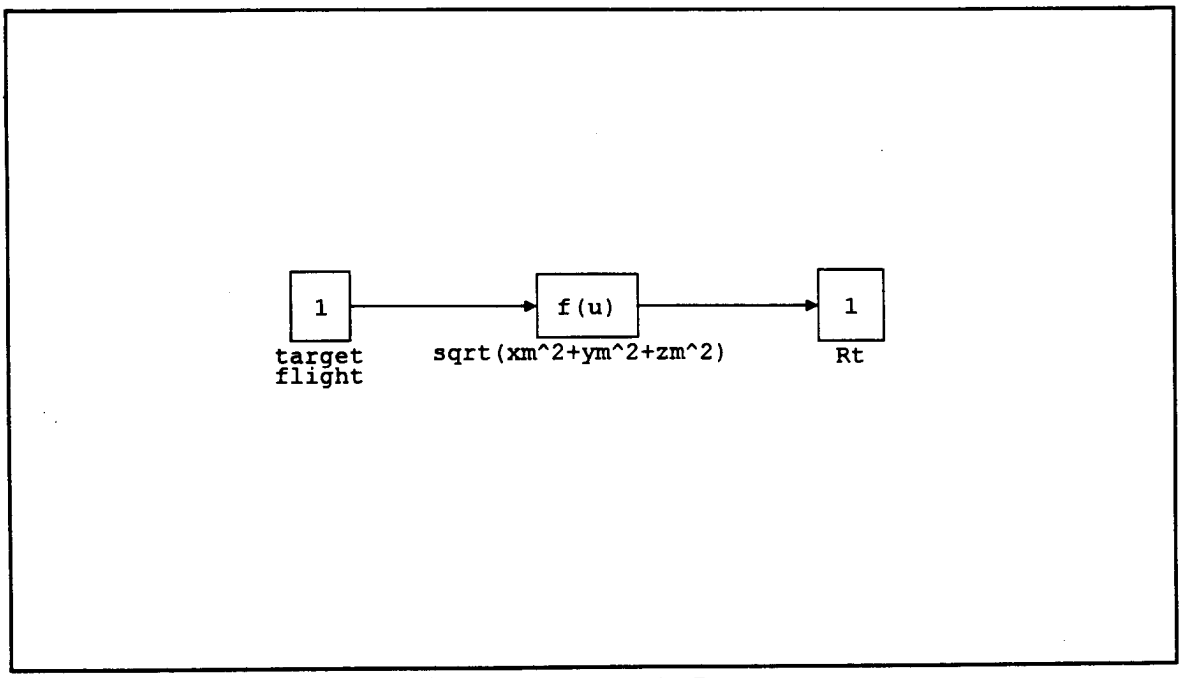

Figure 81. Command Guidance Target Range.

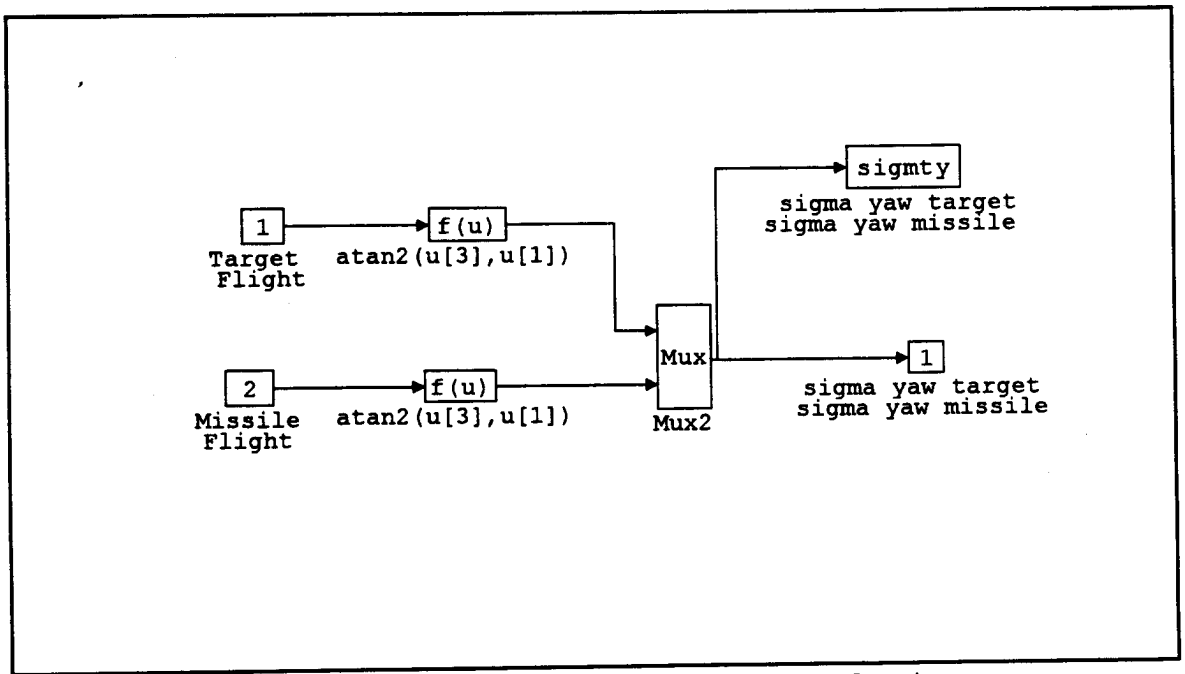

Figure 82. Command Guidance Sigma Yaw Calculation.

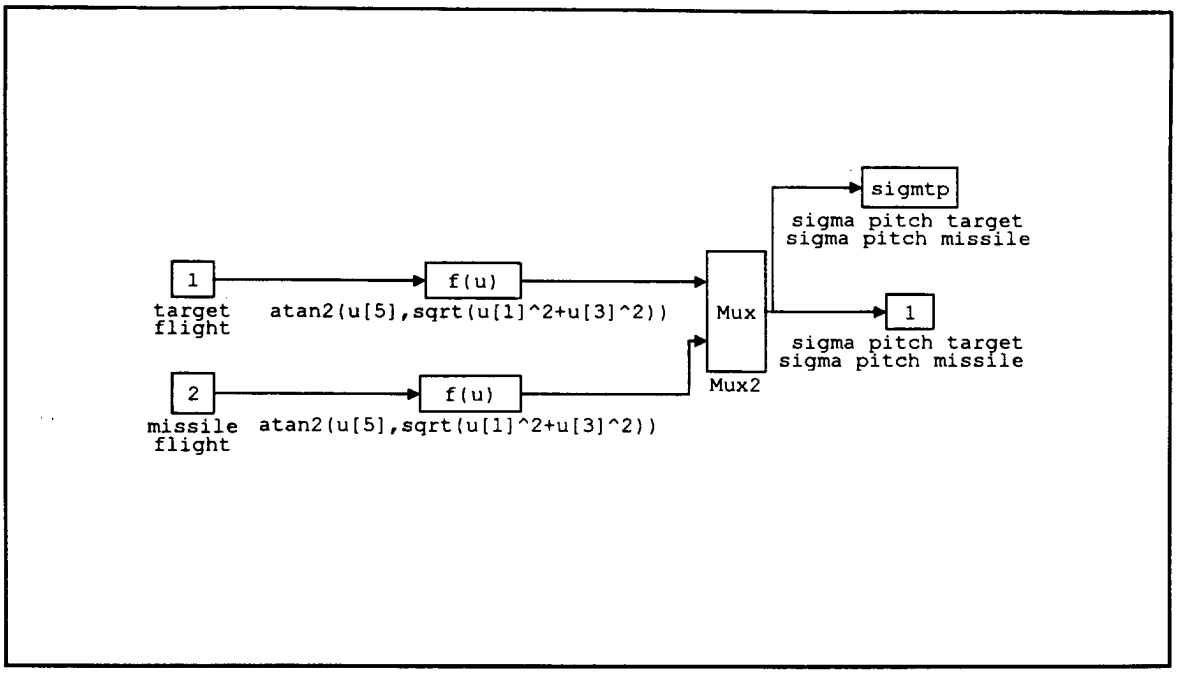

Figure 83. Command Guidance Sigma Pitch Calculation.

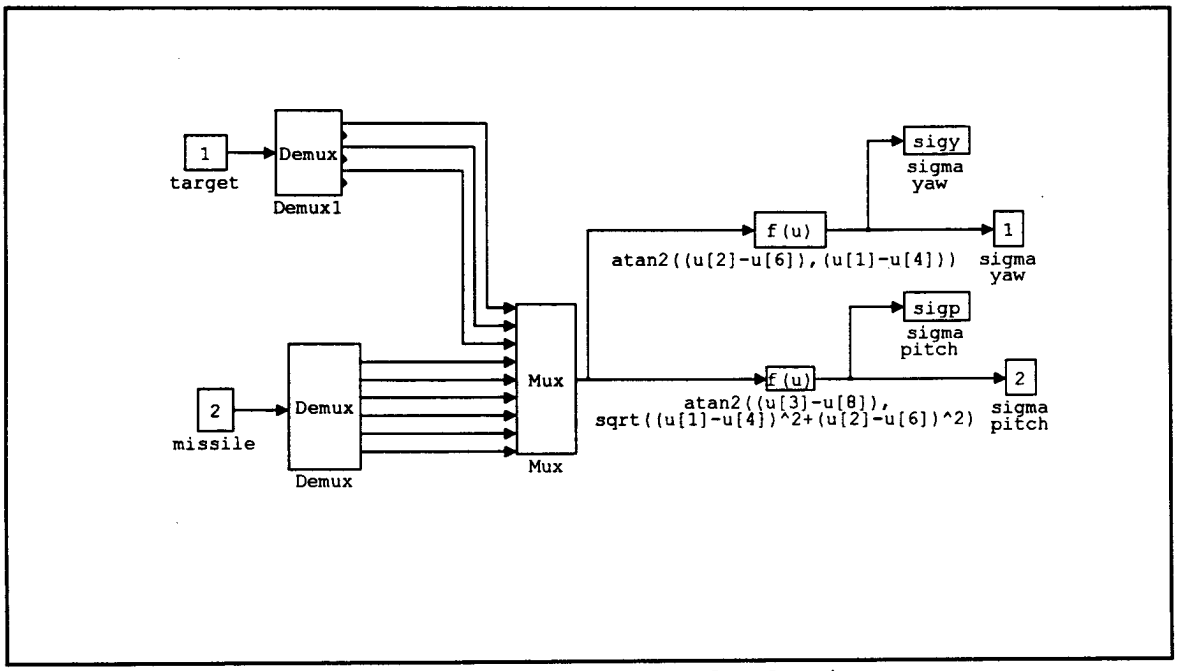

Figure 84. Command Guidance Sigma Calculation.

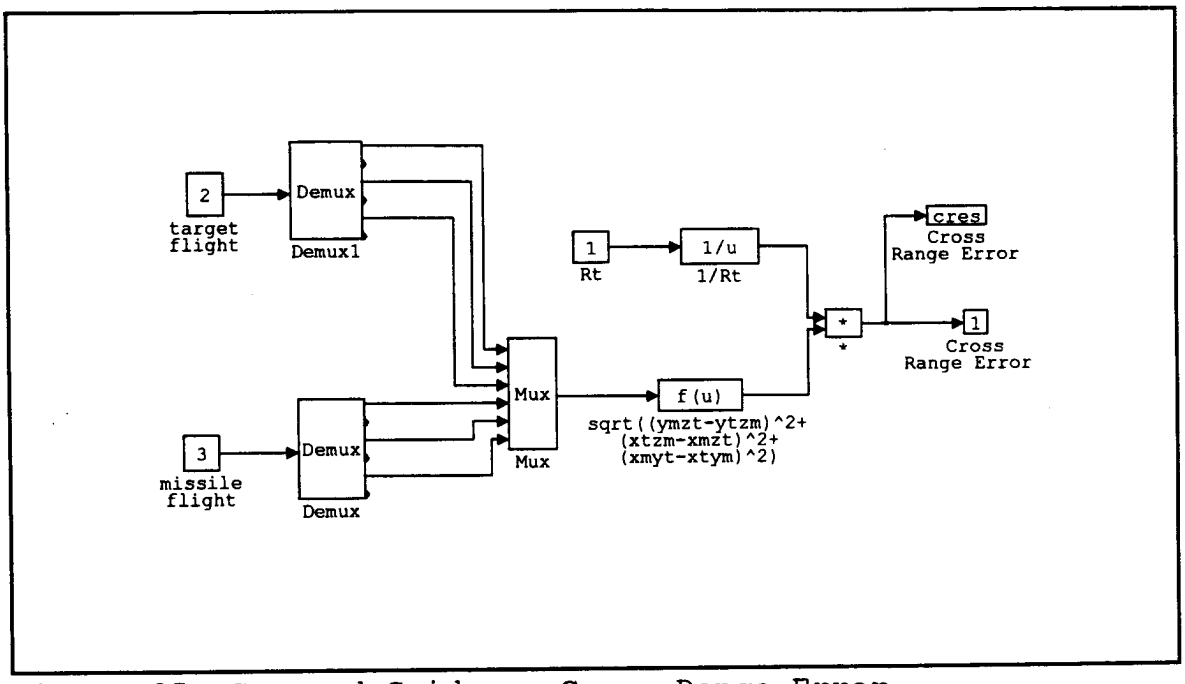

Figure 85. Command Guidance Cross Range Error.

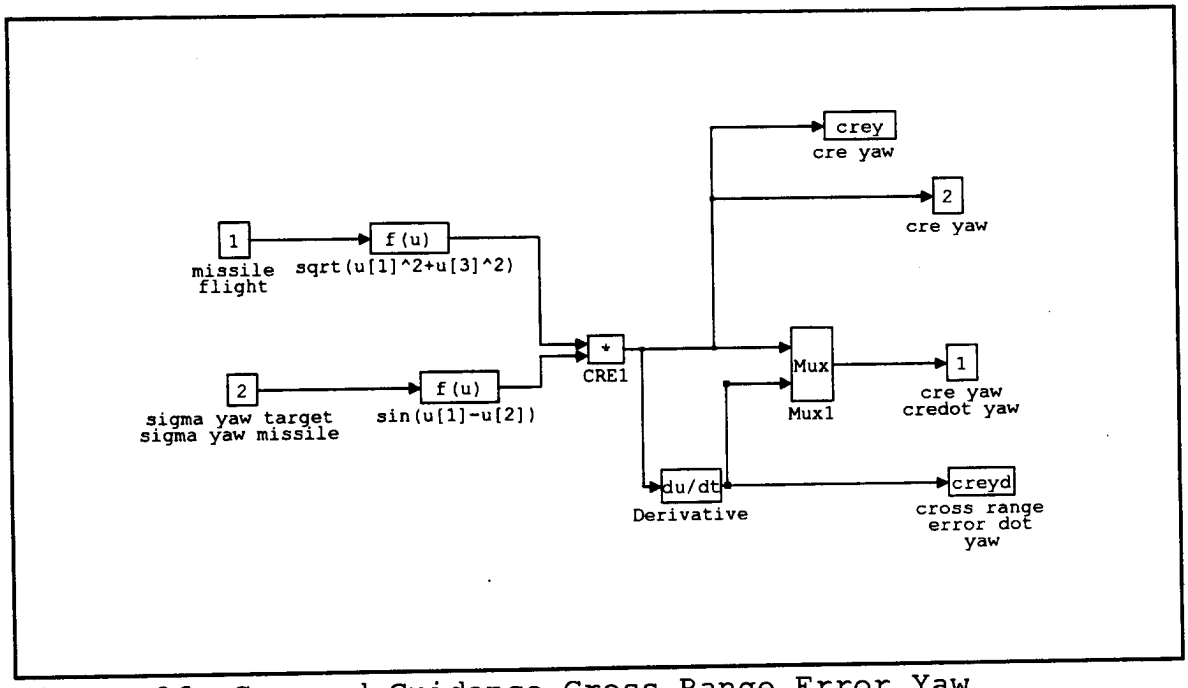

Figure 86. Command Guidance Cross Range Error Yaw.

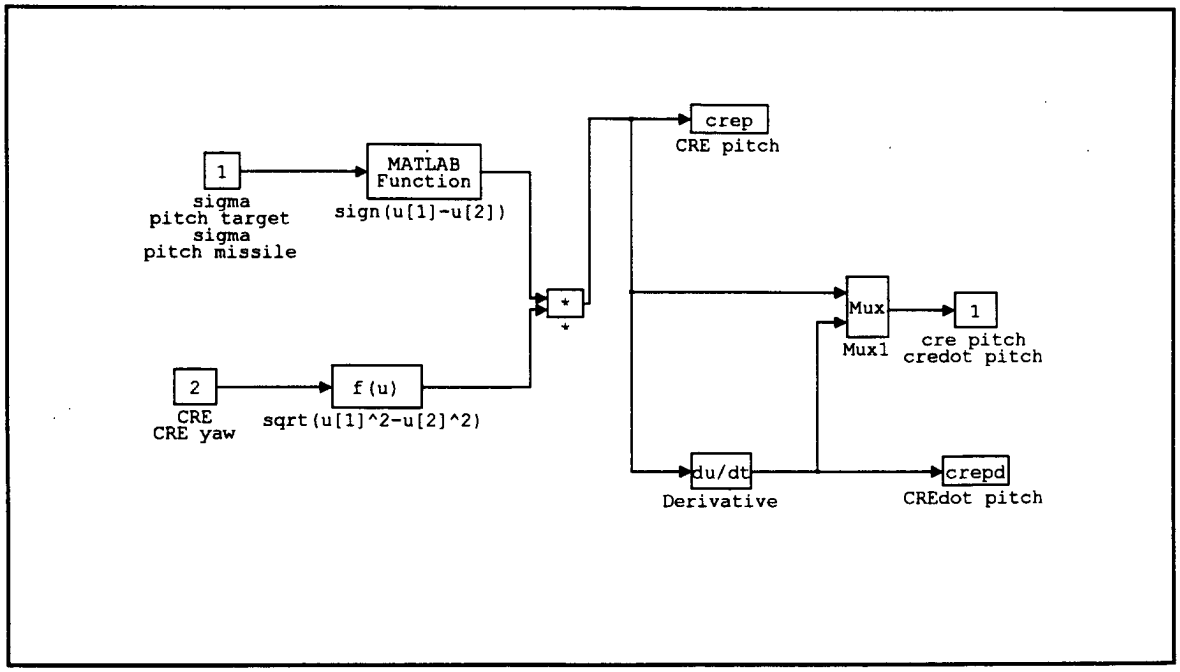

Figure 87. Command Guidance Cross Range Error Pitch.

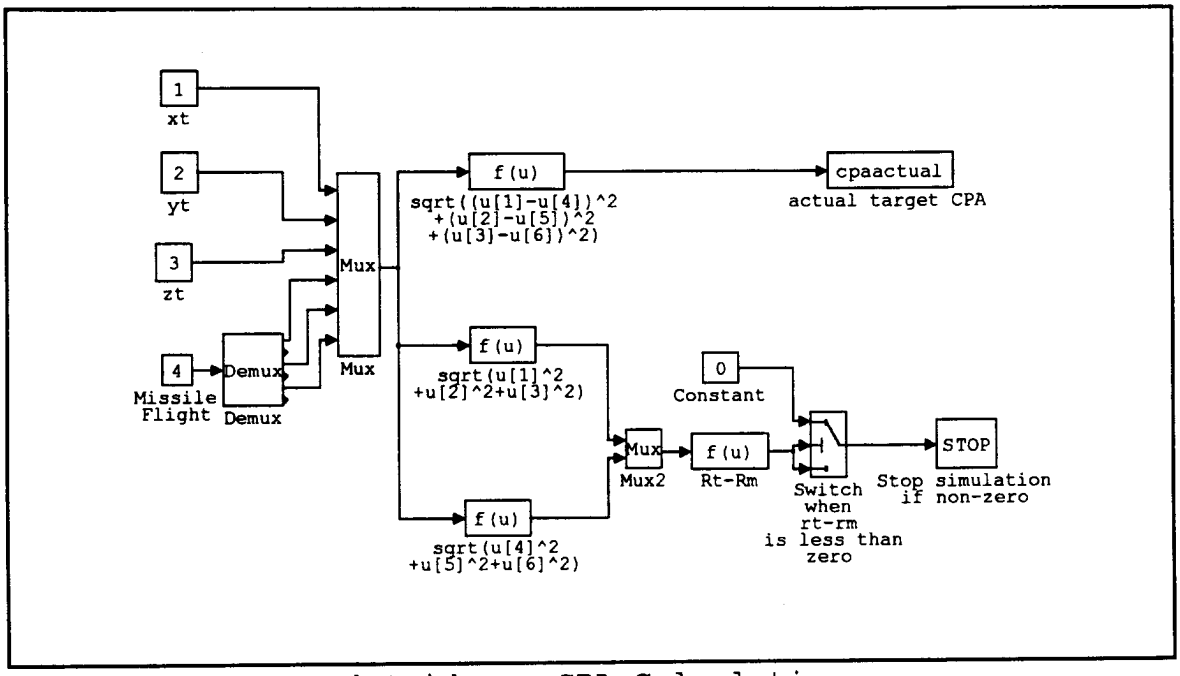

Figure 88. Command Guidance CPA Calculation.

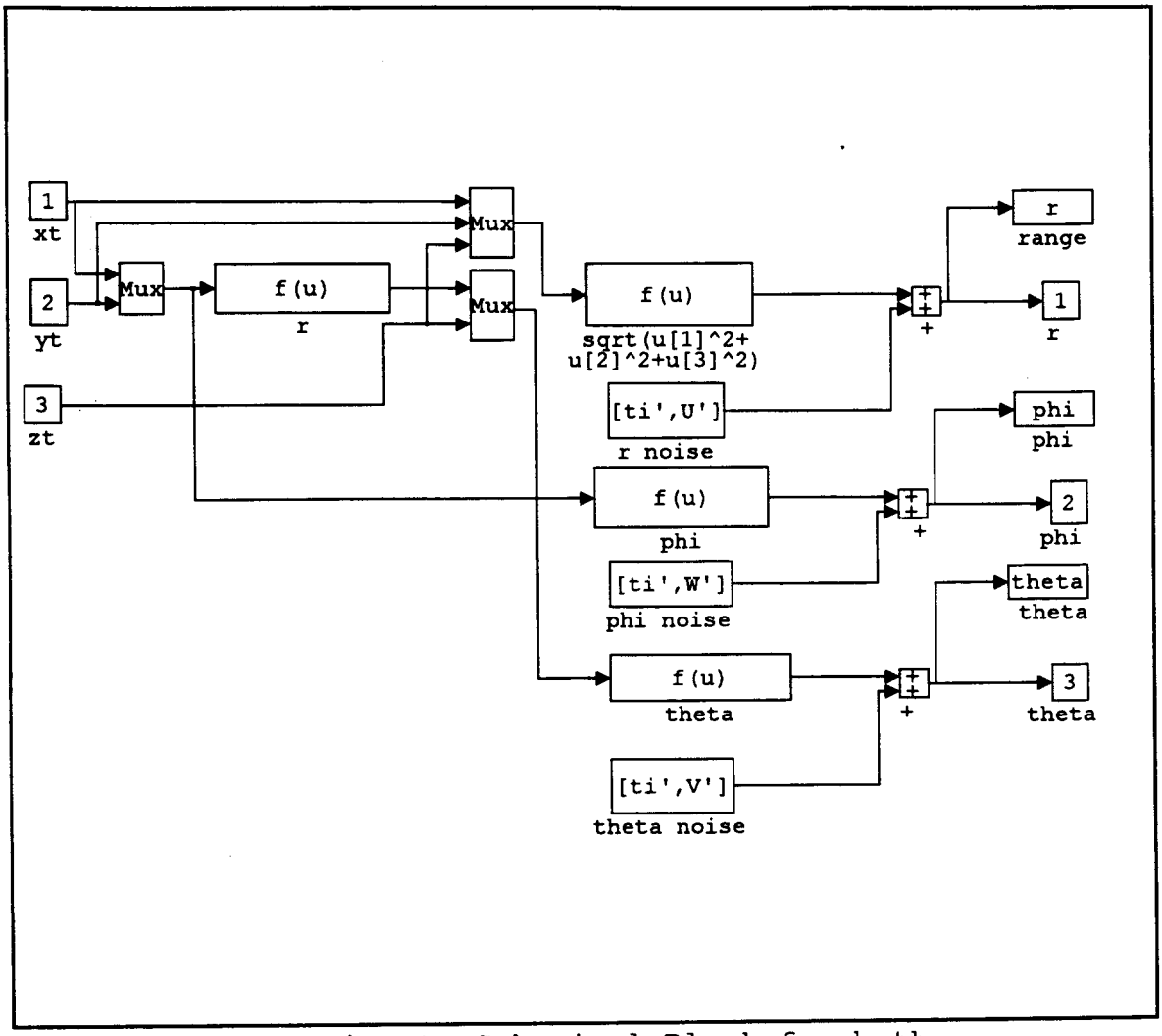

Figure 89. Cartesian to Spherical Block for both Simulations.

H. MISCELLANEOUS MATLAB CODE

```
% This program generates the noise used in the target flight.
randn('seed',26579);
ti=[0:.001:30];
for i= 1:30001
%Range noise
  U(i) = randn*15;
%Pitch angle noise
  V(i) = randn*pi/180;
%Yaw angle Noise
  W(i) = randn*pi/180;
end
%This program sets the initial conditions for the Kalman
%Filter. It is run at the beginning of each simulation.
clear P
clear xhat
global P
global xhat
%initial covariance matrix
  P=1e6*eye(6);
%initial estimated target position
  xhat=[10000 -500  1000 -500 0 500]';
%This function runs a Kalman filter algorithm
%for the given A, B, C matices for constant velocity flight
function[xhat,P]=klmn(u,P,xhat);
%initialization
A=[0 1 0 0 0 0;
   0 0 0 0 0 0;
   0 0 0 1 0 0;
   0 0 0 0 0 0;
   0 0 0 0 0 1;
```

```
   0 0 0 0 0 0];
B=[0;0;0;0;0;0];
C=[1 0 0 0 0 0;
   0 0 1 0 0 0 ;
   0 0 0 0 1 0];
%Time step and q parameter for the Kalman Filter
q=1;
dt=.001;
%Continuous to discrete conversion
[phi,del]=c2d(A,B,dt);
%Specify position and angle vectors
  pos=[u(1);u(2);u(3)];
  ang=[u(4);u(5);u(6)];
%Calculate Sigma Matrix
  sigma=[((q^2)*(dt)^3)/3 ((q^2)*(dt)^2)/2;
       ((q^2)*(dt)^2)/2 (q^2)*(dt)];
%Calculate Q Matrix
  Q=[sigma zeros(2,2) zeros(2,2);
     zeros(2,2) sigma zeros(2,2);
     zeros(2,2) zeros(2,2) sigma];
%Calculate Rstar Matrix
  Rstar=[225 0 0;0 (1*pi/180)^2 0;0 0 (1*pi/180)^2];
%Kalman iteration
  xhatkp1 = phi*xhat;
  Pkp1 = phi*P*phi' + Q;
  H = calch(ang);
  R = H*Rstar*H';
  K = Pkp1*C'*inv(C*Pkp1*C'+R);
  Pk1k1 = (eye(6)-K*C)*Pkp1*(eye(6)-K*C)' + K*R*K';
  xk1k1 = xhatkp1 + K*(pos(:,1)-(C*xhatkp1));
  global xhat;
```

```
  xhat = xk1k1;
  global P;
  P = Pk1k1;
%This function calculates the H matrix for computation
%in a Kalman filter
function [H]=calch(x)
 a=(tan(x(2)))^2;
 b=(tan(x(3)))^2;
 c=(sec(x(2)))^2;
 d=(sec(x(3)))^2;
 e=tan(x(2));
 f=tan(x(3));
H = [1/((a*b+a+b+1)^.5) -x(1)*(b*e*c+c*e)/((a*b+a+b+1)^1.5)
-x(1)*(a*d*f+d*f)/((a*b+a+b+1)^1.5);
e / ( ( a * b + a + b + 1 ) ^ . 5 )
-x(1)*(a*c*(b+1))/((a*b+a+b+1)^1.5)+x(1)*c/((a*b+a+b+1)^.5)
-x(1)*e*f*d*(a+1)/((a*b+a+b+1)^1.5);
f/((1+b)^.5) 0 -x(1)*b*d/((1+b)^1.5)+x(1)*d/((1+b)^.5)];
```

BIBLIOGRAPHY

Blackelock, J.H., *Automatic Control of Aircraft and Missiles*, Wiley-Interscience Publishing, New York, NY. 1991.

Davis, H.F., *Introduction to Vector Analysis*, Wm.C. Brown Publishing, Dubuque, IA. 1991.

Hostetter, G.H., Santana, M.S., Stubberud, A.R., *Digital Control System Design*, Saunders College Publishing, Fort Worth, TX. 1994.

Peppas, D.I, "A Computer Analysis of Proportional Navigation and Command to Line of Sight of a Command Guided Missile for a Point Defence System," M.S. Thesis, Naval Postgraduate School, Monterey CA, December 1992.

Titus, H.A., Missile Guidance, unpublished notes, Naval Postgraduate School, Monterey, CA.

INITIAL DISTRIBUTION LIST

		No. Copies
1.	Defense Technical Information Center Cameron Station Alexandria, Virginia 22304-6145	2
2.	Library, Code 52 Naval Postrgaduate School Monterey, California 93943-5101	2
3.	Chairman, Code EC Department of Electrical and Computer Engineering Naval Postgraduate School Monterey, California 93943-5121	1
4.	Professor H.A. Titus, Code EC/Ts Department of Electrical and Computer Engineering Naval Postgraduate School Monterey, California 93943-5121	1
5.	Professor R.G. Hutchins, Code EC/Hu Department of Electrical and Computer Engineering Naval Postgraduate School Monterey, California 93943-5121	1
6.	Professor P. Pace, Code EC/Pc Department of Electrical and Computer Engineering Naval Postgraduate School Monterey, California 93943-5121	1
7.	Lieutenant Patrick Costello 9 Rhonda Dr. Scarborough, Maine 04074	1